Australian Government
Department of Defence
Defence Science and
Technology Organisation

DSTO

Statistical Analysis of Northern Australian Land Backgrounds

Luke Rosenberg and
Michael Wegener

DSTO-TR-1456

Australian Government
Department of Defence
Defence Science and
Technology Organisation

Statistical Analysis of Northern Australian Land Backgrounds

Luke Rosenberg and Michael Wegener

Weapons Systems Division
Systems Sciences Laboratory

DSTO-TR-1456

ABSTRACT

A substantial amount of work into the statistical analysis of both visual and infra-red imagery has been undertaken in the recent years at DSTO. This report is a summary of the results from the analysis of a trial held in Northern Australia in 1997. The first and second order statistics of land background infra-red pixel intensities were estimated and Gaussian histogram and power-law auto-covariance models were rigorously tested, before a stochastic simulation of the data was performed. As the simulation technique required Gaussian statistics, a point-wise non-linear transform was applied to those ensemble images with non-Gaussian histograms.

RELEASE LIMITATION

Approved for public release

Published by

DSTO Systems Sciences Laboratory
PO Box 1500
Edinburgh South Australia 5111 Australia

Telephone: (08) 8259 5555
Fax: (08) 8259 6567

AR-012-812
July 2004

Statistical Analysis of Northern Australian Land Backgrounds

Executive Summary

Knowledge of the background statistics is required for the design of suitable background clutter suppression and target extraction filters. This information can also be used for computer generation of realistic stochastic models for system performance analysis and generation of large numbers of random backgrounds for Monte-Carlo testing. This report is a summary of the first and second order statistics of natural terrain imagery in Northern Australia during the 1997 trial. The statistics are also applied to generate synthetic images over these terrains.

The ensembles were formed by parsing each recorded run and grouping images containing the predominate vegetation class. Using the assumption that the underlying random processes are stationary in the wide-sense, the ensemble histograms and auto-covariance can be calculated. These then become estimates of the true distribution and correlation for that vegetation classes.

Using Dietrich and Newsam's, [1] technique for generating arbitrary stationary Gaussian random fields using the first and second order statistics of an existing image, synthetic images can be simulated. For sequences without an underlying Gaussian distribution, the non-linear transform developed by Chapple *et al.* [2] can be used to generate a non-Gaussian random field with a marginal probability density and correlation structure that agrees with that of actual IR background imagery.

The analysis shows that the majority of natural terrain background is non-Gaussian and the power-law model for the auto-covariance matches for the majority of the vegetation classes. Most of the transformed synthetic images appear to visually match the sample images, but there does appear to be some difference in the brightness for images which are not transformed but pass the Gaussian hypothesis test. However, if the transformation is applied to these images before synthesis, reasonable simulated images result.

This page intentionally left blank

Authors

Luke Rosenberg
Weapons Systems Division

Luke Rosenberg received his BE (Elec.) with Honours from Adelaide University in 1999 and joined the Missile Simulation Group at DSTO in January 2000. During this time he has completed a Masters degree in Signal and Information Processing through Adelaide University and CSSIP. He is presently in the second year of his PhD at Adelaide University, looking into interference suppression for multi-channel Synthetic Aperture Radar.

Michael Wegener
Surveillance Systems Division

Michael Wegener received his degrees of Dipl.-Inform (equiv. MSc. C.S.) and Dr.-Ing. (PhD EE) from the University of Hamburg, Germany, and the Federal Armed Forces University, Hamburg, in 1980 and 1984, respectively. In 1996, he received a Graduate Diploma in Management (Technology Management) from the Alfred Deakin University, Geelong. Michael has joined DSTO in 1988 and has since worked in many areas of Image Analysis and Electro-Optical Systems analysis. His research interest include hyperspectral imaging, passive electro-optical systems performance modelling and environmental modelling. Before joining DSTO he spent three years at The Flinders University of South Australia developing the hard- and software for a NOAA HRPT Satellite receiver, and lecturing on topics in the areas of Data Analysis and Remote Sensing.

This page intentionally left blank

Contents

This page intentionally left blank

1. Introduction

1.1 Aim

Many advanced image processing algorithms used for automatic detection/recognition of objects in natural terrain, depend on the spatial statistics of the background, [3]. Knowledge of the background statistics is required for the design of suitable background clutter suppression and target extraction filters, [4]. This information can also be used for computer generation of realistic stochastic models for system performance analysis and generation of large numbers of random backgrounds for Monte-Carlo testing, [1]-[2].

To aid in this analysis, visual and infra-red image data in the 0.4μm to 0.8μm (visible), 3μm to 5μm (MWIR) and 8μm to 12μm (LWIR) bands were collected during a series of trials in both Southern and Northern Australia. The visual trial was conducted in July 1993, followed by four trials using infra-red bands in December 1995, February 1996, July 1997 and August 1998. The first two of these trials were conducted by the Wide Area Surveillance Systems Division (WASSD), now Surveillance Systems Division (SSD) and the other three by the Weapons Systems Division (WSD).

A total of eight reports, [1]-[2] and [4]-[8], have been written focussing on different parts of this analysis, each one using only a small subset of the data which has been collected. This report aims to fill in the gaps, by analysing an entire data set from the 1997 trial and rigorously test the main findings of papers [1]-[2] and [5]-[8], The other two reports focus on specific application of the results and will not be considered here.

1.2 Trials Background

The visual trial in 1993 and the MWIR trial in 1995 were conducted by the Image Exploitation group in WASSD. Analyses of the data from these trials led to papers [1], [5] and [6]. This work was then continued by both the Electro-Optical Seekers and Missile Simulation groups in WSD. A further three trials were conducted in the MWIR and LWIR in 1996, 1997 and 1998, which led to a further two papers, [7]-[8]. More recently, the work in [1] has been extended and papers [2]-[4] have been written.

In the WSD trials, a pair of Agema 900 imaging radiometers were used to capture the imagery in both the MWIR and the LWIR bands. The imagers were mounted inside a RAAF Dakota Aircraft, pointing sideways out of the parachute door. The imagers' lines of sights (LOS) were aligned, but not 'pixel registered'[1], due to different aberrations in their optical systems. During data collection, the aircraft travelled at a speed of approximately 120 knots.

1. If the imagers were 'pixel registered', then every pixel recorded by the LWIR system has exactly one corresponding pixel in the same row and column recorded by the MWIR and vice versa.

The purpose of the initial WSD trial in February 1996 was to collect data at various sensor look-down angles between 10^0 and 60^0. It turned out that the range of depression angles between 25^0 and 50^0 could not be used, as the imagers' field of views (FOV) were affected by one of the aircraft engine's exhaust gasses. Second, data collection at shallow look down angles smaller then 15^0 resulted in unusable images due to high atmospheric attenuation. Data collection during the 1996 wet season trial was therefore limited to sensor look-down angles of 60^0.

As the images recorded in the 1996 trials were generally of low contrast and very noisy, due to high atmospheric absorption and low temperature contrast due to cloud cover, the trial was repeated in July 1997 to collect dry season background data of the same areas overflown in February 1996. The image data collected in the dry season proved to be of far better quality due to lower atmospheric absorption and higher temperature contrast caused by high solar loading. The third trial in August 1998 collected data at shallow sensor depression angles around 15^0. In addition, any incomplete data from previous data sets were collected. The exact locations of the trials are given in the classified appendix.

The geographical area over which image data was collected, was selected from a vegetation map of the Northern Territory (NT) [see classified appendix]. This approach was used to ensure that the vegetation types most commonly found in the NT were covered.

1.3 Imager Details

The Agema 900 uses a pair of scanned cooled detectors made of Indium-Antimonide (InSb) for the MWIR and Cadmium-Mercury-Telluride (CMT) for the LWIR. Image frames are collected at a rate of 2Hz with a FOV of 2.5^0 vertical by 5^0 horizontal.

As the system's modulation transfer function affects the horizontal spatial resolution, each frame was recorded digitally as a 136x272 pixel image to maintain the correct aspect ratio. This gave a collection rate with approximately 50% overlap between one image and the next and modified the frame rate to approximately 1Hz.

The radiance distribution projected onto the imaging plane of the sensor is related to the radiance distribution from the terrain (self-emitted plus reflected solar) by convolution with the optics point-spread function. For the purpose of the analysis contained within this report, the effect of this convolution is insignificant, and has been neglected.

Each pixel has a 12-bit dynamic range before the AGEMA software linearises the response on the detector. A non-linear mapping from the integer range 0-4095 (12 bit) to 0-8191 (13-bit) causes a large number of empty bins in the ensemble histogram. These empty bins are later removed by a median filter of length five. Although not mathematically exact, the effect on the intensity distribution is negligible. After linearisation, the measured pixel intensities are taken to be directly related to the intensity of the radiation emanating from the scene, including atmospheric propagation effects. No attempt was made to account for atmosphetic attenuation and path radiance as it does not significantly affect the shape of either the histogram or the

auto-covariance function.

1.4 Document Overview

Most current generation image processing algorithms implemented in electro-optic surveillance systems use only first and second order statistics. Therefore, the analysis of the data in this report has been limited to the first and second order statistics of the radiance intensity distribution.

Previous results indicate that the radiance intensity distributions of the natural terrain backgrounds from the WSD trials[1] are nearly always wide-sense stationary but not necessarily Gaussian, [7]-[8]. Therefore, the analysis in this report starts by assuming the ensemble images are wide-sense stationary. The ensemble histogram is then formed and the hypothesis that the distribution is Gaussian is tested. The hypothesis threshold is tested by the Root Mean Square (RMS) error and a Chi-squared test.

The auto-covariance estimate is split into horizontal and vertical slices. A power-law model is applied to the slices and a threshold test based on the Root Mean Square (RMS) error is used to test the model. A full auto-covariance calculation of a single sample image is then used to create a stochastic simulation. For images with non-Gaussian statistics, a point-wise non-linear transformation is applied.

The first part of this report explains the background to this work and a detailed description of the different analysis techniques. The second part is a listing of the results and comparisons between MWIR and LWIR histograms, auto-covariance slices and stochastic simulations for each different vegetation class.

2. Analysis Techniques

2.1 Forming an Ensemble

Given the imagers' FOVs (2.5^0 vertical x 5^0 horizontal), the number of pixels (136 vertically x 272 horizontally) and a known look-down angle and height, the area covered by a single pixel on the ground can be calculated for each run. The pixel size strictly applies to pixels closest to the image centre only. For pixels on the top and bottom rows, there is a variation of approximately ±4% that was not corrected for.

In this analysis, each recorded run was parsed and images of the predominate vegetation class were extracted to form an ensemble. Runs with the same predominate vegetation class and pixel size, were combined to form a larger ensemble. This approach lets each vegetation class be independent.

1. Wide-sense stationarity depends on many things, such as sensor orientation and the field of view. These conditions were met for the WSD trial.

2.2 Random Field Analysis

In the following, each image in an ensemble is treated as a truncated segment of a different realisation of a two-dimensional discrete-space random field. With this assumption,

$$x^i(m,n) \quad \text{with } m = 1,2,\ldots,136;\ n = 1,2,\ldots,272 \text{ and } i = 1,2,\ldots,L \tag{1}$$

where L is the number of images in the ensemble, represents the pixel at (m,n) for the i-th image.

This approach is different from the approach used by Yaglom [9], who assumes in his analysis that every image in the ensemble is a single realisation of an ergodic random field. Although, the ergodic assumption is intuitively appealing as the sensors record different patches of the same class of terrain, difficulties will arise later if the assumption does not hold. The approach used for this analysis does not rely on this assumption, therefore the results will remain valid regardless of whether the underlying process is ergodic.

Two different approaches can also be used to undertake the correlation analysis on the image ensemble. First, correlation analysis can be carried out after subtracting from every individual image in the ensemble its own mean, [10], and second the ensemble mean can be subtracted from the individual images, [2] and [6]. The first approach makes the inherent assumption that the auto-covariance estimates decay to insignificantly small values within the spatial extent of one image frame. As this requirement cannot be guaranteed for the type of imagery analysed here, the second approach is being taken in this study. If the auto-covariance estimate indeed drops to an insignificant level within the spatial extent of one image frame, then both approaches will give identical results. If, on the other hand, the correlation structures in the image extend beyond one image frame, the approach used here will give a better approximation of the auto-covariance estimate. As the spatial extent of the ensembles' correlation was not known at the beginning of this study, the second approach is used.

2.3 The Gaussian Hypothesis

2.3.1 Background

The analysis of the first and second order statistics of the image ensembles is based on the assumption that the underlying random processes are stationary in the wide-sense. Mathematically, the mean calculated over an entire ensemble of infinitely many realisations of the random field,

$$\mu = E[x(m,n)], \tag{2}$$

and its auto-covariance at lag (k,l),

$$C(k,l) = E[(x(m,n) - \mu)(x(m+k,n+l) - \mu)], \tag{3}$$

are independent of position *(m,n)*.

In this report, the image ensembles were not tested for wide-sense stationarity due to the findings in [7]-[8]. In addition, if the random processes were Gaussian it would imply strict-sense stationarity. This condition is tested rigorously in this report by using an RMS comparison and a Chi-squared test.

2.3.2 Histogram

To test the Gaussian hypothesis, an ensemble histogram is calculated and overlayed with a Gaussian plot as shown in Figure 1. The ensemble histogram is obtained by grouping all of the pixels from each of the images in the ensemble, and then counting the fraction of the pixels that have grey-level 0,1,2,...,8191.

The Gaussian model is based on a single-variate distribution with the mean ($\tilde{\mu}$) and variance ($\tilde{\sigma}^2$), which are determined by minimising the RMS between the Gaussian model and the ensemble histogram. The Gaussian model is given by

$$h_2(x) = \frac{1}{\sqrt{2\pi\tilde{\sigma}^2}} \exp\left[\frac{-(x-\tilde{\mu})^2}{2\tilde{\sigma}^2}\right]. \tag{4}$$

The RMS error can then be calculated by the following:

$$RMS = \sqrt{\frac{1}{8192}\sum_{x=0}^{8191}(h_2(x) - h_1(x))^2}\ , \tag{5}$$

where $h_1(x)$ is the ensemble histogram and $h_2(x)$ is the Gaussian model at position x. Since both $h_1(x)$ and $h_2(x)$ are normalised, the RMS value is expressed as a percentage.

The Chi-squared test needs to be constructed with bins of at least five samples (Cochran's Rule, [11]). The ensemble histogram is hence trimmed to remove any points smaller then five and the result is a new histogram $\tilde{h}_1$ with its bins now labelled m (m = 1,...,M). The trimmed points are not used in the comparison.

The test statistic is then computed as:

$$\tau = \sum_{m=1}^{M} \frac{(\tilde{h}_1(m) - h_2(m))}{h_2(m)} \tag{6}$$

with corresponding P-value: $P(\chi^2_{M-1-2} > \tau)$. The degrees of freedom (DOF) is *M-1-2*, as two parameters were estimated in the Gaussian model.

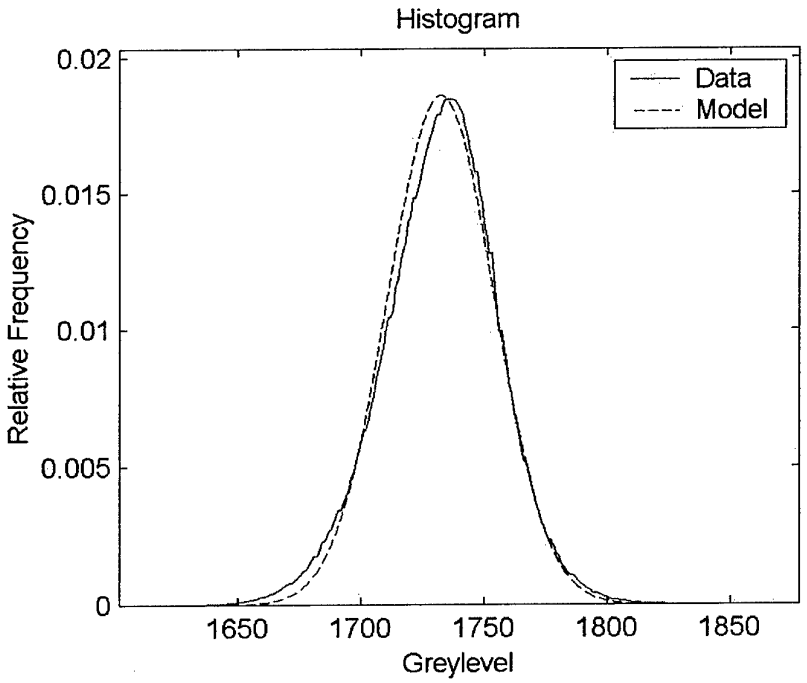

Figure 1 – Histogram with Gaussian overlay

2.3.3 Determining Threshold

The hypothesis threshold for whether the ensemble histogram is Gaussian or not is determined by the RMS value and the Chi-squared value. The limits imposed were less than 10% error for the RMS and a Chi-squared value greater than 5%.

The results of this test were also used to determine if the image needed to be transformed when constructing a stochastic simulation.

2.4 First and Second Order Statistics

The mean and auto-covariance of a wide-sense stationary field can theoretically be obtained using (2) and (3). However, since they require an infinite number of realisations of the random processes, these equations must be modified to reflect the fact that the sample size is finite.

Given that the underlying random processes are wide-sense stationary and that the individual images are statistically independent, the best possible estimate of the mean of the random process is given by

$$\hat{\mu} = \frac{1}{M * N * L} \sum_{i=1}^{L} \sum_{m=1}^{M} \sum_{n=1}^{N} x^i(m,n), \tag{7}$$

with variance

$$\sigma_{\hat{\mu}}^2 = E[(\hat{\mu}-\mu)^2] \approx \frac{1}{L*(L-1)}\sum_{i=1}^{L}(\hat{\mu}^i-\hat{\mu})^2\,, \tag{8}$$

where $\hat{\mu}^i$ is the mean of the *i*-th image.

This estimate of the mean approaches the true mean, μ, of the random field as the size of the ensemble approaches infinity.

An estimate of the auto-covariance function is obtained from the finite sample size in a similar way

$$\hat{C}(k,l) = \frac{1}{(M-k)*(N-l)*L}\sum_{i=1}^{L}\sum_{m=1}^{M-k}\sum_{n=1}^{N-l}(x^i(m,n)-\hat{\mu})(x^i(m+k,n+l)-\hat{\mu})\,, \tag{9}$$

with variance

$$\sigma_{\hat{C}}^2 = E[(\hat{C}(k,l)-C(k,l))^2] \approx \frac{1}{L*(L-1)}\sum_{i=1}^{L}(\hat{C}^i(k,l)-\hat{C}(k,l))^2\,, \tag{10}$$

where $\hat{C}^i(k,l)$ is the auto-covariance of the *i*-th image.

Again as the sample size increases to infinity, this estimate approaches the true auto-covariance function *C(k,l)*.

As the estimates $\hat{C}(k,l)$ and $\hat{\mu}$ are obtained from a large amount of independent images, it follows from the Central Limit Theorem, [12] that both can be taken to be Gaussian random variables with mean μ and auto-covariance *C(k,l)*, respectively. Figure 2 is an example of the auto-correlation function, plotted in three dimensions.

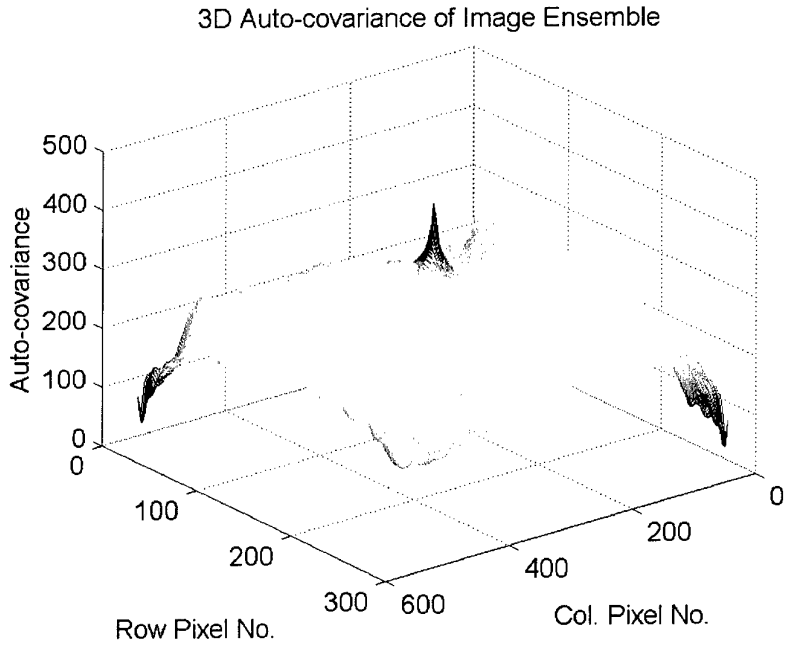

Figure 2 – 3D Auto-covariance plot of an Image Ensemble

As the lag increases away from the central peak, there are increasing fluctuations. These fluctuations represent increasing statistical variation and is associated with the fact that fewer data samples are available at larger lags. To simplify the analysis, the auto-covariance is calculated for each horizontal and vertical lag. They are then averaged to give horizontal and vertical slices. Figure 3 demonstrates this process with one standard deviation error bars also shown.

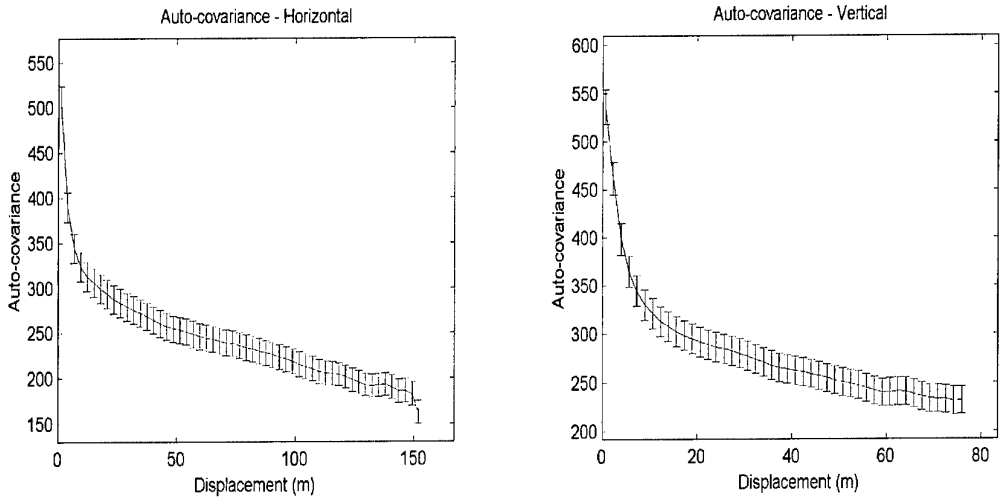

Figure 3 – Auto-covariance for Horizontal and Vertical slices

2.4.1 Auto-covariance Models

In previously papers, [5]-[7],[10] attempts were made to model the auto-covariance functions both as an exponential and with a power-law model.

The exponential function was suggested by N. Ben-Yosef *et al.* [10] and has an equation of the form

$$C(k,l) = A * \exp(-\gamma\sqrt{(\Delta_x k)^2 + (\Delta_y l)^2}), \tag{11}$$

where Δ_x and Δ_y are the horizontal and vertical dimensions of a pixel and $A > 0$ and $\gamma > 0$ are constants.

It was found in [5]-[6] that this model did not match the auto-covariance estimates measured. Instead, a power-law model was tested by [5] and [7] for an isotropic random field, which exhibits a power-law fall-off

$$C(k,l) = \frac{a}{(b^2 + k^2 + l^2)^{\nu}}, \tag{12}$$

where $a > 0, b > 0$ and $\nu > 0$ are constants.

It was found in [5] and [7], that the power-law rather then the exponential model provided a better match for the auto-covariance estimates measured. Consequently, this is the model that we have decided to use. The method for matching the power-law model to the data was simplified by reducing the number of parameters by one. The horizontal and vertical slices were used to test the simplified model, which now reduces to

$$C(k) = \frac{a}{M(b^2 + k^2)^{\nu}} \text{ and } C(l) = \frac{a}{N(b^2 + l^2)^{\nu}}. \tag{13}$$

The best fit parameters were obtained by a numeric maximum likelihood estimation technique on the correlation data over about half of the available range of lags, [13]. They were then adjusted to minimize the RMS between the auto-covariance estimate and the model. Figure 4 is an example of two power-law fits.

2.4.2 Determining Threshold

A basic threshold test was used for determing if the power law model fit the data. The RMS value is 3% and was chosen by trial and error.

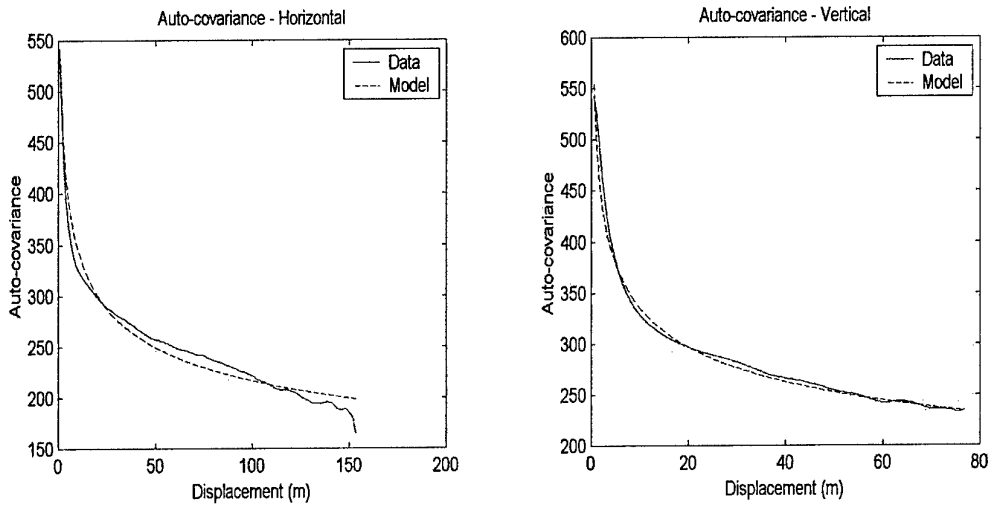

Figure 4 – Power-law model for Horizontal and Vertical Auto-covariance slices

2.5 Stochastic Simulation

2.5.1 Background

Stochastic image models play an important role in many areas of statistical image processing, [14]. Dietrich and Newsam, [1] investigated this and developed a technique for generating arbitrary stationary Gaussian random fields using the first and second order statistics of an existing image. This technique was used to generate synthetic images of the visual data collected from the 1993 trial and later in the 1995 MWIR trial, [6].

More recently, a non-linear transform was developed by Chapple *et al.* [2] to generate a non-Gaussian random field with a marginal probability density and correlation structure that agrees with that of actual IR background imagery. This technique was then used for target detection/recognition in [3]-[4].

2.5.2 Stochastic Image Simulation of Gaussian Random Fields

The simulation process begins by calculating the auto-covariance estimate for an ensemble image. It is then multiplied by a circular super-Gaussian taper to reduce artefacts associated with the variance in the estimate at large lags. This is then used as the correlation structure in the next part of the simulation. The circular super-Gaussian taper, which acts as a window to the auto-covariance estimate, is calculated by

$$w(k) = \exp\left[-\left(\frac{|k|}{P}\right)^4\right], \tag{14}$$

where k is the auto-correlation and $P > 0$ represents the radius of the taper.
In this analysis, a value of P was chosen to include most of the slowly falling correlation tail. The process then continues by computing the Fast Fourier Transform (FFT) of the auto-covariance estimate, setting any negative values to zero, performing an element-wise square root, and then multiplying the result by a white noise random function with Gaussian statistics. The FFT of the resulting matrix is then separated into real and imaginary parts, both of which are independent realisations of the stationary zero-mean Gaussian random field with the required correlation structure. The simulation is completed by adding the estimate of the mean of the random field. Figure 5 is a visual representation of this process.

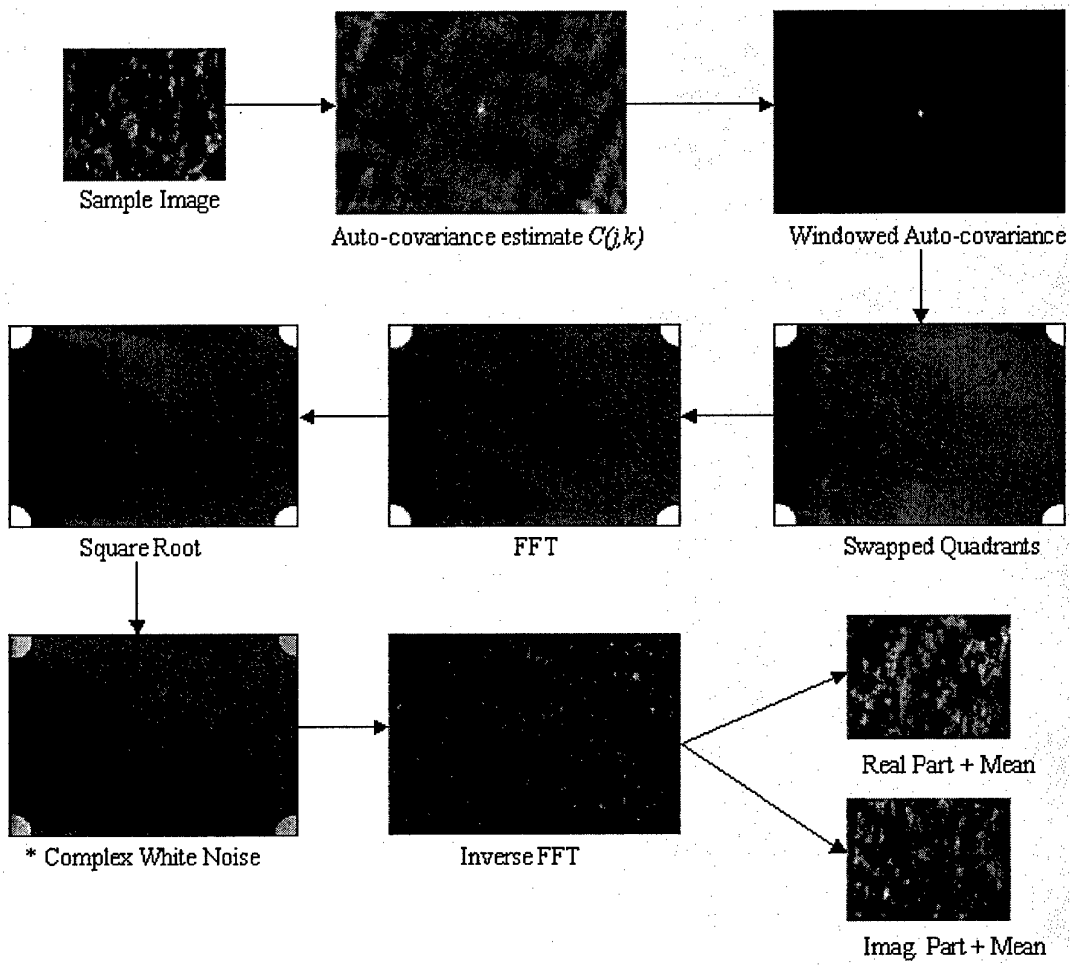

Figure 5 – Gaussian Simulation Process

There are two sources of error in this simulation approach. The first is due to the tapering of the correlation data and is unavoidable because of the fact that the variance in an auto-covariance estimate will always increase at large lags as a result of the small number of data samples. The second is due to setting to zero the negative values in the FFT of the tapered auto-covariance estimate. Bertilone *et al.* [6] has shown the latter

error has a magnitude of 10^{-6}, which is insignificant in this simulation. Figure 6 is a comparison between a sample image and a simulated one.

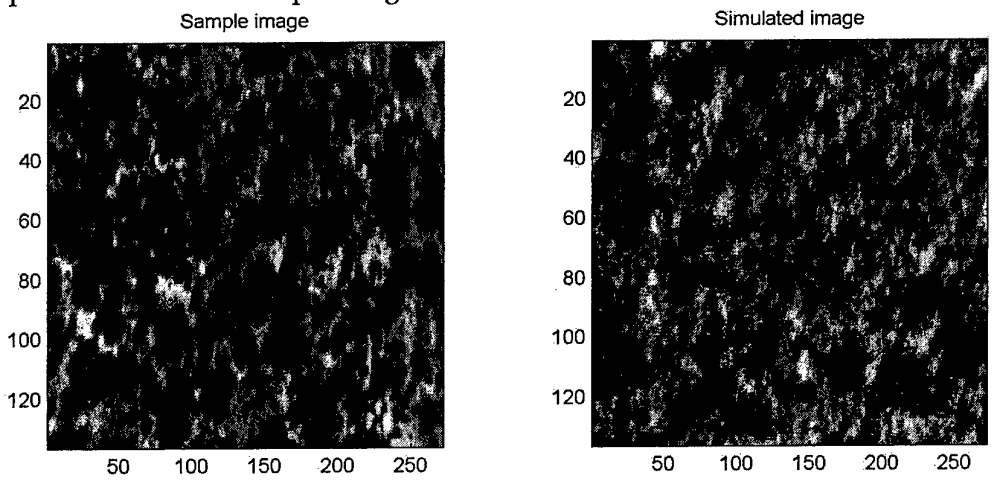

Figure 6 – Comparison of Sample and Simulated Images

2.5.3 Non-Linear Transform

One of the conditions for Dietrich and Newsam's method to work is for the ensemble image to have Gaussian statistics. If the simulation is performed on a sample image without this distribution, many features are visually incorrect and the histogram of the new image is very different from the sample image. Chapple *et al.* [2] has developed a technique whereby the images are transformed by a point-wise non-linear transform to generate an ensemble with a Gaussian histogram. After the image has been simulated, an inverse non-linear transform is used to restore the original histogram. Figure 7 shows a comparison between a synthesized image with and without transformation. It is clear in Figure 7b that without the transform, the contrast is lacking and much of the detail is not represented correctly.

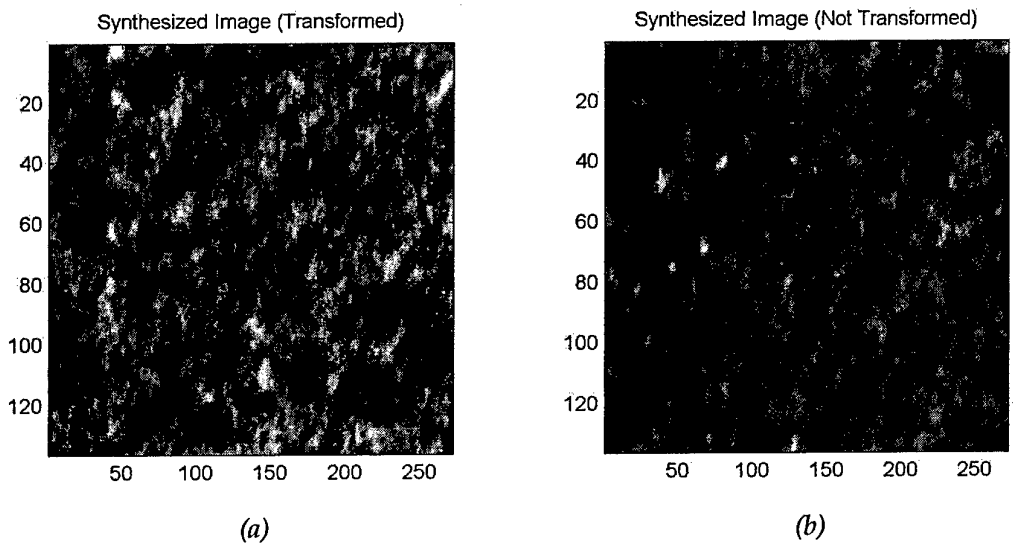

Figure 7 – Comparison of Simulated Image (Transformed vs. Not Transformed)

The transformation function $F(x)$ is used to convert values $X(m,n)$ to values $Y(m,n) = F(X(m,n))$ with a Gaussian distribution with zero mean and a variance of one. For a probability density $P_X(x)$, the required transformation is

$$F(x) = \sqrt{2} erf^{-1}(2\int_0^x P_X(x')dx' - 1). \tag{15}$$

A new image is then created with this distribution and is substituted for the ensemble image. To recreate the final images, the inverse non-linear transform, $F^{-1}(x)$ is applied to the simulated images. Figure 8 shows typical plots of the non-linear transform and the inverse non-linear transform.

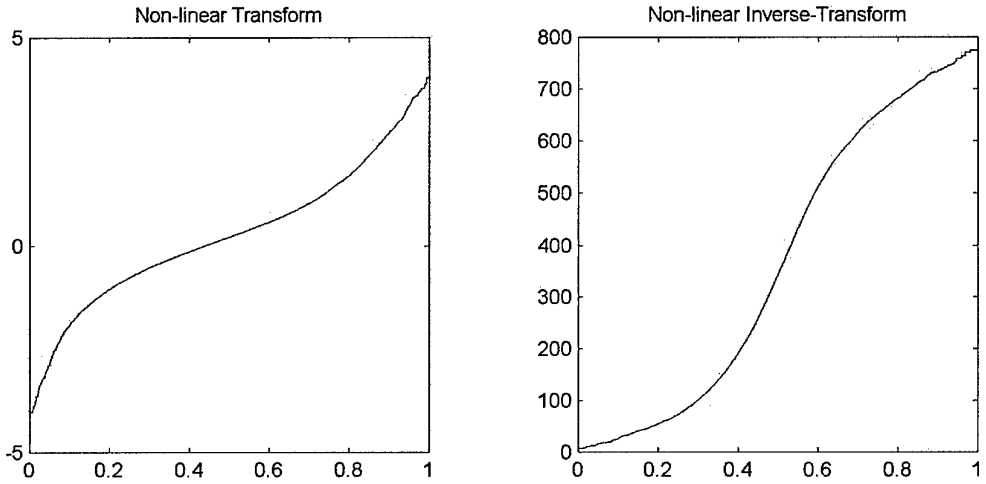

Figure 8 – Transform and Inverse Transform

For a sample ensemble image with a non-Gaussian distribution, Figure 9 shows the histogram after using the above transform to create a sample image.

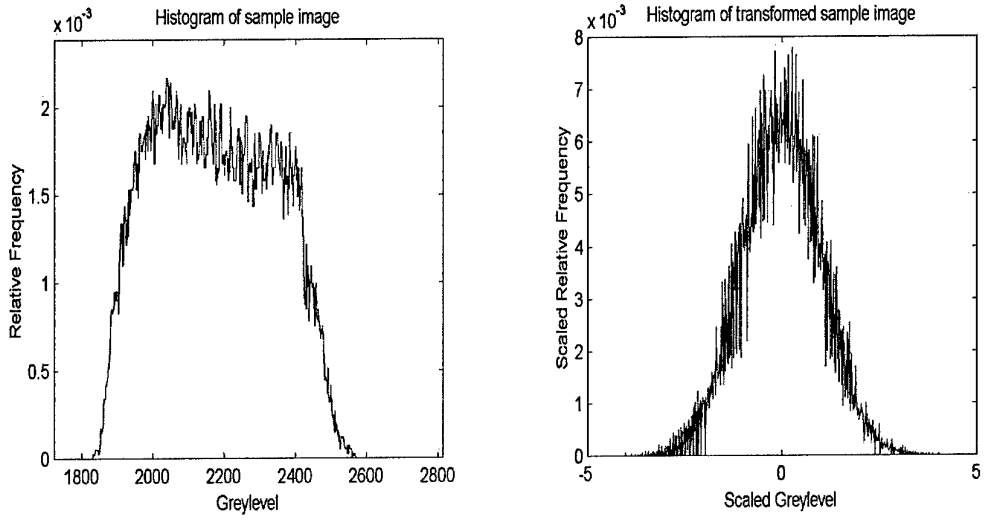

(a) *(b)*

Figure 9 – Original and Transformed Histograms of a Sample Image

After the transformation, Figure 9b now shows a Gaussian distribution with zero mean and a variance of one. After creating the simulated images, Figure 10 shows a comparison between the histogram of the original simulated image and one after the inverse transform has been applied.

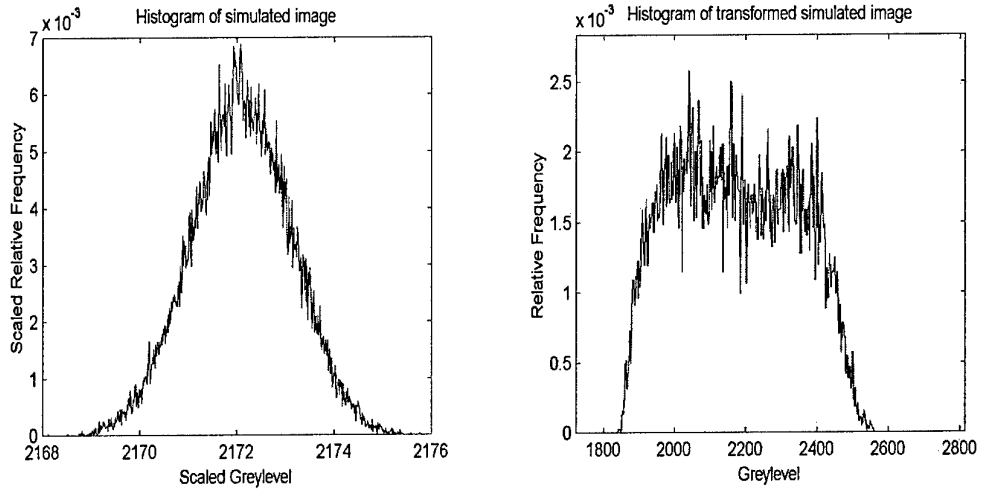

(a) (b)

Figure 10 – Original and Transformed Histograms of a Simulated Image

Its clear that the original distribution has been restored with very little difference between Figure 9a and Figure 10b. To verify the second order statistics, Figure 11 is a comparison between the sample and simulated horizontal and vertical auto-covariance slices.

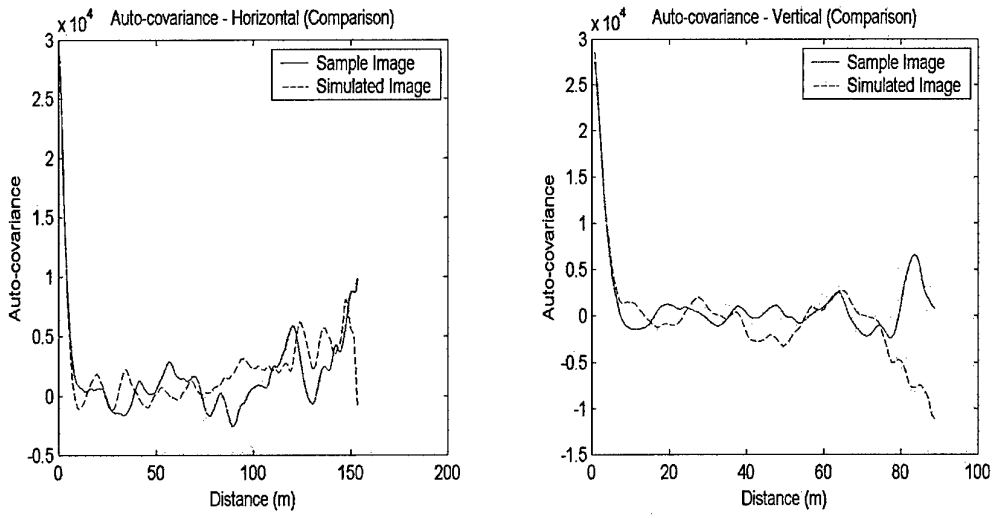

Figure 11 – Auto-covariance Slices of the Sample and Simulated Image

The peak at the start is well matched in both plots, but the remainder of the tail is subject to a statistical fluctuation associated with the small sample size and windowing the centre of the auto-covariance estimate.

3. 1997 Trial

3.1 Sequence Summary from AGEMA 900 IMAGER

During the 1997 trial, three groups of runs were taken on different days and at different times in the day. The predominate vegetation class has been determined and forms the basis of the analysis for each run (see section 2.1 for information on how the classes were chosen). Table 1 is a brief summary of each run. The key for the vegetation classes is in the classified appendix.

Table 1 – 1997 Sequence Summary

Flight Date and Conditions	Run Number	Altitude (feet)	Depression Angle (degrees)	Vegetation Classes in Run	Predominate Vegetation Class
FLIGHT DATE: 30-6-97, NIGHT	1	10K	60	9, 105, 11, 4, 48	4
	2	10K	60	48, 4, 105	4
	3	5K	60	9, 105, 11, 4,	9
	4	5K	60	54, 48, 4	54
	5	1.7K	60	11,4	11
	6	1.7K	15	48	48
	7	1.0K	tracking	N/A	N/A
	8	1.0K	tracking	N/A	N/A
FLIGHT DATE: 1-7-97, DAY	9	10K	60	105, 21, 11, 32, 4, 9	32
FLIGHT DATE: 3-7-97, DAY	10	10K	60	48, 11, 21, 105	11
	11	10K	60	21, 15, 51	21
	12	10K	60	13, 51, 15, 4, 21	15
	13	5K	60	9, 21, 11, 32	32
	14	5K	60	48, 11, 51	11
	15	5K	60	21, 15, 51	21
	16	5K	60	13, 51, 15, 4, 21	15
	17	10K	60	4, 106	106
	18	10K	60	53, 4, 106	53
	19	5K	60	4, 106	106
	20	5K	60	53, 4, 106	53
	21	10K	60	18, 106	106
	22	10K	60	106, 3, 47	3
	23	10K	60	3, 105	3
	24	5K	60	18, 106	106
	25	5K	60	106, 3, 47	3
	26	5K	60	3, 105	3

3.2 Explanation of Run Analysis

The layout of the following section is in four parts:

- The first is a general summary of the run and the ensemble.
- The second part is an analysis of the histogram for the LWIR and the MWIR.
- The third part is a comparison between the horizontal and vertical auto-covariance slices for the LWIR and MWIR.
- The final part is a comparison between sample and simulated images of the ensemble.

If the Gaussian threshold test is passed, both the transformed and non-transformed simulated images are compared. In addition to the threshold tests, a visual test is

added to each of the comparisons. The rating of this test is either 'yes', 'partial' or 'no' depending on the plots.

3.3 Runs 1-2

3.3.1 General Information

Flight Date: 30-6-97 NIGHT
Altitude: 10K ft
Depression Angle: 60 deg.
Vegetation Classes in Run: 9, 105, 11, 4, 48
Predominate Vegetation Class: 4

Ensemble Size is: 79
Number of Valid Images is: 79
Vertical Resolution is: 1.30m
Horizontal Resolution is: 1.13m

3.3.2 Histogram

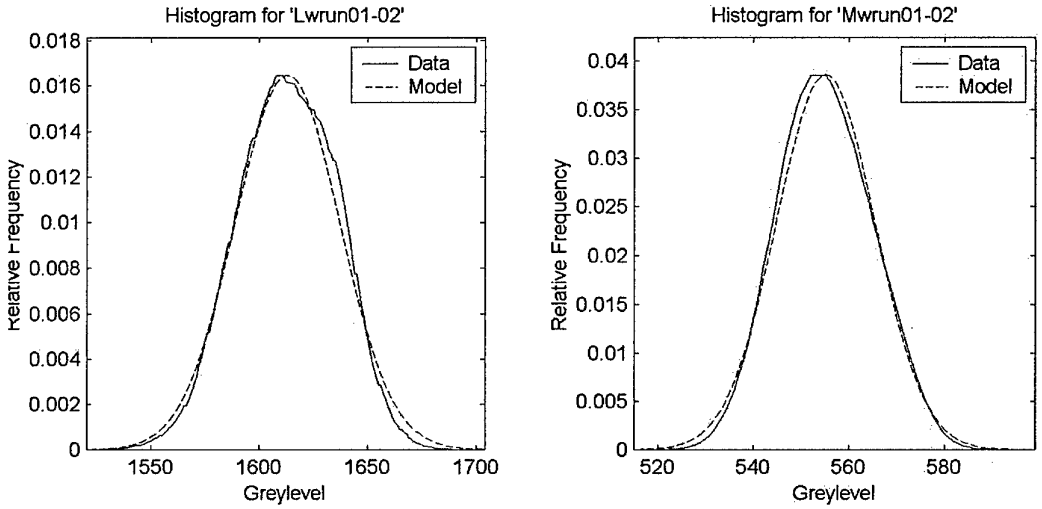

Figure 12 – Gaussian Fit – Histogram of Runs 01-02

Histogram Information for 'Lwrun01-02'

Normal Model Parameters:
    Mean is: 1612.89
    Variance is: 587.43
RMS error is: 5.32%
Chi2 P-value is: 100.00%
Model Accepted by Threshold: Yes
Model Accepted Visually: Yes

Histogram Information for 'Mwrun01-02'

Normal Model Parameters:
Mean is: 555.06
Variance is: 107.00
RMS error is: 10.17%
Chi2 P-value is: 100.00%
Model Accepted by Threshold: No
Model Accepted Visually: Yes

3.3.3 Auto-covariance – Horizontal

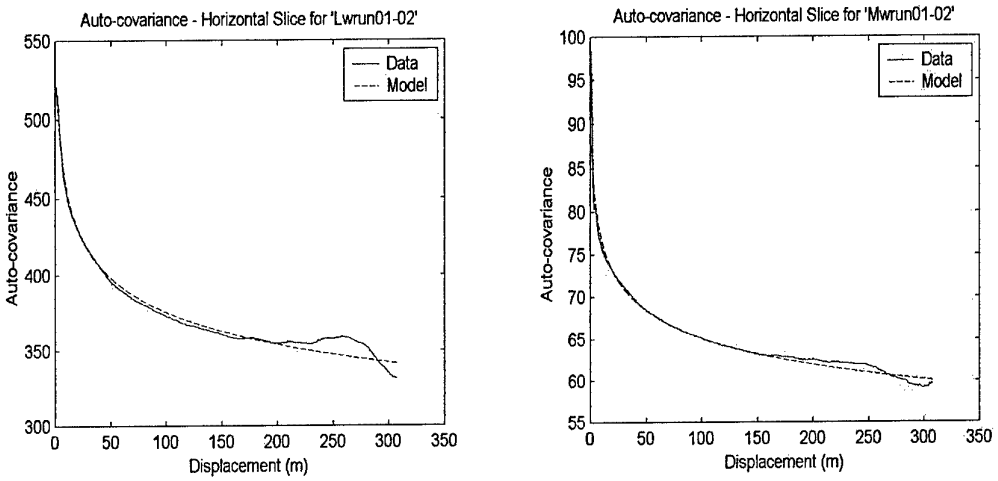

Figure 13 – Power Law Fit - Horizontal Slice of Runs 01-02

Auto-covariance - Horizontal for 'Lwrun01-02'

Mean Standard deviation between images is: 47.91
Power Law Model Parameters:
a_est is: 535.04
b_est is: 0.00
w_est is: 0.04
RMS error is: 1.30%
Model Accepted by Threshold: Yes
Model Accepted Visually: Yes

Auto-covariance - Horizontal for 'Mwrun01-02'

Mean Standard deviation between images is: 8.37
Power Law Model Parameters:
a_est is: 89.98
b_est is: 0.00
w_est is: 0.04
RMS error is: 0.91%

Model Accepted by Threshold: Yes
Model Accepted Visually: Yes

3.3.4 Auto-covariance – Vertical

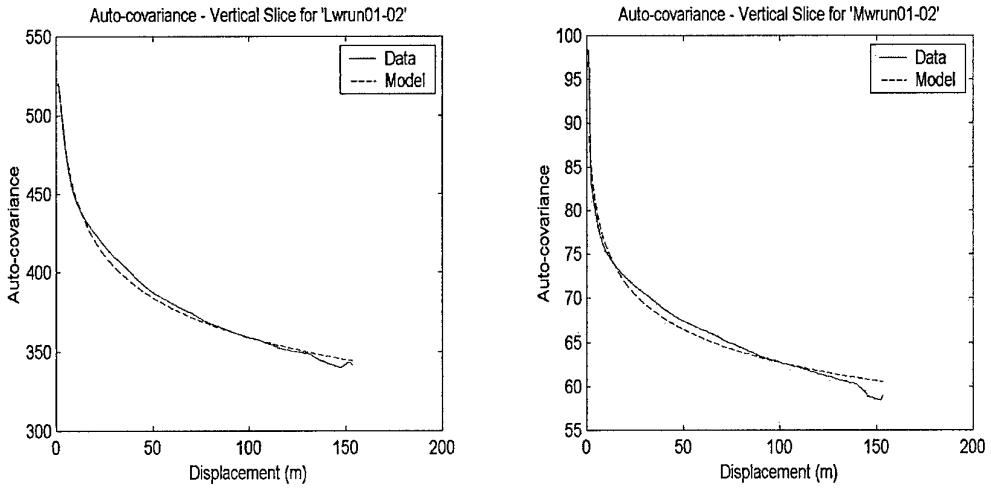

Figure 14 – Power Law Fit - Vertical Slice of Runs 01-02

Auto-covariance - Vertical for 'Lwrun01-02'

Mean Standard deviation between images is: 47.72
Power Law Model Parameters:
a_est is: 575.59
b_est is: 2.41
w_est is: 0.05
RMS error is: 0.69%
Model Accepted by Threshold: Yes
Model Accepted Visually: Yes

Auto-covariance - Vertical for 'Mwrun01-02'

Mean Standard deviation between images is: 8.29
Power Law Model Parameters:
a_est is: 94.15
b_est is: 0.00
w_est is: 0.04
RMS error is: 1.44%
Model Accepted by Threshold: Yes
Model Accepted Visually: Yes

3.3.5 Image Synthesis:

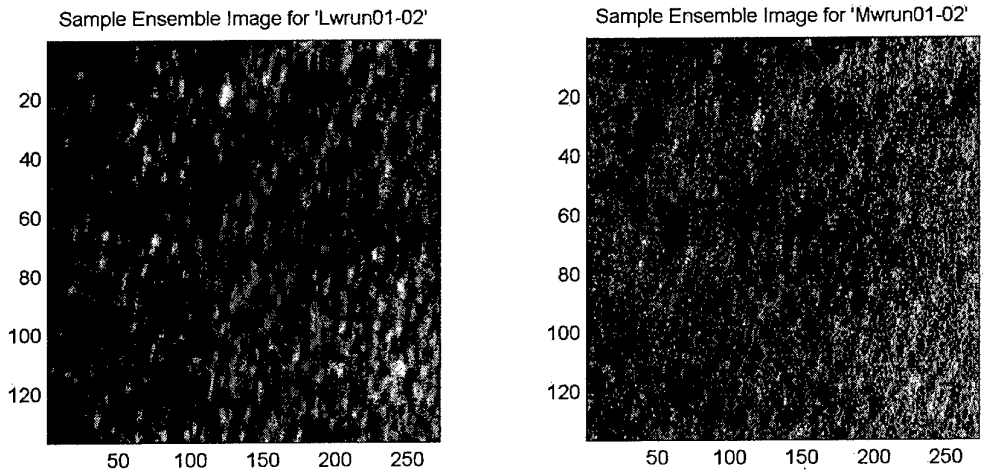

Figure 15 – Original Images from Runs 01-02

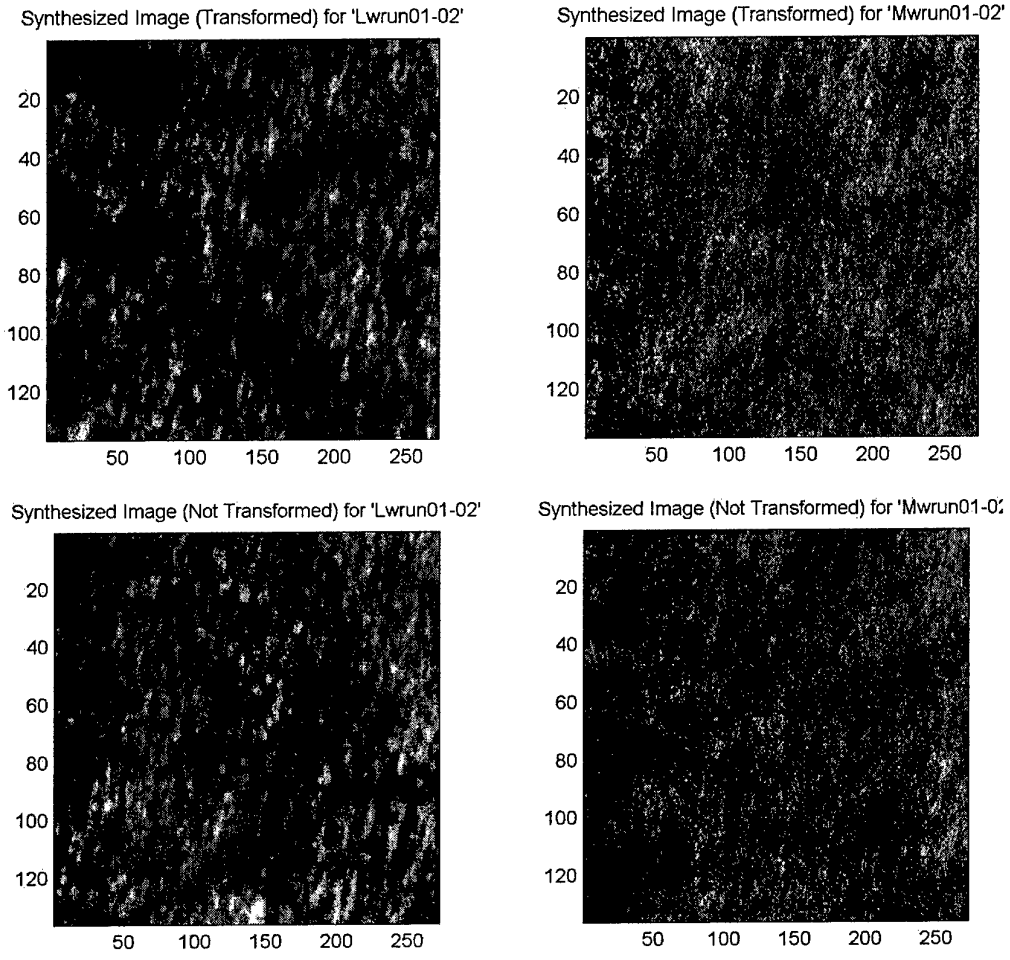

Figure 16 – Synthetic Images for Run 01-02

3.4 Run 3

3.4.1 General Information

Flight Date: 30-6-97 NIGHT
Altitude: 5K ft
Depression Angle: 60 deg.
Vegetation Classes in Run: 9, 105, 11, 4
Predominate Vegetation Class: 9

Ensemble Size is: 250
Number of Valid Images is: 68
Vertical Resolution is: 0.65m
Horizontal Resolution is: 0.56m

3.4.2 Histogram

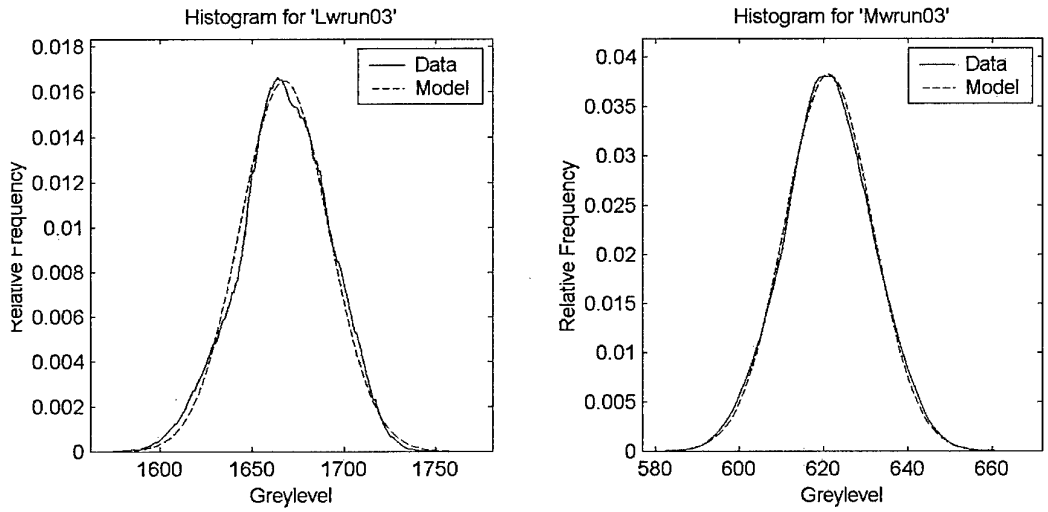

Figure 17 – Gaussian Fit – Histogram of Run 3

Histogram Information for 'Lwrun03'

Normal Model Parameters:
    Mean is: 1667.42
    Variance is: 585.37
RMS error is: 4.78%
Chi2 P-value is: 100.00%
Model Accepted by Threshold: Yes
Model Accepted Visually: Yes

Histogram Information for 'Mwrun03'

Normal Model Parameters:
Mean is: 621.15
Variance is: 109.00
RMS error is: 5.10%
Chi2 P-value is: 100.00%
Model Accepted by Threshold: Yes
Model Accepted Visually: Yes

3.4.3 Auto-covariance – Horizontal

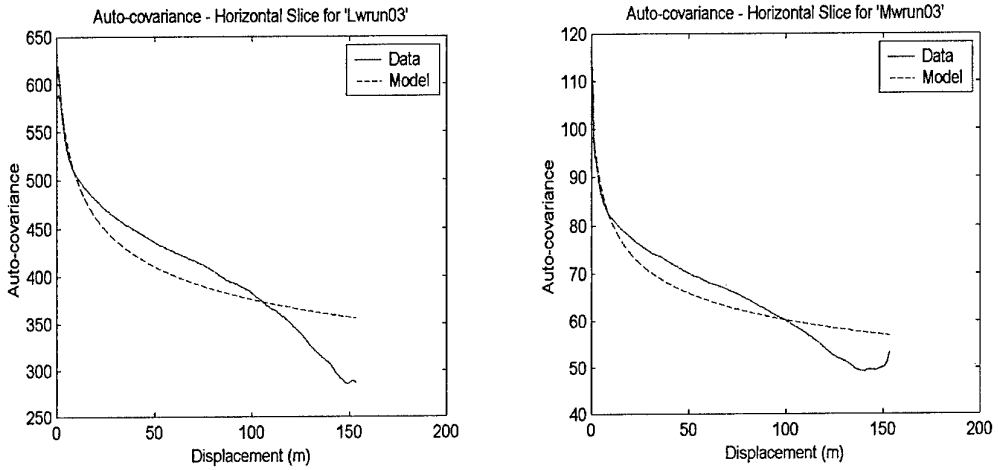

Figure 18 – Power Law Fit - Horizontal Slice of Run 3

Auto-covariance - Horizontal for 'Lwrun03'

Mean Standard deviation between images is: 59.79
Power Law Model Parameters:
a_est is: 654.11
b_est is: 1.48
w_est is: 0.06
RMS error is: 9.25%
Model Accepted by Threshold: No
Model Accepted Visually: No

Auto-covariance - Horizontal for 'Mwrun03'

Mean Standard deviation between images is: 9.80
Power Law Model Parameters:
a_est is: 112.67
b_est is: 0.80
w_est is: 0.07
RMS error is: 7.45%
Model Accepted by Threshold: No

Model Accepted Visually: No

3.4.4 Auto-covariance – Vertical

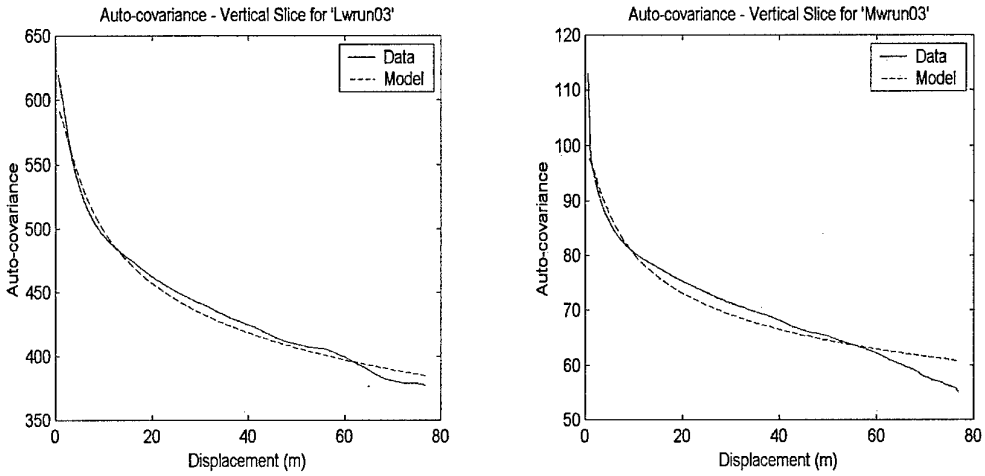

Figure 19 – Power Law Fit - Vertical Slice of Run 3

Auto-covariance - Vertical for 'Lwrun03'

Mean Standard deviation between images is: 62.34
Power Law Model Parameters:
a_est is: 672.35
b_est is: 2.29
w_est is: 0.06
RMS error is: 1.34%
Model Accepted by Threshold: Yes
Model Accepted Visually: Partially

Auto-covariance - Vertical for 'Mwrun03'

Mean Standard deviation between images is: 9.83
Power Law Model Parameters:
a_est is: 137.40
b_est is: 8.28
w_est is: 0.10
RMS error is: 2.95%
Model Accepted by Threshold: Yes
Model Accepted Visually: Partially

3.4.5 Image Synthesis:

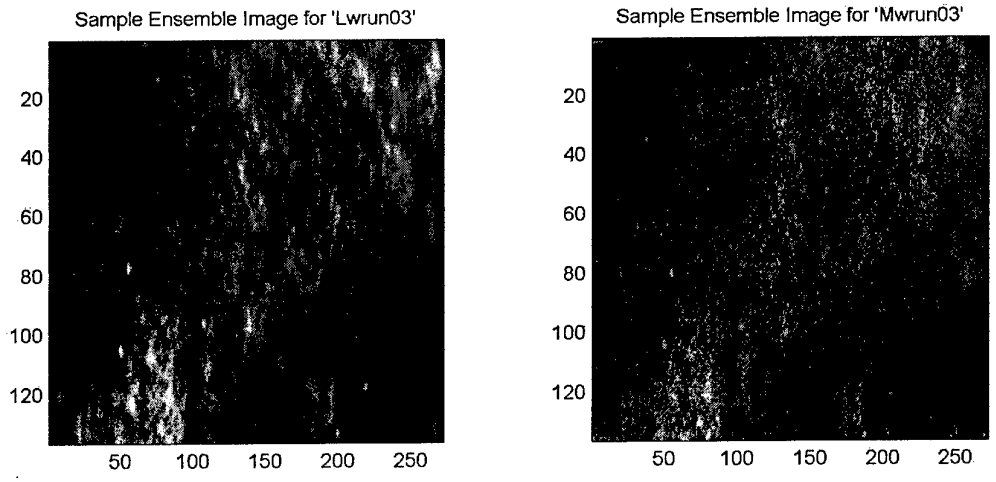

Figure 20 – Original Images from Run 3

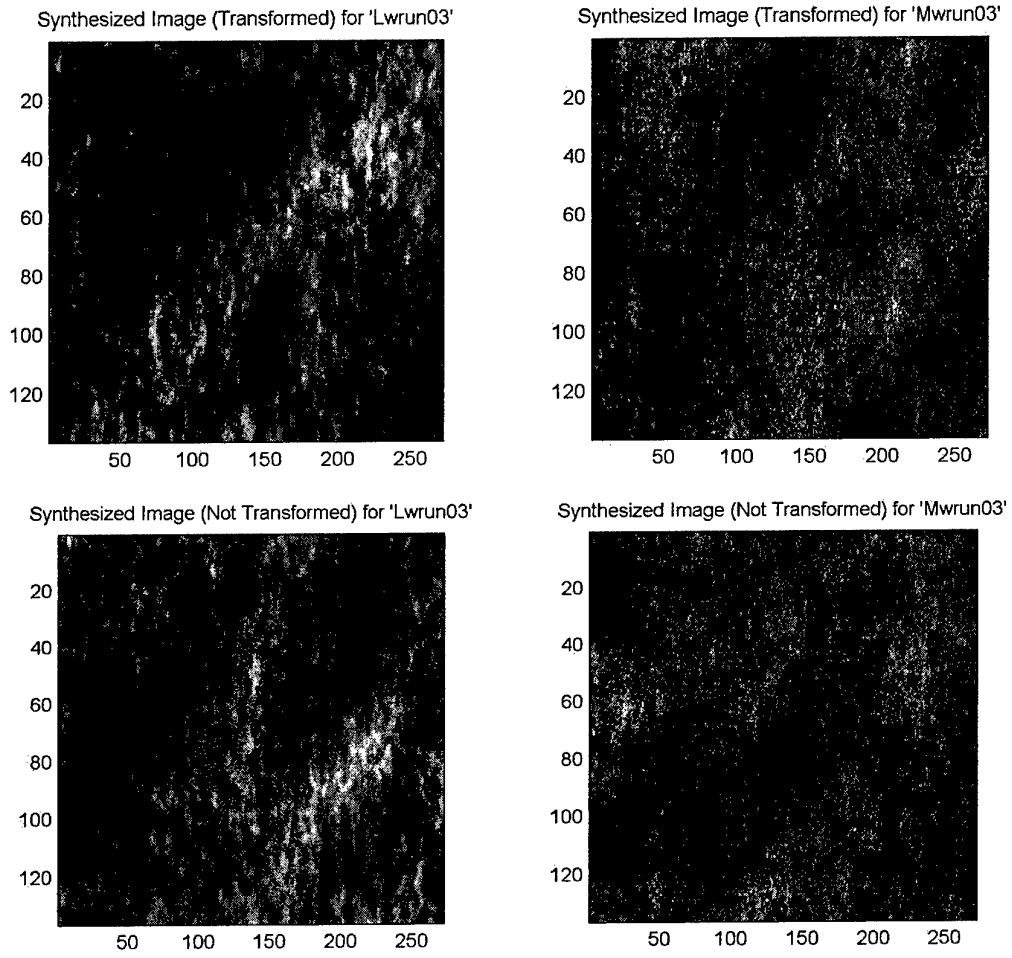

Figure 21 – Synthetic Images for Run 3

3.5 Run 4

3.5.1 General Information

Flight Date: 30-6-97 NIGHT
Altitude: 5K ft
Depression Angle: 60 deg.
Vegetation Classes in Run: 48, 4, 105
Predominate Vegetation Class: 54

Ensemble Size is: 251
Number of Valid Images is: 100
Vertical Resolution is: 0.65m
Horizontal Resolution is: 0.56m

3.5.2 Histogram

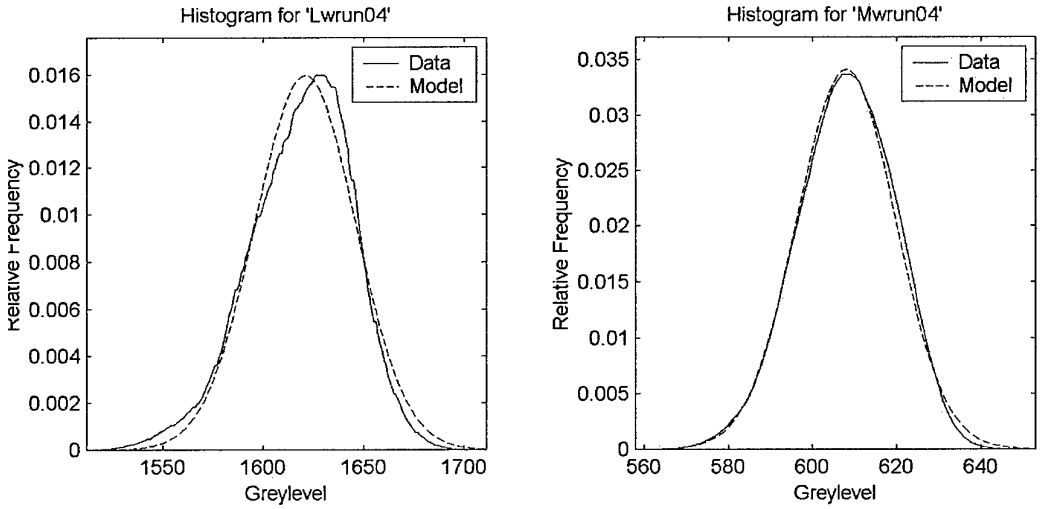

Figure 22 – Gaussian Fit – Histogram of Run 4

Histogram Information for 'Lwrun04'

Normal Model Parameters:
    Mean is: 1620.83
    Variance is: 624.96
RMS error is: 7.41%
Chi2 P-value is: 99.91%
Model Accepted by Threshold: Yes
Model Accepted Visually: Partially

Histogram Information for 'Mwrun04'

Normal Model Parameters:
Mean is: 607.98
Variance is: 137.03
RMS error is: 6.82%
Chi2 P-value is: 100.00%
Model Accepted by Threshold: Yes
Model Accepted Visually: Yes

3.5.3 Auto-covariance - Horizontal

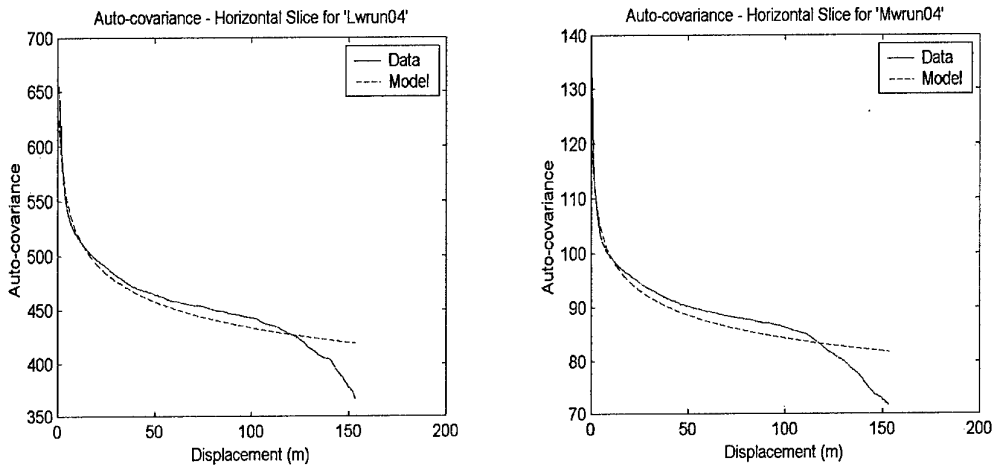

Figure 23 – Power Law Fit - Horizontal Slice of Run 4

Auto-covariance - Horizontal for 'Lwrun04'

Mean Standard deviation between images is: 63.36
Power Law Model Parameters:
a_est is: 622.52
b_est is: 0.21
w_est is: 0.04
RMS error is: 3.33%
Model Accepted by Threshold: No
Model Accepted Visually: Partially

Auto-covariance - Horizontal for 'Mwrun04'

Mean Standard deviation between images is: 11.56
Power Law Model Parameters:
a_est is: 236.97
b_est is: 30.12
w_est is: 0.12
RMS error is: 5.09%
Model Accepted by Threshold: No

Model Accepted Visually: Partially

3.5.4 Auto-covariance – Vertical

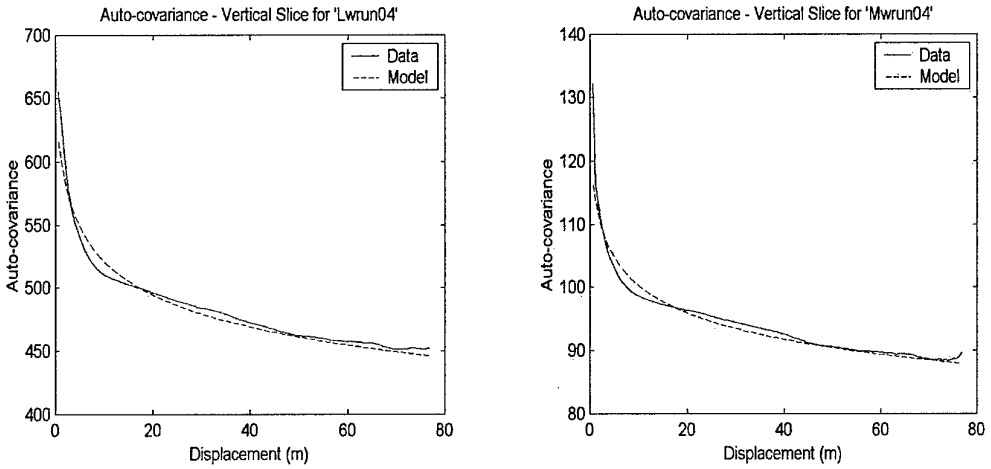

Figure 24 – Power Law Fit - Vertical Slice of Run 4

Auto-covariance - Vertical for 'Lwrun04'

Mean Standard deviation between images is: 62.57
Power Law Model Parameters:
a_est is: 613.29
b_est is: 0.00
w_est is: 0.04
RMS error is: 0.90%
Model Accepted by Threshold: Yes
Model Accepted Visually: Partially

Auto-covariance - Vertical for 'Mwrun04'

Mean Standard deviation between images is: 11.38
Power Law Model Parameters:
a_est is: 115.44
b_est is: 0.00
w_est is: 0.03
RMS error is: 1.10%
Model Accepted by Threshold: Yes
Model Accepted Visually: Partially

3.5.5 Image Synthesis:

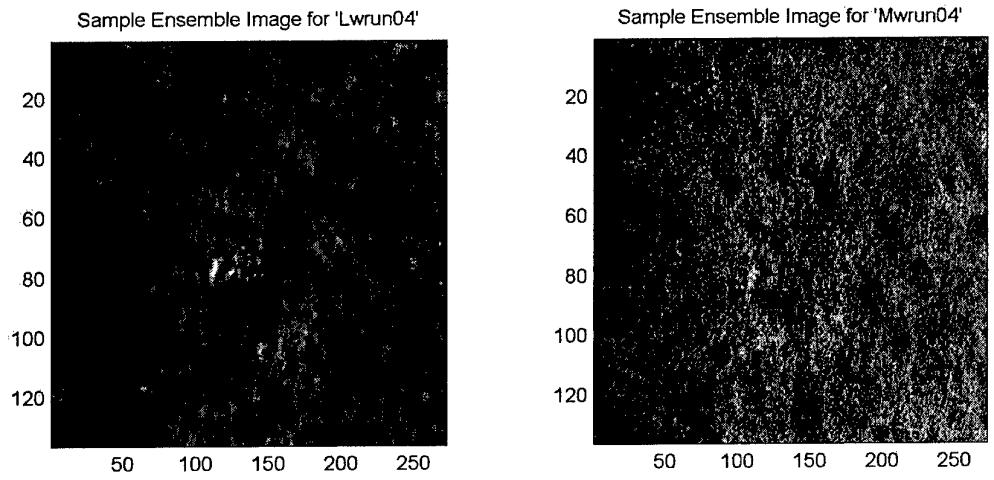

Figure 25 – Original Images from Run 4

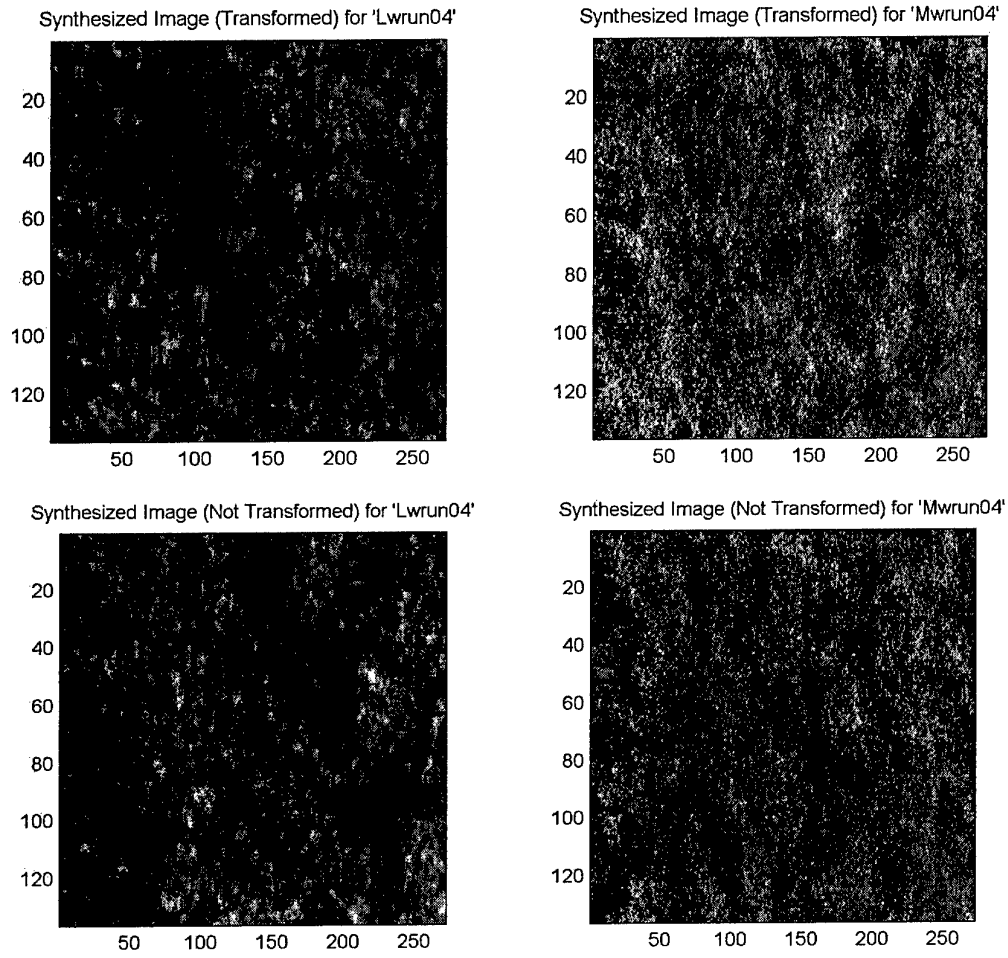

Figure 26 – Synthetic Images for Run 4

3.6 Run 5

3.6.1 General Information

Flight Date: 30-6-97 NIGHT
Altitude: 1.7K ft
Depression Angle: 60 deg.
Vegetation Classes in Run: 11,4
Predominate Vegetation Class: 54

Ensemble Size is: 244
Number of Valid Images is: 53
Vertical Resolution is: 0.22m
Horizontal Resolution is: 0.19m

3.6.2 Histogram

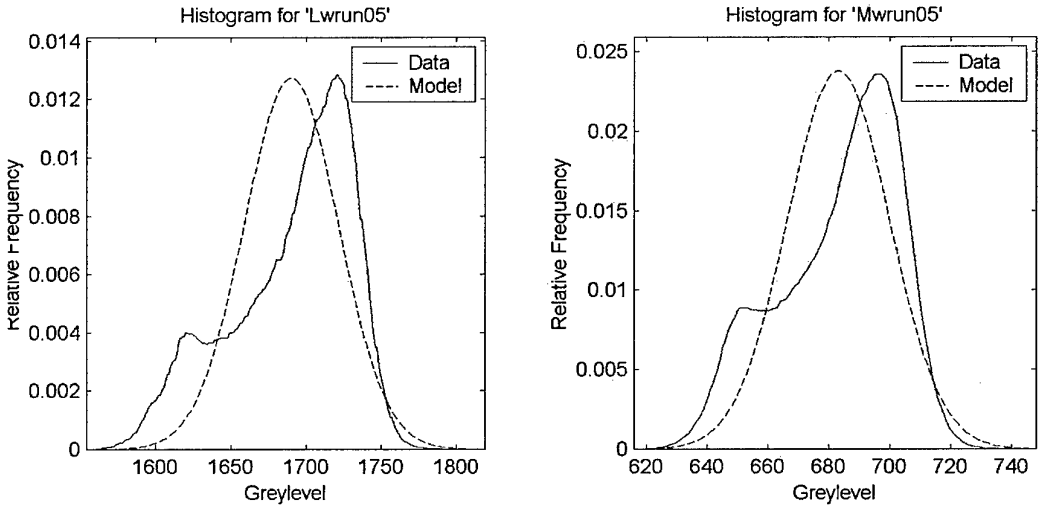

Figure 27 – Gaussian Fit – Histogram of Run 5

Histogram Information for 'Lwrun05'

Normal Model Parameters:
    Mean is: 1690.06
    Variance is: 984.18
RMS error is: 25.99%
Chi2 P-value is: 0.00%
Model Accepted by Threshold: No
Model Accepted Visually: No

Histogram Information for 'Mwrun05'

Normal Model Parameters:
Mean is: 683.10
Variance is: 281.89
RMS error is: 42.06%
Chi2 P-value is: 0.00%
Model Accepted by Threshold: No
Model Accepted Visually: No

3.6.3 Auto-covariance - Horizontal

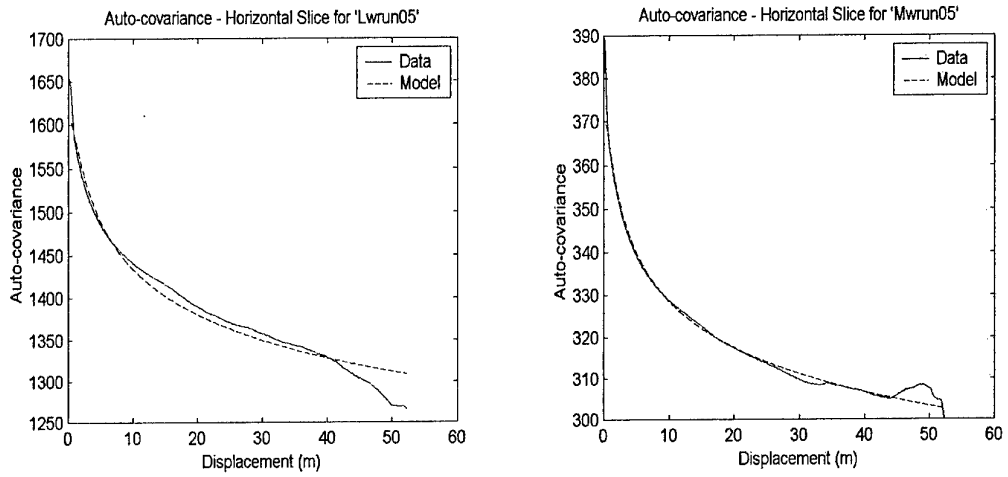

Figure 28 – Power Law Fit - Horizontal Slice of Run 5

Auto-covariance - Horizontal for 'Lwrun05'

Mean Standard deviation between images is: 247.20
Power Law Model Parameters:
a_est is: 1627.02
b_est is: 1.04
w_est is: 0.03
RMS error is: 1.13%
Model Accepted by Threshold: Yes
Model Accepted Visually: Partially

Auto-covariance - Horizontal for 'Mwrun05'

Mean Standard deviation between images is: 51.55
Power Law Model Parameters:
a_est is: 365.08
b_est is: 0.17
w_est is: 0.02
RMS error is: 0.44%
Model Accepted by Threshold: Yes

Model Accepted Visually: Yes

3.6.4 Auto-covariance – Vertical

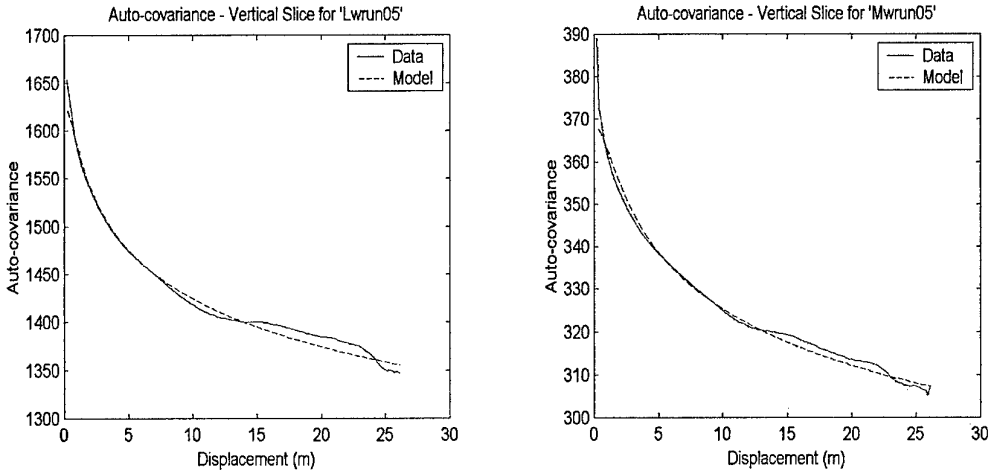

Figure 29 – Power Law Fit - Vertical Slice of Run 5

Auto-covariance - Vertical for 'Lwrun05'

Mean Standard deviation between images is: 252.79
Power Law Model Parameters:
a_est is: 1594.86
b_est is: 0.44
w_est is: 0.02
RMS error is: 0.44%
Model Accepted by Threshold: Yes
Model Accepted Visually: Yes

Auto-covariance - Vertical for 'Mwrun05'

Mean Standard deviation between images is: 53.01
Power Law Model Parameters:
a_est is: 367.37
b_est is: 0.28
w_est is: 0.03
RMS error is: 0.52%
Model Accepted by Threshold: Yes
Model Accepted Visually: Yes

3.6.5 Image Synthesis:

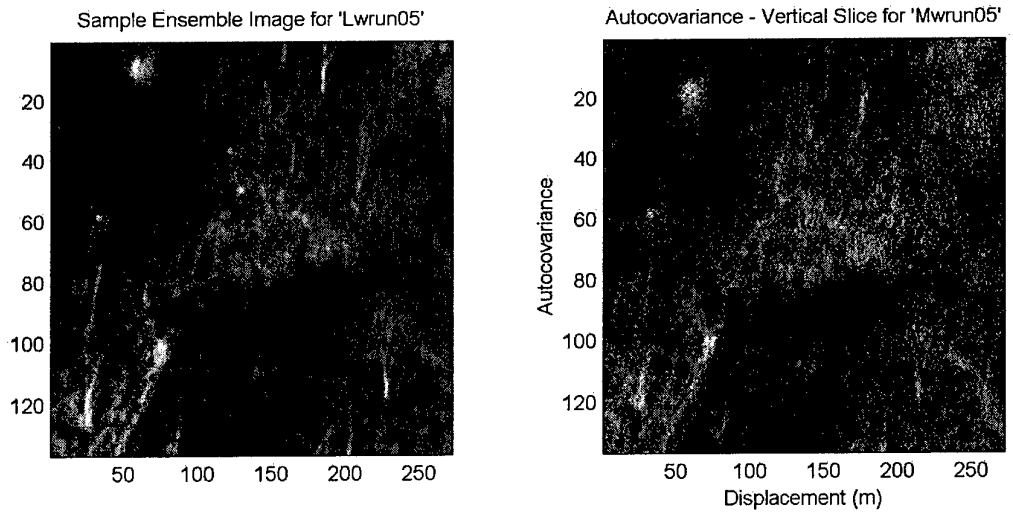

Figure 30 – Original Images from Run 5

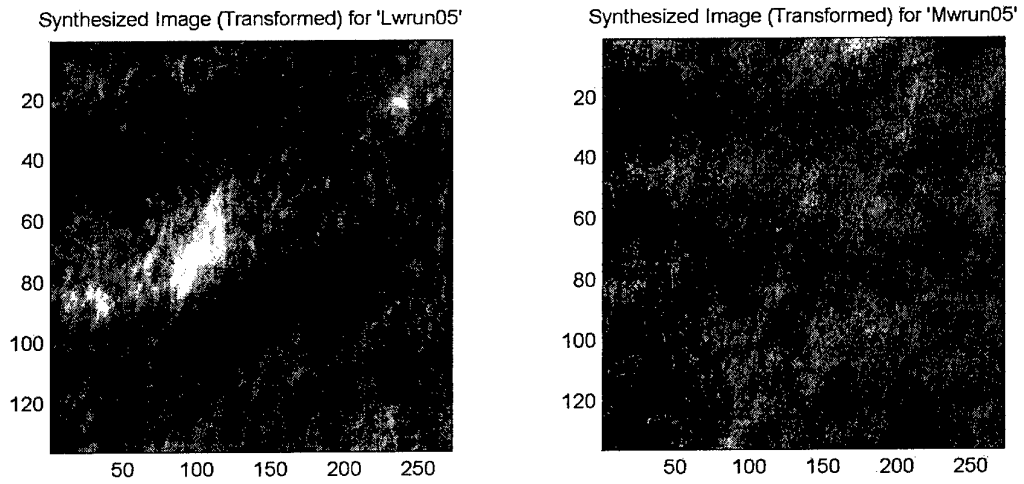

Figure 31 – Synthetic Images for Run 5

3.7 Run 6

3.7.1 General Information

Flight Date: 30-6-97 NIGHT
Altitude: 1.7K ft
Depression Angle: 60 deg.
Vegetation Classes in Run: 48
Predominate Vegetation Class: 48

Ensemble Size is: 151
Number of Valid Images is: 39
Vertical Resolution is: 2.48m
Horizontal Resolution is: 0.64m

3.7.2 Histogram

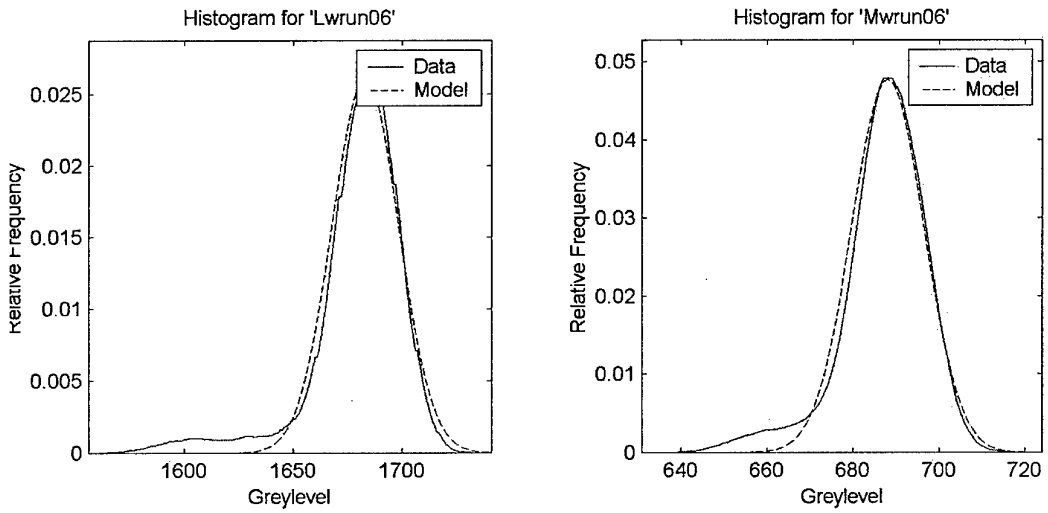

Figure 32 – Gaussian Fit – Histogram of Run 6

Histogram Information for 'Lwrun06'

Normal Model Parameters:
    Mean is: 1683.04
    Variance is: 234.60
RMS error is: 9.94%
Chi2 P-value is: 0.00%
Model Accepted by Threshold: No
Model Accepted Visually: No

Histogram Information for 'Mwrun06'

Normal Model Parameters:
Mean is: 688.01
Variance is: 70.00
RMS error is: 18.25%
Chi2 P-value is: 0.00%
Model Accepted by Threshold: No
Model Accepted Visually: No

3.7.3 Auto-covariance – Horizontal

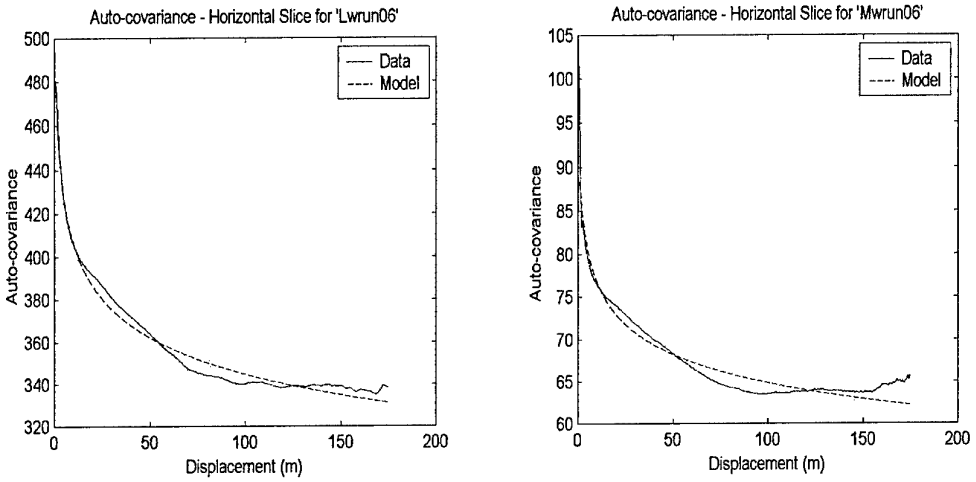

Figure 33 – Power Law Fit - Horizontal Slice of Run 6

Auto-covariance - Horizontal for 'Lwrun06'

Mean Standard deviation between images is: 185.94
Power Law Model Parameters:
a_est is: 479.50
b_est is: 0.74
w_est is: 0.04
RMS error is: 1.13%
Model Accepted by Threshold: Yes
Model Accepted Visually: No

Auto-covariance - Horizontal for 'Mwrun06'

Mean Standard deviation between images is: 27.38
Power Law Model Parameters:
a_est is: 90.96
b_est is: 0.00
w_est is: 0.04
RMS error is: 1.95%
Model Accepted by Threshold: Yes

Model Accepted Visually: No

3.7.4 Auto-covariance – Vertical

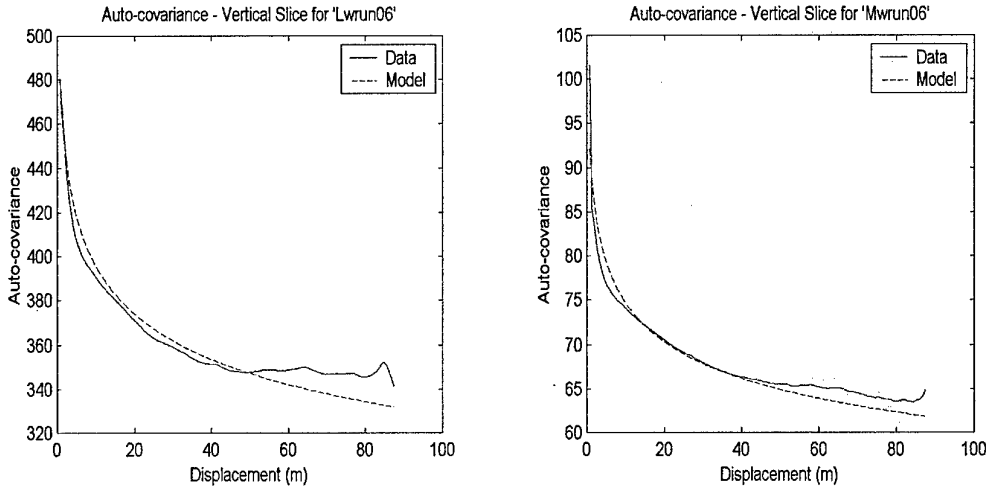

Figure 34 – Power Law Fit - Vertical Slice of Run 6

Auto-covariance - Vertical for 'Lwrun06'

Mean Standard deviation between images is: 184.95
Power Law Model Parameters:
a_est is: 452.59
b_est is: 0.00
w_est is: 0.03
RMS error is: 1.35
Model Accepted by Threshold: Yes
Model Accepted Visually: Partially

Auto-covariance - Vertical for 'Mwrun06'

Mean Standard deviation between images is: 27.53
Power Law Model Parameters:
a_est is: 89.54
b_est is: 0.00
w_est is: 0.04
RMS error is: 1.37
Model Accepted by Threshold: Yes
Model Accepted Visually: Partially

3.7.5 Image Synthesis:

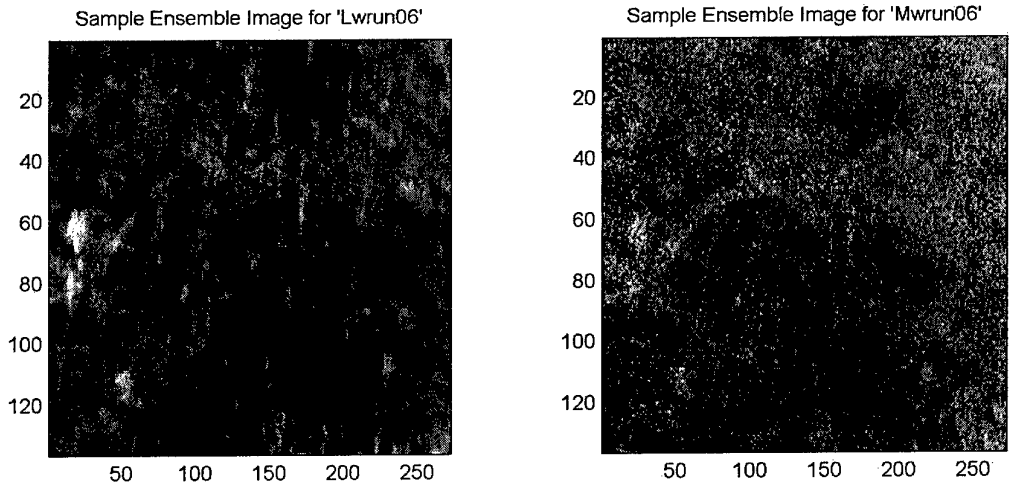

Figure 35 – Original Images from Run 6

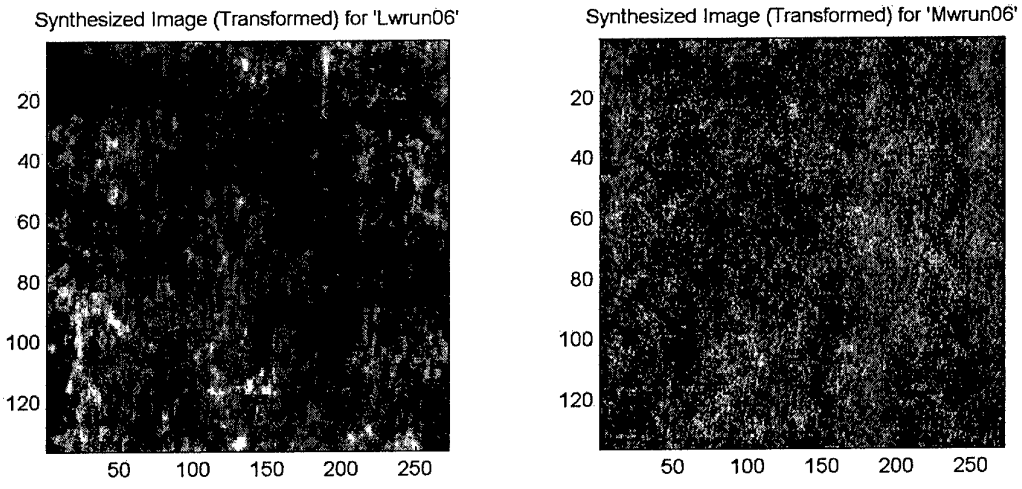

Figure 36 – Synthetic Images for Run 6

3.8 Run 9

3.8.1 General Information

Flight Date: 1-7-97 DAY
Altitude: 10K ft
Depression Angle: 60 deg.
Vegetation Classes in Run: 105, 21, 11, 32, 4, 9
Predominate Vegetation Class: 32

Ensemble Size is: 150
Number of Valid Images is: 47
Vertical Resolution is: 1.30m
Horizontal Resolution is: 1.13m

3.8.2 Histogram

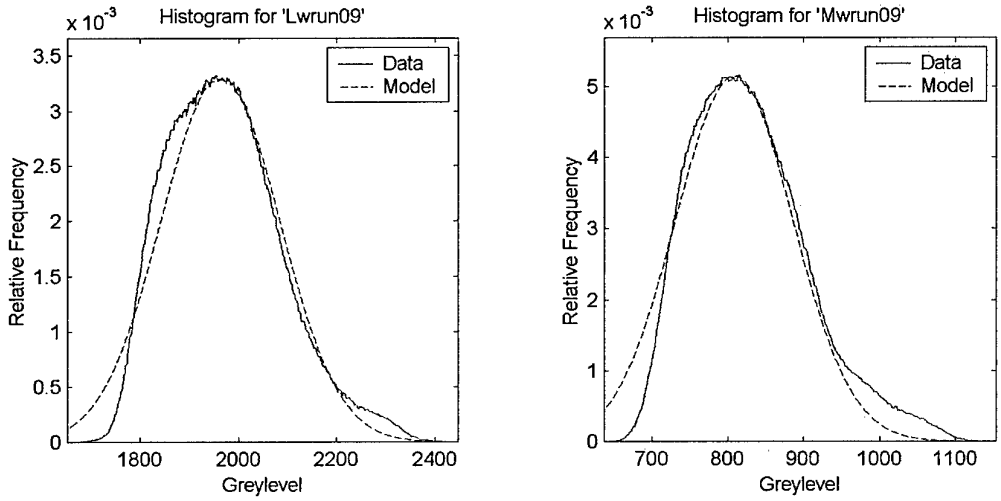

Figure 37 – Gaussian Fit – Histogram of Run 9

Histogram Information for 'Lwrun09'

Normal Model Parameters:
    Mean is: 1963.37
    Variance is: 14521.48
RMS error is: 2.16%
Chi2 P-value is: 100.00%
Model Accepted by Threshold: Yes
Model Accepted Visually: No

Histogram Information for 'Mwrun09'

Normal Model Parameters:
Mean is: 808.51
Variance is: 6007.26
RMS error is: 3.70%
Chi2 P-value is: 100.00%
Model Accepted by Threshold: Yes
Model Accepted Visually: No

3.8.3 Auto-covariance – Horizontal

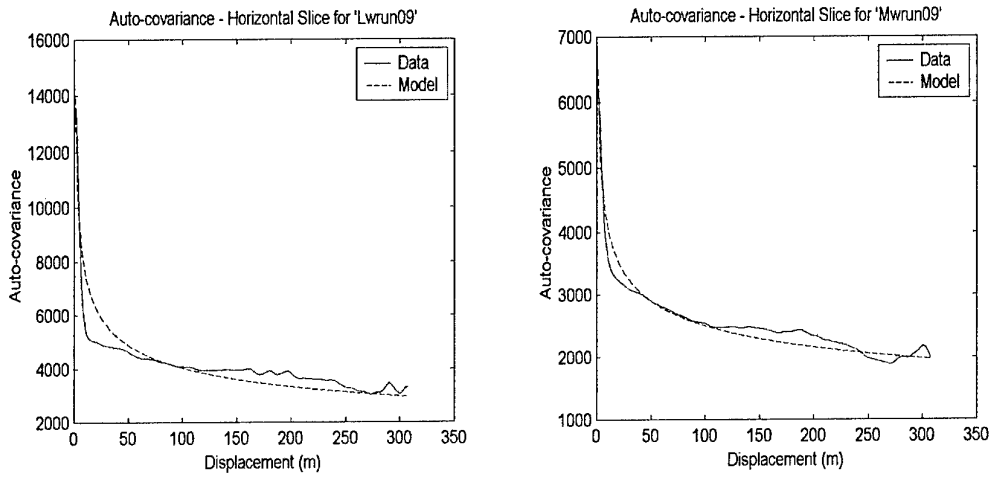

Figure 38 – Power Law Fit - Horizontal Slice of Run 9

Auto-covariance - Horizontal for 'Lwrun09'

Mean Standard deviation between images is: 907.60
Power Law Model Parameters:
a_est is: 14512.17
b_est is: 0.00
w_est is: 0.14
RMS error is: 10.82%
Model Accepted by Threshold: No
Model Accepted Visually: No

Auto-covariance - Horizontal for 'Mwrun09'

Mean Standard deviation between images is: 551.53
Power Law Model Parameters:
a_est is: 6714.88
b_est is: 0.00
w_est is: 0.11
RMS error is: 5.48%

Model Accepted by Threshold: No
Model Accepted Visually: No

3.8.4 Auto-covariance – Vertical

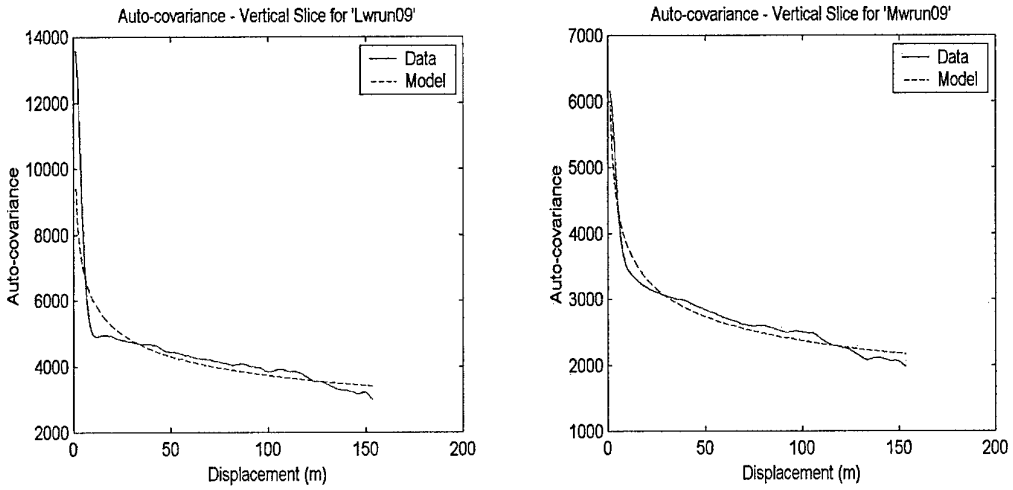

Figure 39 – Power Law Fit - Vertical Slice of Run 9

Auto-covariance - Vertical for 'Lwrun09'

Mean Standard deviation between images is: 883.06
Power Law Model Parameters:
a_est is: 9734.98
b_est is: 0.00
w_est is: 0.10
RMS error is: 7.90%
Model Accepted by Threshold: No
Model Accepted Visually: No

Auto-covariance - Vertical for 'Mwrun09'

Mean Standard deviation between images is: 518.84
Power Law Model Parameters:
a_est is: 6142.74
b_est is: 0.00
w_est is: 0.10
RMS error is: 4.62%
Model Accepted by Threshold: No
Model Accepted Visually: No

3.8.5 Image Synthesis:

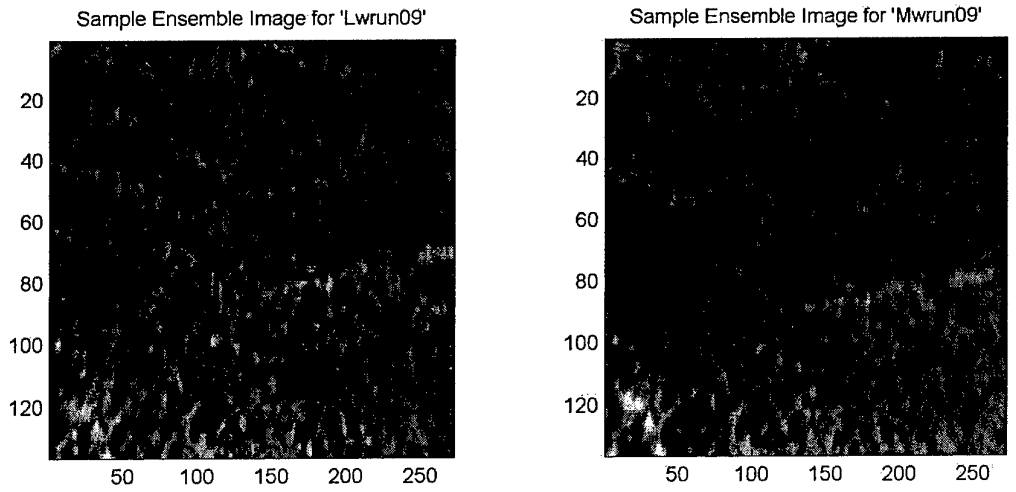

Figure 40 – Original Images from Run 9

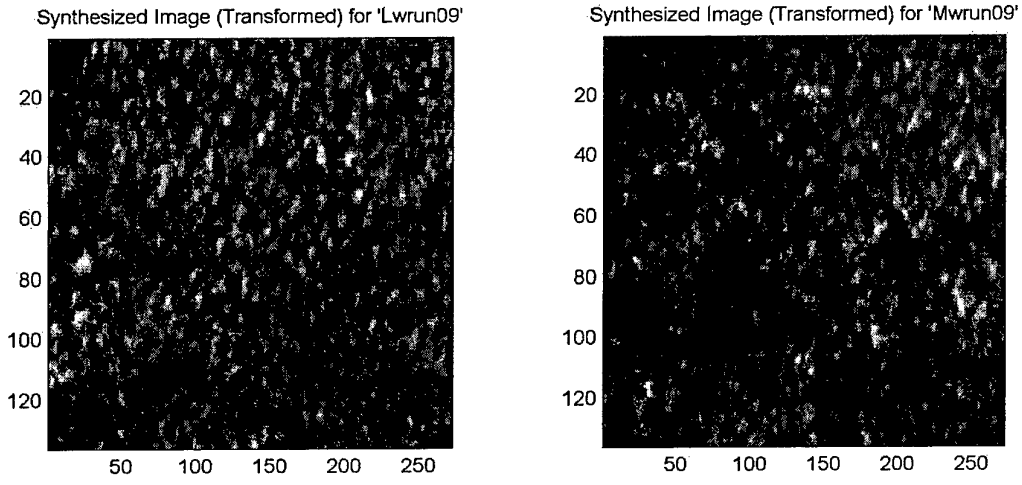

Figure 41 – Synthetic Images for Run 9

3.9 Run 10

3.9.1 General Information

Flight Date: -7-97 DAY
Altitude: 0K ft
Depression Angle: 60 deg.
Vegetation Classes in Run: 48, 11, 21, 105
Predominate Vegetation Class: 11

Ensemble Size is: 146
Number of Valid Images is: 35
Vertical Resolution is: 1.30m
Horizontal Resolution is: 1.13m

3.9.2 Histogram

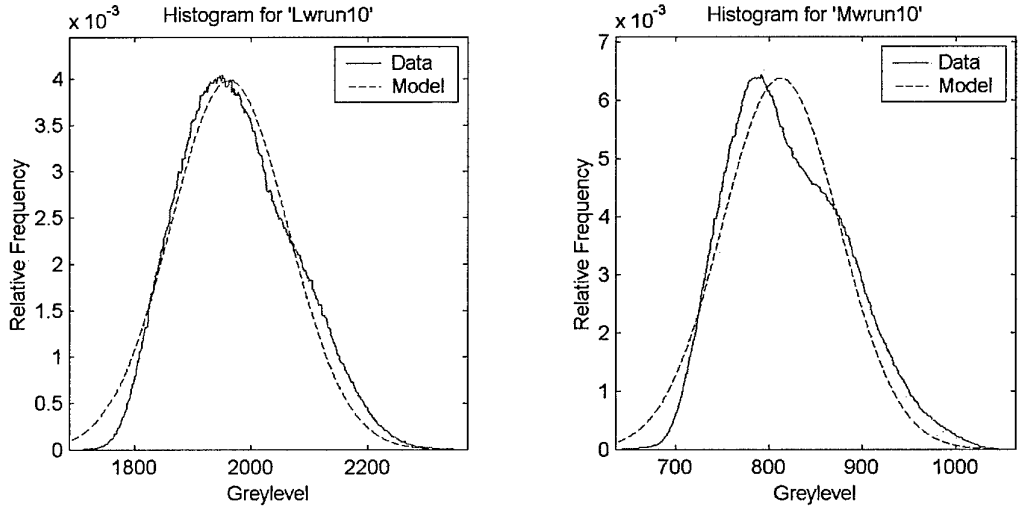

Figure 42 – Gaussian Fit – Histogram of Run 10

Histogram Information for 'Lwrun10'

Normal Model Parameters:
    Mean is: 1961.99
    Variance is: 10000.00
RMS error is: 2.20%
Chi2 P-value is: 100.00%
Model Accepted by Threshold: Yes
Model Accepted Visually: No

Histogram Information for 'Mwrun10'

Normal Model Parameters:
Mean is: 812.46
Variance is: 3907.81
RMS error is: 5.24%
Chi2 P-value is: 100.00%
Model Accepted by Threshold: Yes
Model Accepted Visually: No

3.9.3 Auto-covariance – Horizontal

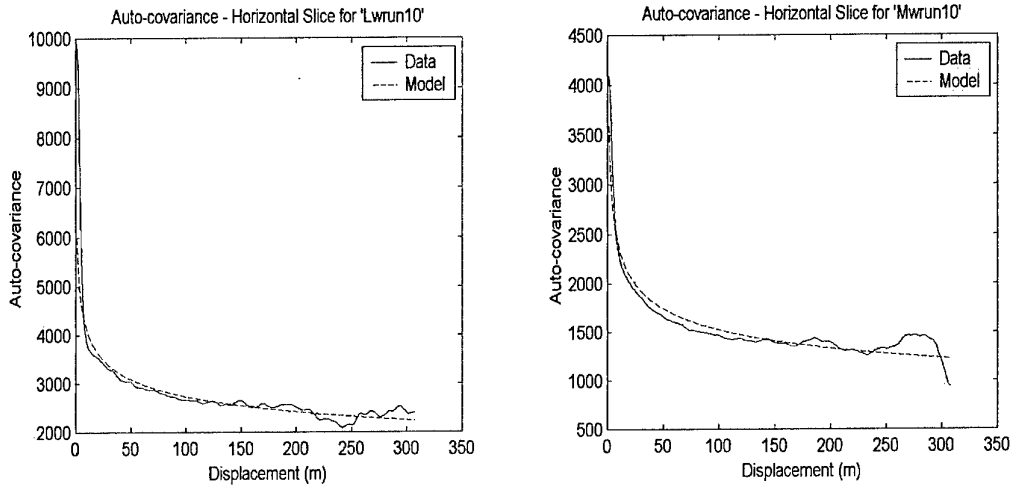

Figure 43 – Power Law Fit - Horizontal Slice of Run 10

Auto-covariance - Horizontal for 'Lwrun10'

Mean Standard deviation between images is: 496.04
Power Law Model Parameters:
a_est is: 6591.87
b_est is: 0.00
w_est is: 0.10
RMS error is: 6.27%
Model Accepted by Threshold: No
Model Accepted Visually: Partially

Auto-covariance - Horizontal for 'Mwrun10'

Mean Standard deviation between images is: 305.81
Power Law Model Parameters:
a_est is: 3958.77
b_est is: 0.74
w_est is: 0.10
RMS error is: 7.15%

Model Accepted by Threshold: No
Model Accepted Visually: Partially

3.9.4 Auto-covariance – Vertical

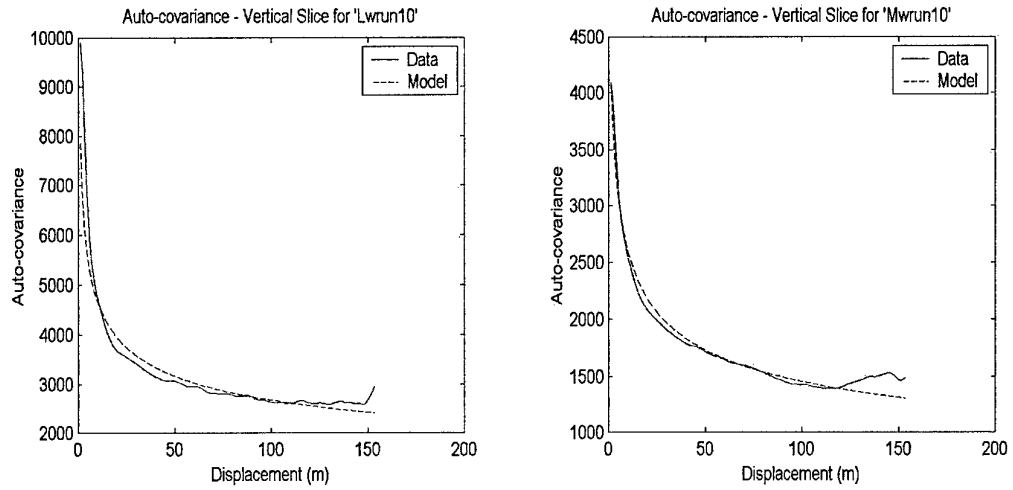

Figure 44 – Power Law Fit - Vertical Slice of Run 10

Auto-covariance - Vertical for 'Lwrun10'

Mean Standard deviation between images is: 555.61
Power Law Model Parameters:
a_est is: 8157.81
b_est is: 0.00
w_est is: 0.12
RMS error is: 6.12%
Model Accepted by Threshold: No
Model Accepted Visually: Partially

Auto-covariance - Vertical for 'Mwrun10'

Mean Standard deviation between images is: 288.02
Power Law Model Parameters:
a_est is: 4670.79
b_est is: 1.25
w_est is: 0.13
RMS error is: 5.01%
Model Accepted by Threshold: No
Model Accepted Visually: Yes

3.9.5 Image Synthesis:

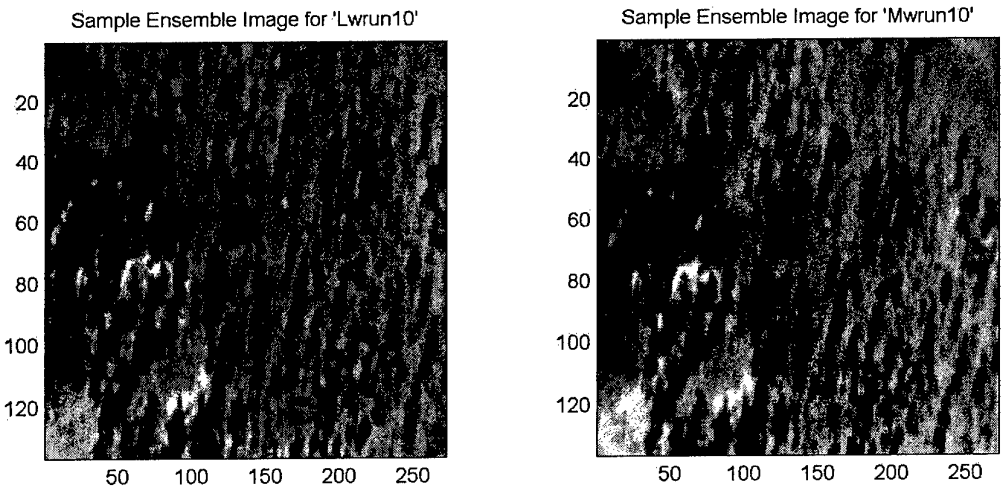

Figure 45 – Original Images from Run 10

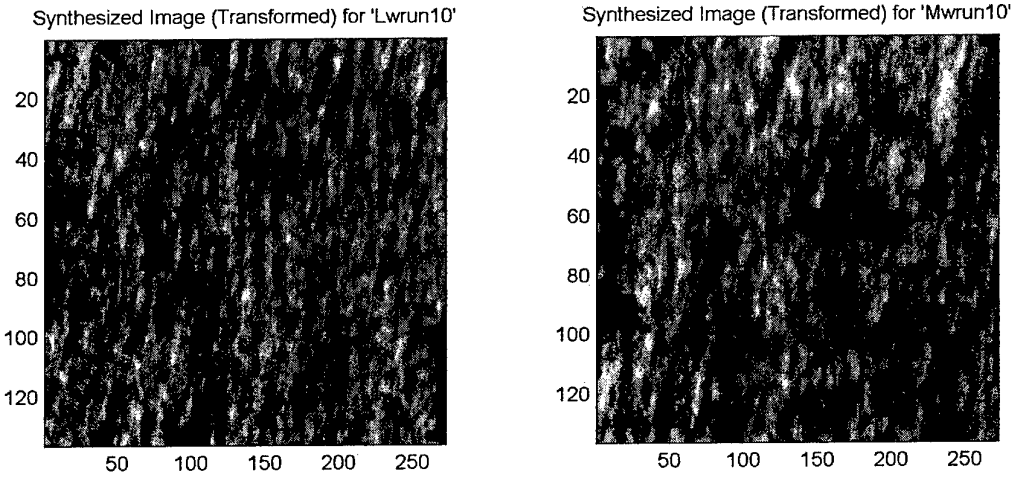

Figure 46 – Synthetic Images for Run 10

3.10 Run 11

3.10.1 General Information

Flight Date: 3-7-97 DAY
Altitude: 10K ft
Depression Angle: 60 deg.
Vegetation Classes in Run: 21, 15, 51
Predominate Vegetation Class: 21

Ensemble Size is: 150
Number of Valid Images is: 17
Vertical Resolution is: 1.30m
Horizontal Resolution is: 1.13m

3.10.2 Histogram

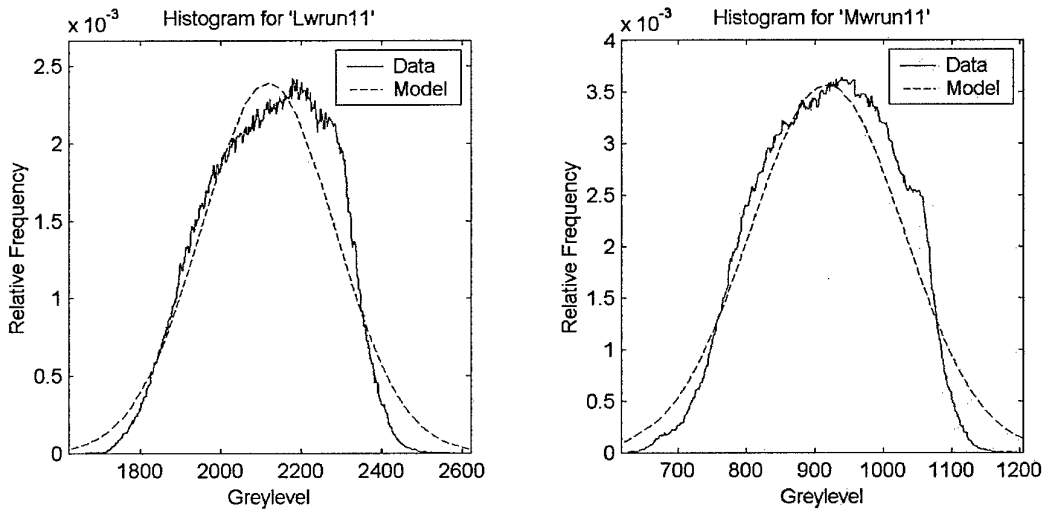

Figure 47 – Gaussian Fit – Histogram of Run 11

Histogram Information for 'Lwrun11'

Normal Model Parameters:
    Mean is: 2118.03
    Variance is: 27839.50
RMS error is: 2.16%
Chi2 P-value is: 100.00%
Model Accepted by Threshold: Yes
Model Accepted Visually: No

Histogram Information for 'Mwrun11'

Normal Model Parameters:
Mean is: 917.71
Variance is: 12503.97
RMS error is: 3.14%
Chi2 P-value is: 100.00%
Model Accepted by Threshold: Yes
Model Accepted Visually: No

3.10.3 Auto-covariance – Horizontal

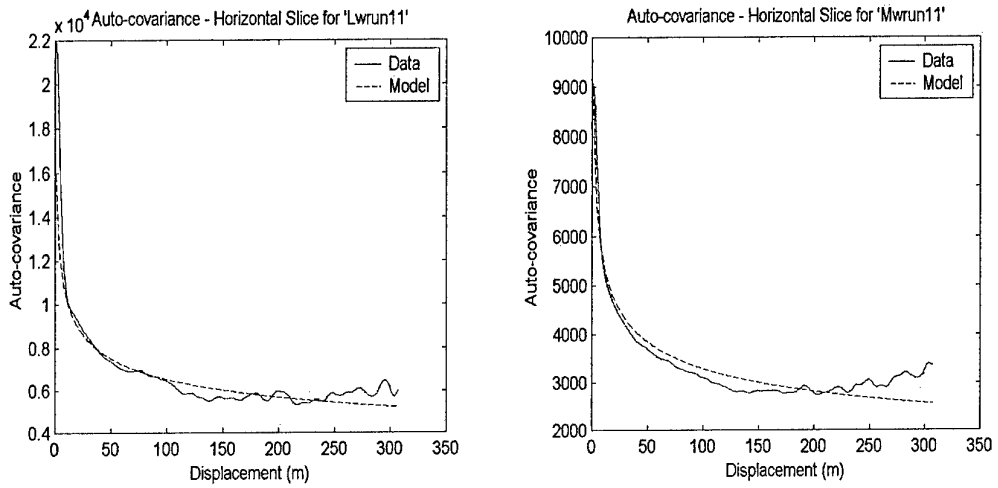

Figure 48 – Power Law Fit - Horizontal Slice of Run 11

Auto-covariance - Horizontal for 'Lwrun11'

Mean Standard deviation between images is: 2527.34
Power Law Model Parameters:
a_est is: 18431.15
b_est is: 0.00
w_est is: 0.11
RMS error is: 7.50%
Model Accepted by Threshold: No
Model Accepted Visually: Partially

Auto-covariance - Horizontal for 'Mwrun11'

Mean Standard deviation between images is: 1080.30
Power Law Model Parameters:
a_est is: 9711.80
b_est is: 0.00
w_est is: 0.12
RMS error is: 9.10%

Model Accepted by Threshold: No
Model Accepted Visually: Partially

3.10.4 Auto-covariance – Vertical

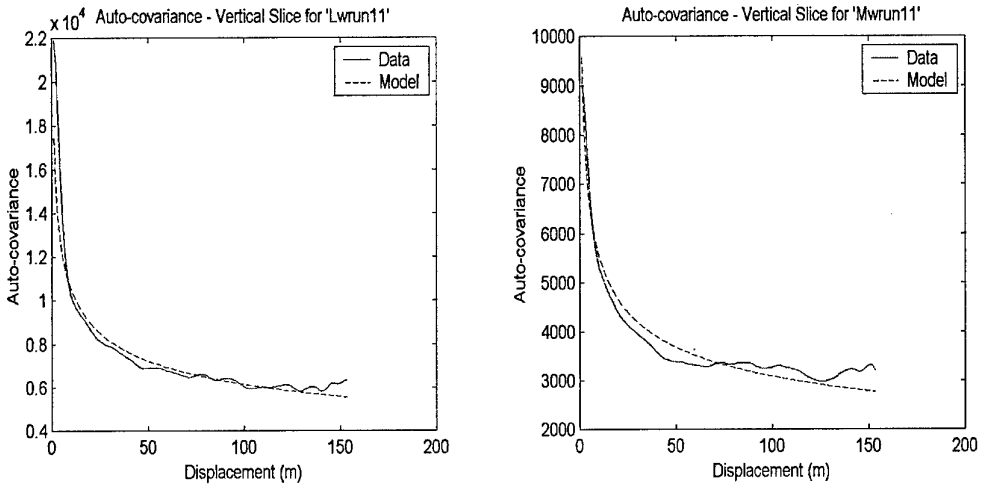

Figure 49 – Power Law Fit - Vertical Slice of Run 11

Auto-covariance - Vertical for 'Lwrun11'

Mean Standard deviation between images is: 2616.55
Power Law Model Parameters:
a_est is: 18068.13
b_est is: 0.00
w_est is: 0.12
RMS error is: 5.70%
Model Accepted by Threshold: No
Model Accepted Visually: Partially

Auto-covariance - Vertical for 'Mwrun11'

Mean Standard deviation between images is: 1145.11
Power Law Model Parameters:
a_est is: 9941.85
b_est is: 0.00
w_est is: 0.13
RMS error is: 7.07%
Model Accepted by Threshold: No
Model Accepted Visually: No

3.10.5 Image Synthesis:

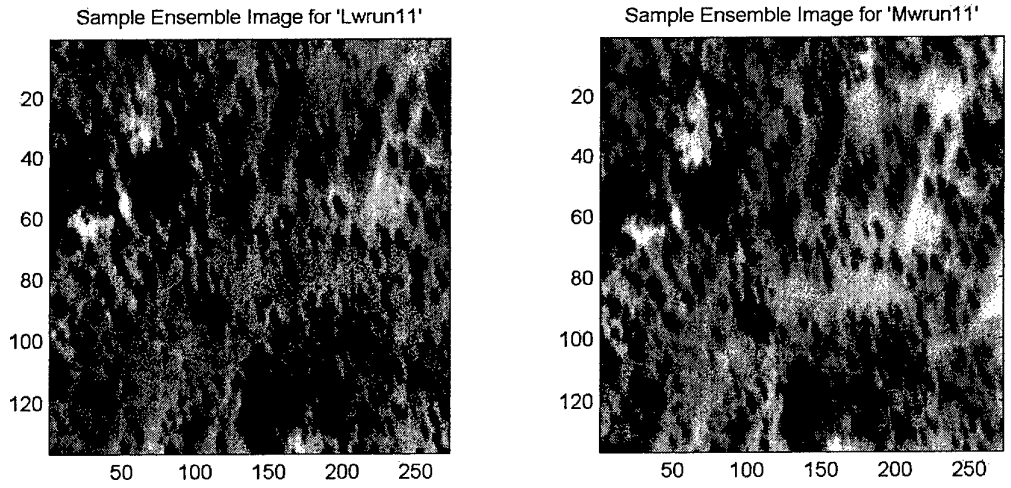

Figure 50 – Original Images from Run 11

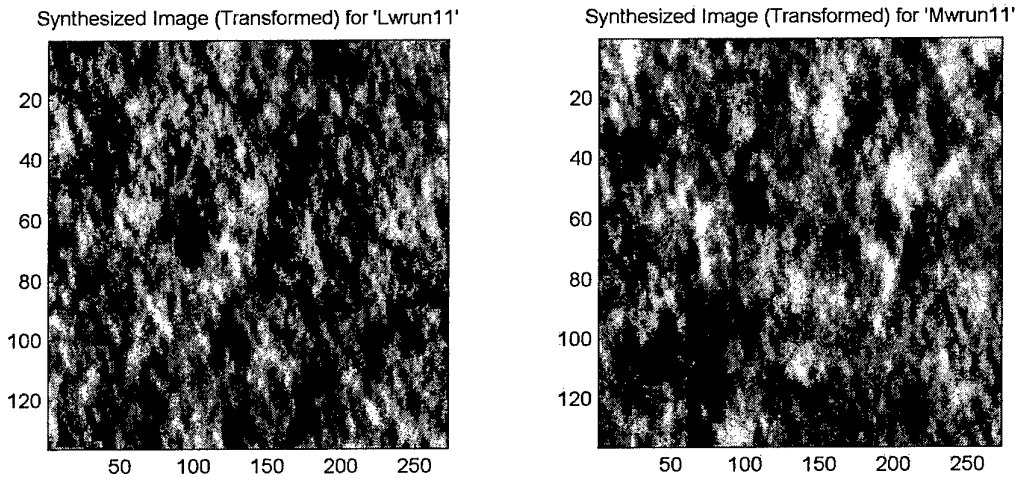

Figure 51 – Synthetic Images for Run 11

3.11 Run 12

3.11.1 General Information

Flight Date: 3-7-97 DAY
Altitude: 10K ft
Depression Angle: 60 deg.
Vegetation Classes in Run: 13, 51, 15, 4, 21
Predominate Vegetation Class: 15

Ensemble Size is: 269
Number of Valid Images is: 31
Vertical Resolution is: 1.30m
Horizontal Resolution is: 1.13m

3.11.2 Histogram

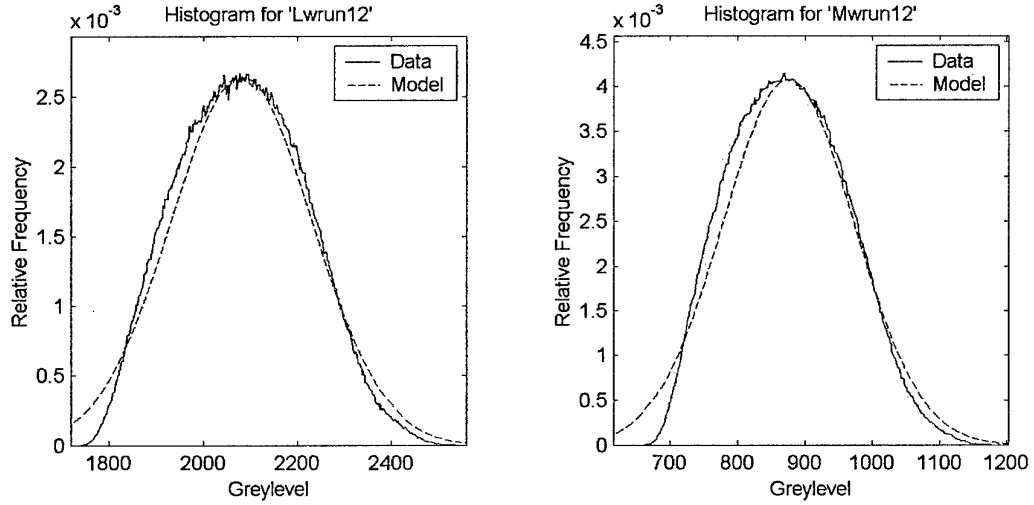

Figure 52 – Gaussian Fit – Histogram of Run 12

Histogram Information for 'Lwrun12'

Normal Model Parameters:
    Mean is: 2081.22
    Variance is: 22712.26
RMS error is: 1.29%
Chi2 P-value is: 100.00%
Model Accepted by Threshold: Yes
Model Accepted Visually: No

Histogram Information for 'Mwrun12'

Normal Model Parameters:
Mean is: 875.47
Variance is: 9580.54
RMS error is: 2.33%
Chi2 P-value is: 100.00%
Model Accepted by Threshold: Yes
Model Accepted Visually: Partially

3.11.3 Auto-covariance – Horizontal

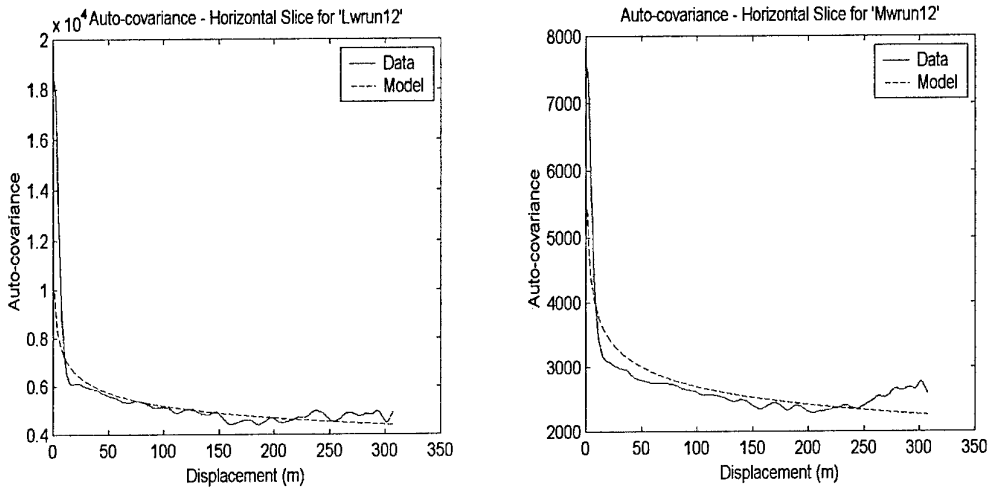

Figure 53 – Power Law Fit - Horizontal Slice of Run 12

Auto-covariance - Horizontal for 'Lwrun12'

Mean Standard deviation between images is: 1369.61
Power Law Model Parameters:
a_est is: 11251.79
b_est is: 0.00
w_est is: 0.08
RMS error is: 7.96%
Model Accepted by Threshold: No
Model Accepted Visually: No

Auto-covariance - Horizontal for 'Mwrun12'

Mean Standard deviation between images is: 610.68
Power Law Model Parameters:
a_est is: 6331.00
b_est is: 0.00
w_est is: 0.09
RMS error is: 9.17%

Model Accepted by Threshold: No
Model Accepted Visually: No

3.11.4 Auto-covariance - Vertical

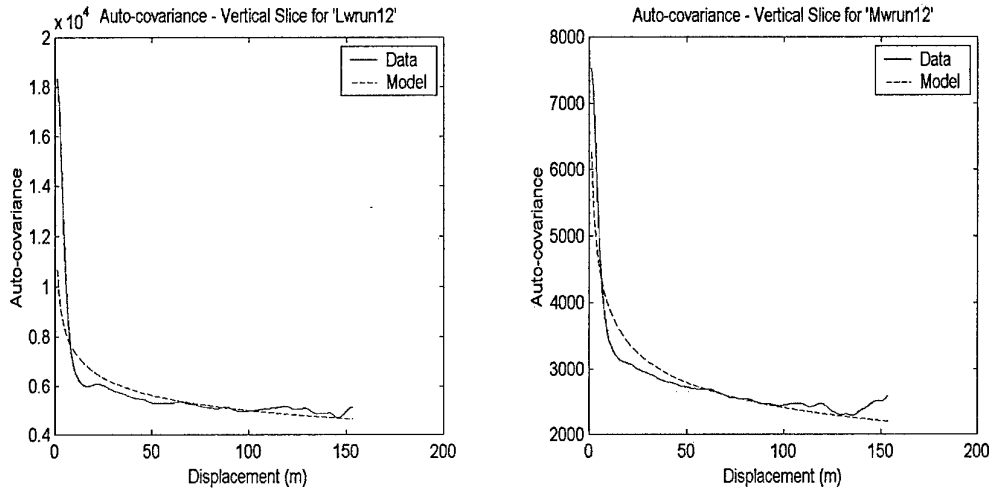

Figure 54 – Power Law Fit - Vertical Slice of Run 12

Auto-covariance - Vertical for 'Lwrun12'

Mean Standard deviation between images is: 1348.69
Power Law Model Parameters:
a_est is: 11000.20
b_est is: 0.00
w_est is: 0.09
RMS error is: 8.77%
Model Accepted by Threshold: No
Model Accepted Visually: No

Auto-covariance - Vertical for 'Mwrun12'

Mean Standard deviation between images is: 598.14
Power Law Model Parameters:
a_est is: 6469.22
b_est is: 0.00
w_est is: 0.11
RMS error is: 6.85%
Model Accepted by Threshold: No
Model Accepted Visually: No

3.11.5 Image Synthesis:

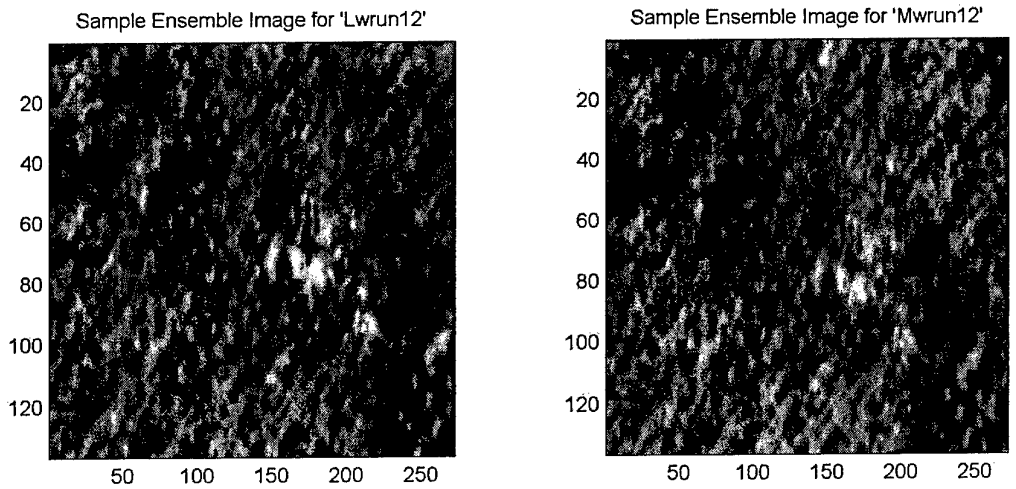

Figure 55 – Original Images from Run 12

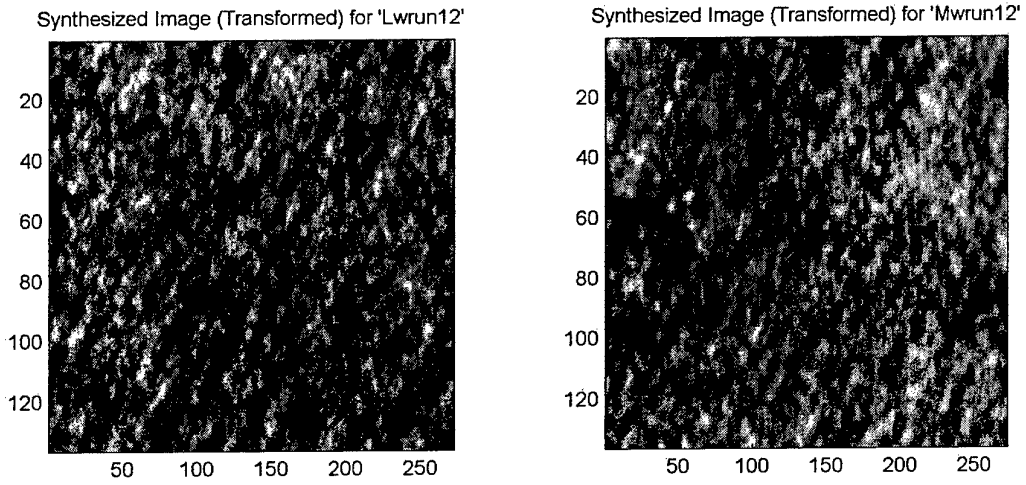

Figure 56 – Synthetic Images for Run 12

3.12 Run 13

3.12.1 General Information

Flight Date: 3-7-97 DAY
Altitude: 5K ft
Depression Angle: 60 deg.
Vegetation Classes in Run: 9, 21, 11, 32
Predominate Vegetation Class: 32

Ensemble Size is: 250
Number of Valid Images is: 62
Vertical Resolution is: 0.65m
Horizontal Resolution is: 0.56m

3.12.2 Histogram

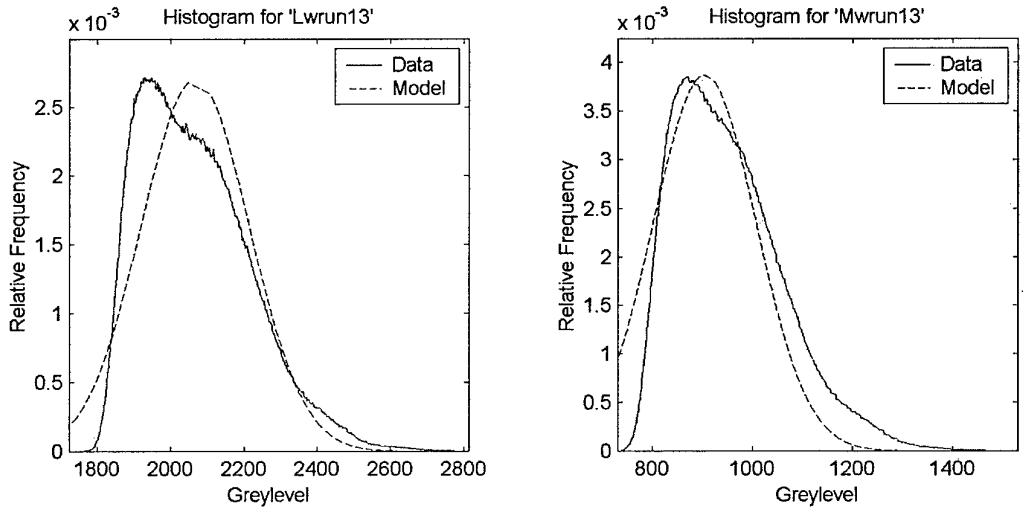

Figure 57 – Gaussian Fit – Histogram of Run 13

Histogram Information for 'Lwrun13'

Normal Model Parameters:
    Mean is: 2066.47
    Variance is: 21795.67
RMS error is: 3.45%
Chi2 P-value is: 99.55%
Model Accepted by Threshold: Yes
Model Accepted Visually: No

Histogram Information for 'Mwrun13'

Normal Model Parameters:
Mean is: 904.15
Variance is: 10624.08
RMS error is: 4.31%
Chi2 P-value is: 100.00%
Model Accepted by Threshold: Yes
Model Accepted Visually: No

3.12.3 Auto-covariance – Horizontal

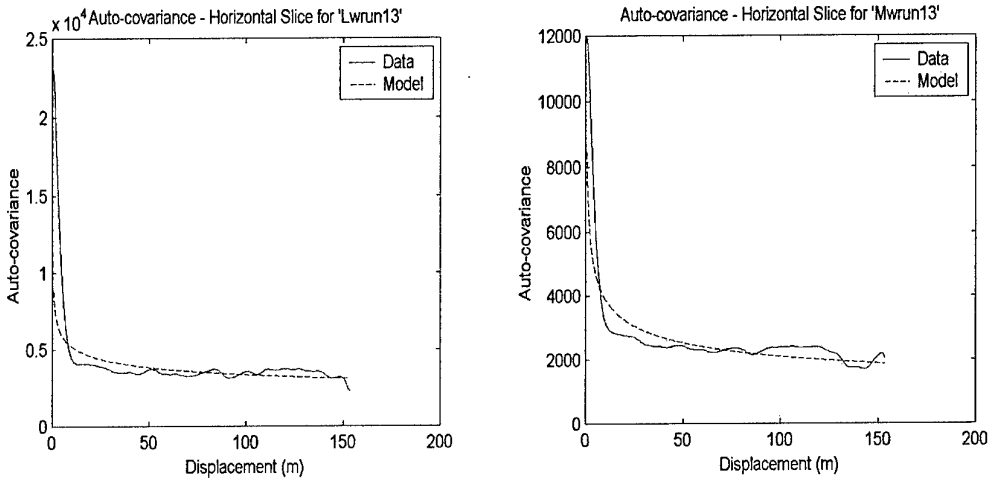

Figure 58 – Power Law Fit - Horizontal Slice of Run 13

Auto-covariance - Horizontal for 'Lwrun13'

Mean Standard deviation between images is: 666.45
Power Law Model Parameters:
a_est is: 8080.16
b_est is: 0.00
w_est is: 0.09
RMS error is: 15.29%
Model Accepted by Threshold: No
Model Accepted Visually: No

Auto-covariance - Horizontal for 'Mwrun13'

Mean Standard deviation between images is: 392.46
Power Law Model Parameters:
a_est is: 8413.28
b_est is: 0.00
w_est is: 0.15
RMS error is: 14.47%

Model Accepted by Threshold: No
Model Accepted Visually: No

3.12.4 Auto-covariance – Vertical

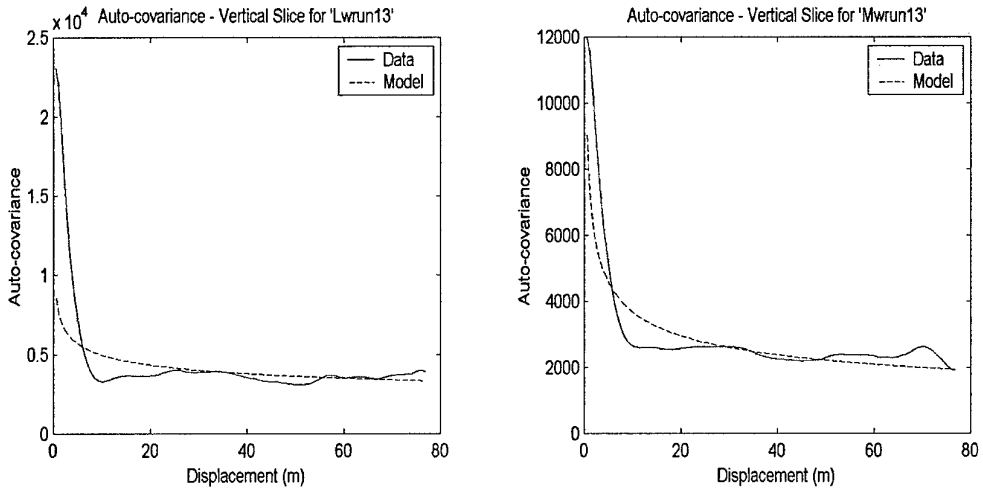

Figure 59 – Power Law Fit - Vertical Slice of Run 13

Auto-covariance - Vertical for 'Lwrun13'

Mean Standard deviation between images is: 641.98
Power Law Model Parameters:
a_est is: 7837.69
b_est is: 0.00
w_est is: 0.10
RMS error is: 20.77%
Model Accepted by Threshold: No
Model Accepted Visually: No

Auto-covariance - Vertical for 'Mwrun13'

Mean Standard deviation between images is: 390.10
Power Law Model Parameters:
a_est is: 7605.90
b_est is: 0.00
w_est is: 0.16
RMS error is: 16.36%
Model Accepted by Threshold: No
Model Accepted Visually: No

3.12.5 Image Synthesis:

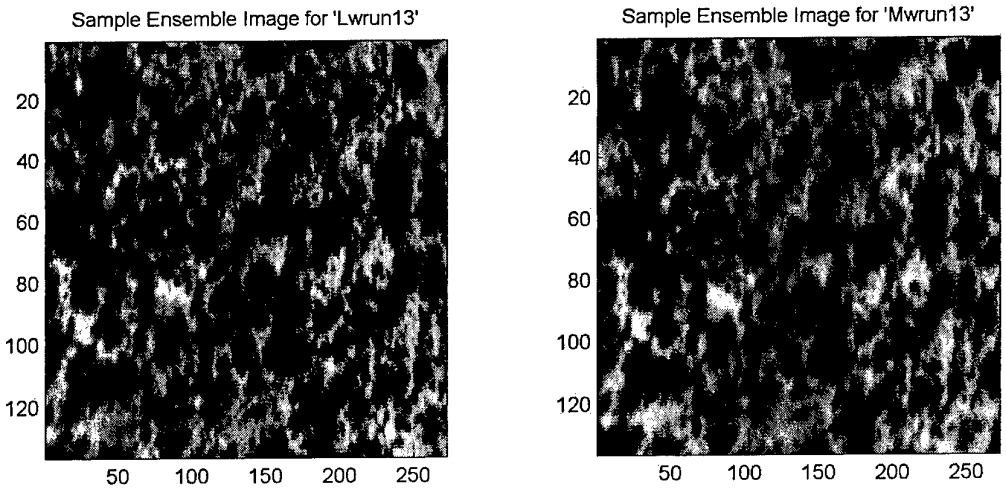

Figure 60 – Original Images from Run 13

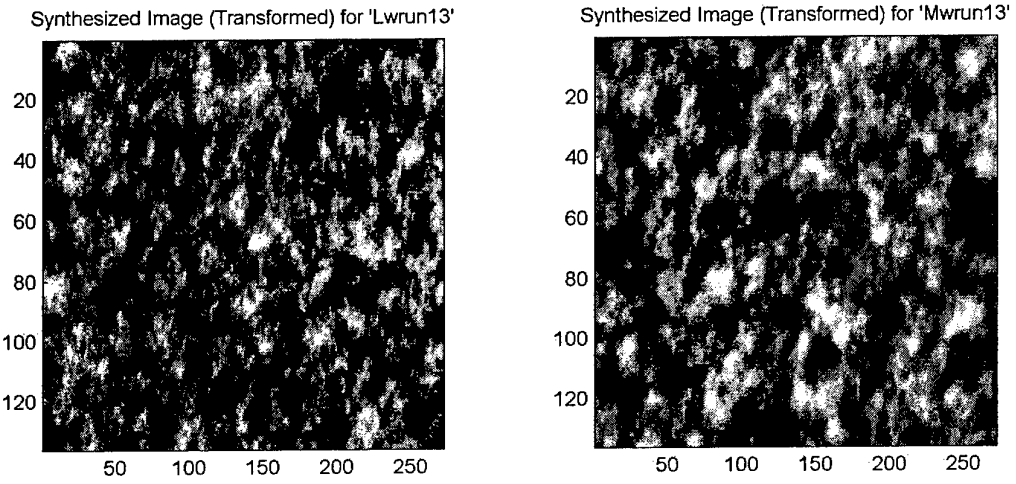

Figure 61 – Synthetic Images for Run 13

3.13 Run 14

3.13.1 General Information

Flight Date: 3-7-97 DAY
Altitude: 5K ft
Depression Angle: 60 deg.
Vegetation Classes in Run: 48, 11, 51
Predominate Vegetation Class 11

Ensemble Size is: 250
Number of Valid Images is: 75
Vertical Resolution is: 0.65m
Horizontal Resolution is: 0.56m

3.13.2 Histogram

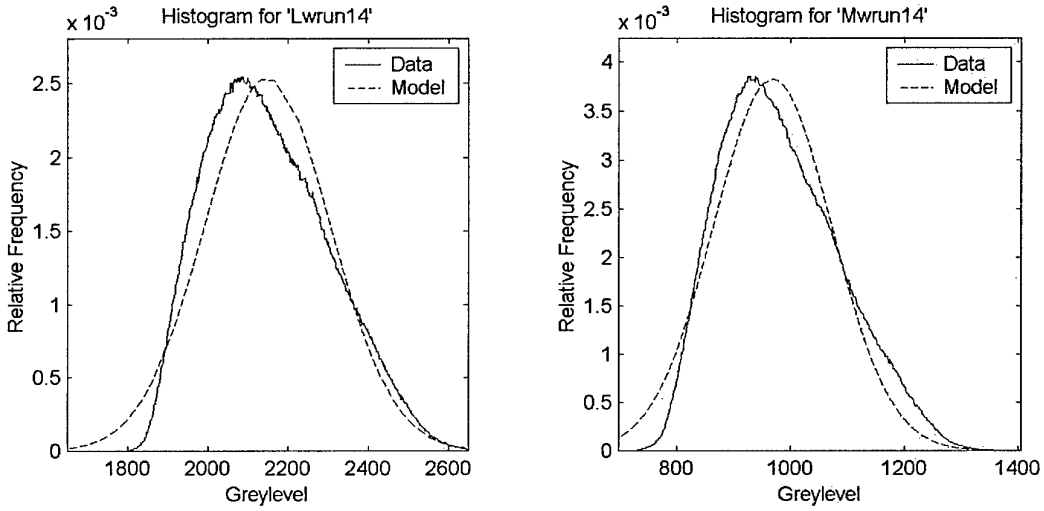

Figure 62 – Gaussian Fit – Histogram of Run 14

Histogram Information for 'Lwrun14'

Normal Model Parameters:
    Mean is: 2147.89
    Variance is: 24725.98
RMS error is: 2.26%
Chi2 P-value is: 100.00%
Model Accepted by Threshold: Yes
Model Accepted Visually: No

Histogram Information for 'Mwrun14'

Normal Model Parameters:
Mean is: 967.89
Variance is: 10878.77
RMS error is: 2.86%
Chi2 P-value is: 100.00%
Model Accepted by Threshold: Yes
Model Accepted Visually: No

3.13.3 Auto-covariance – Horizontal

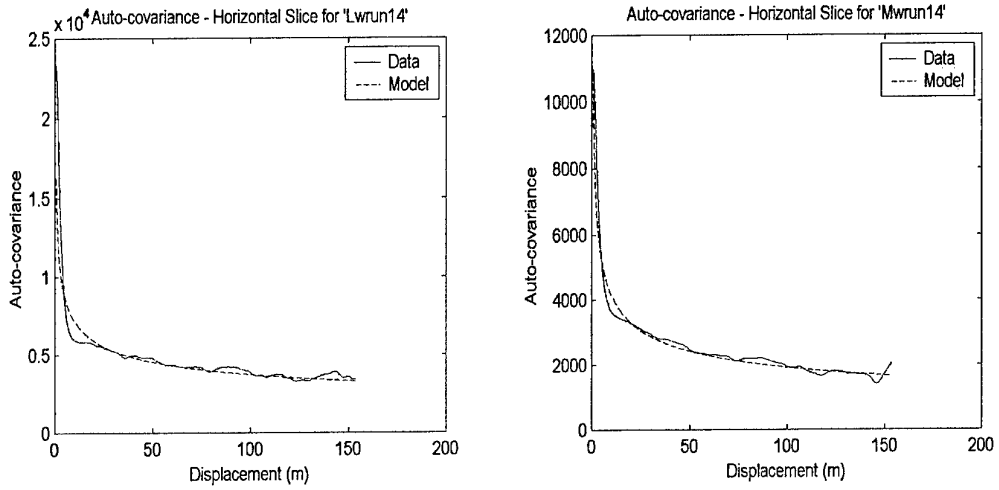

Figure 63 – Power Law Fit - Horizontal Slice of Run 14

Auto-covariance - Horizontal for 'Lwrun14'

Mean Standard deviation between images is: 856.52
Power Law Model Parameters:
a_est is: 22984.96
b_est is: 12.00
w_est is: 0.20
RMS error is: 12.57%
Model Accepted by Threshold: No
Model Accepted Visually: Partially

Auto-covariance - Horizontal for 'Mwrun14'

Mean Standard deviation between images is: 473.18
Power Law Model Parameters:
a_est is: 8896.77
b_est is: 0.19
w_est is: 0.17
RMS error is: 6.44%

Model Accepted by Threshold: No
Model Accepted Visually: Yes

3.13.4 Auto-covariance - Vertical

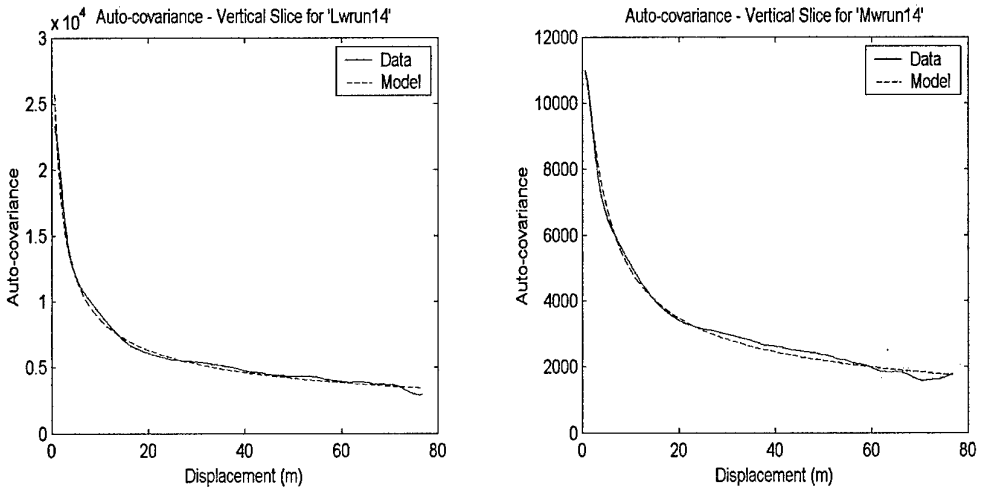

Figure 64 – Power Law Fit - Vertical Slice of Run 14

Auto-covariance - Vertical for 'Lwrun14'

Mean Standard deviation between images is: 784.67
Power Law Model Parameters:
a_est is: 24578.28
b_est is: 0.68
w_est is: 0.23
RMS error is: 4.89%
Model Accepted by Threshold: No
Model Accepted Visually: Yes

Auto-covariance - Vertical for 'Mwrun14'

Mean Standard deviation between images is: 441.07
Power Law Model Parameters:
a_est is: 16219.27
b_est is: 2.07
w_est is: 0.26
RMS error is: 5.68%
Model Accepted by Threshold: No
Model Accepted Visually: Yes

3.13.5 Image Synthesis:

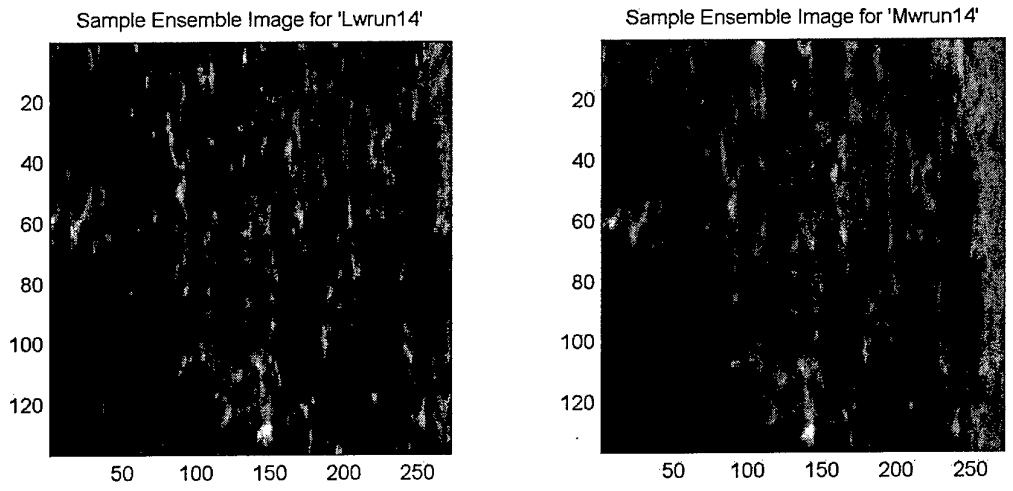

Figure 65 – Original Images from Run 14

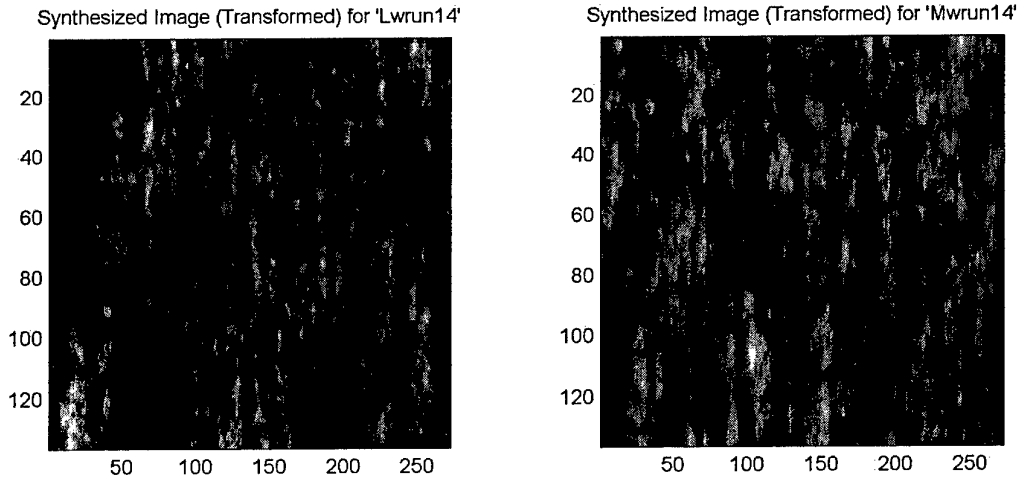

Figure 66 – Synthetic Images for Run 14

3.14 Run 15

3.14.1 General Information

Flight Date: 3-7-97 DAY
Altitude: 5K ft
Depression Angle: 60 deg.
Vegetation Classes in Run: 21, 15, 51
Predominate Vegetation Class: 21

Ensemble Size is: 250
Number of Valid Images is: 49
Vertical Resolution is: 0.65m
Horizontal Resolution is: 0.56m

3.14.2 Histogram

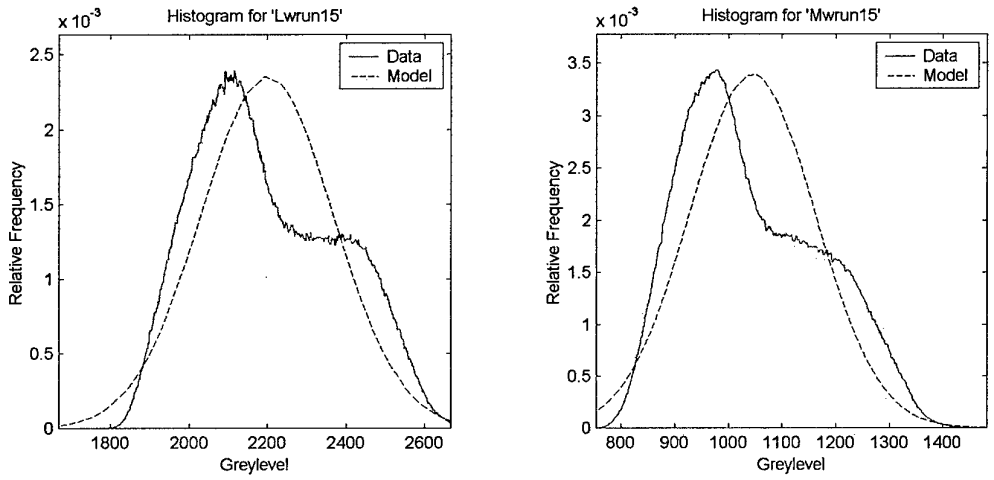

Figure 67 – Gaussian Fit – Histogram of Run 15

Histogram Information for 'Lwrun15'

Normal Model Parameters:
    Mean is: 2198.06
    Variance is: 28755.24
RMS error is: 3.95%
Chi2 P-value is: 100.00%
Model Accepted by Threshold: Yes
Model Accepted Visually: No

Histogram Information for 'Mwrun15'

Normal Model Parameters:
Mean is: 1044.27
Variance is: 13828.69
RMS error is: 6.07%
Chi2 P-value is: 0.02%
Model Accepted by Threshold: No
Model Accepted Visually: No

3.14.3 Auto-covariance – Horizontal

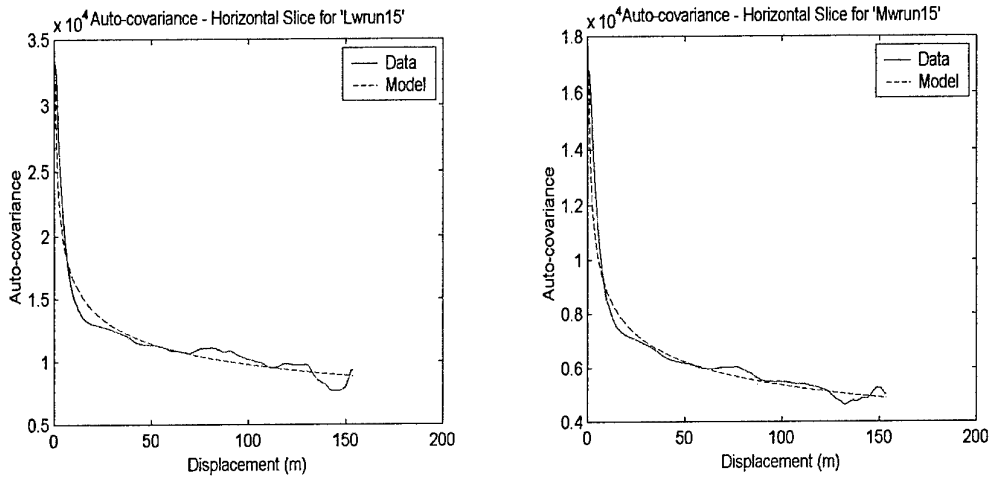

Figure 68 – Power Law Fit - Horizontal Slice of Run 15

Auto-covariance - Horizontal for 'Lwrun15'

Mean Standard deviation between images is: 1523.55
Power Law Model Parameters:
a_est is: 28049.33
b_est is: 0.00
w_est is: 0.12
RMS error is: 6.68%
Model Accepted by Threshold: No
Model Accepted Visually: Partially

Auto-covariance - Horizontal for 'Mwrun15'

Mean Standard deviation between images is: 880.74
Power Law Model Parameters:
a_est is: 16413.18
b_est is: 0.00
w_est is: 0.12
RMS error is: 5.11%

Model Accepted by Threshold: No
Model Accepted Visually: Partially

3.14.4 Auto-covariance – Vertical

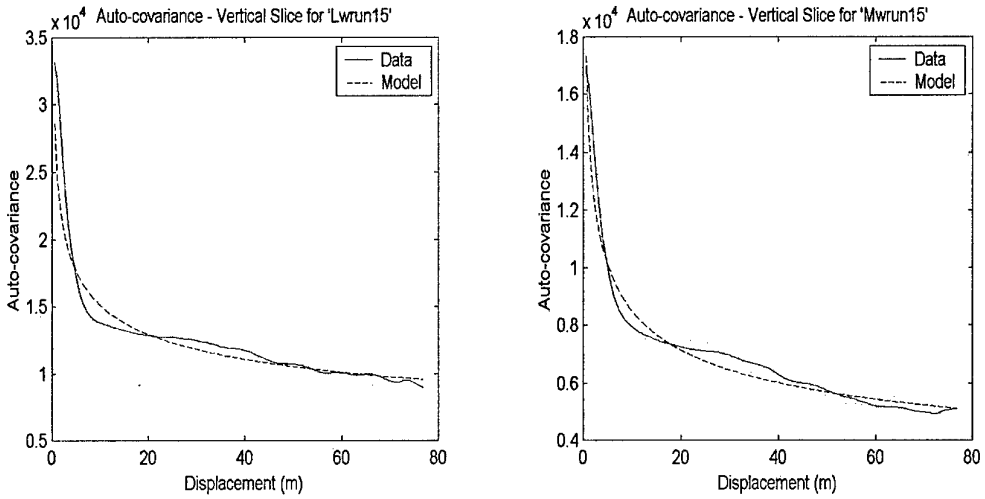

Figure 69 – Power Law Fit - Vertical Slice of Run 15

Auto-covariance - Vertical for 'Lwrun15'

Mean Standard deviation between images is: 1431.44
Power Law Model Parameters:
a_est is: 25309.82
b_est is: 0.00
w_est is: 0.11
RMS error is: 5.64%
Model Accepted by Threshold: No
Model Accepted Visually: Partially

Auto-covariance - Vertical for 'Mwrun15'

Mean Standard deviation between images is: 841.12
Power Law Model Parameters:
a_est is: 15107.65
b_est is: 0.00
w_est is: 0.12
RMS error is: 4.88%
Model Accepted by Threshold: No
Model Accepted Visually: Partially

3.14.5 Image Synthesis:

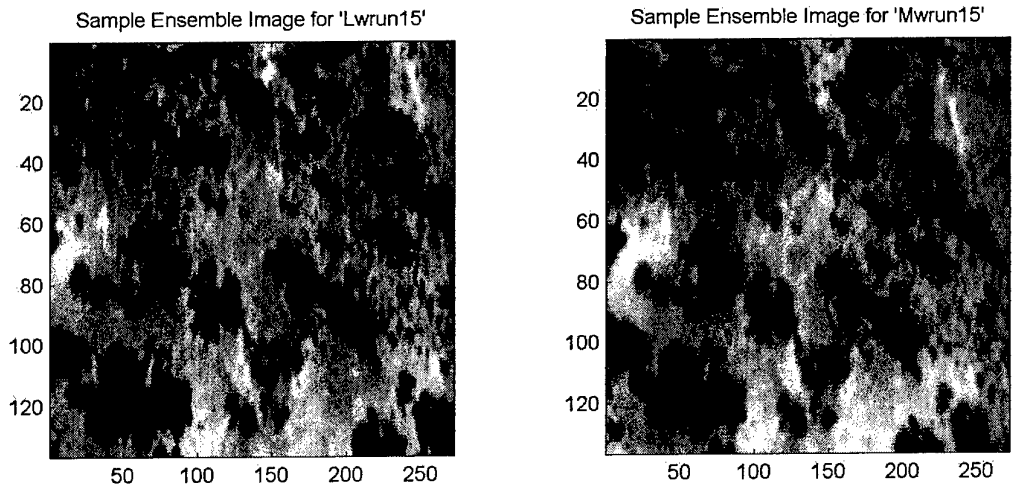

Figure 70 – Original Images from Run 15

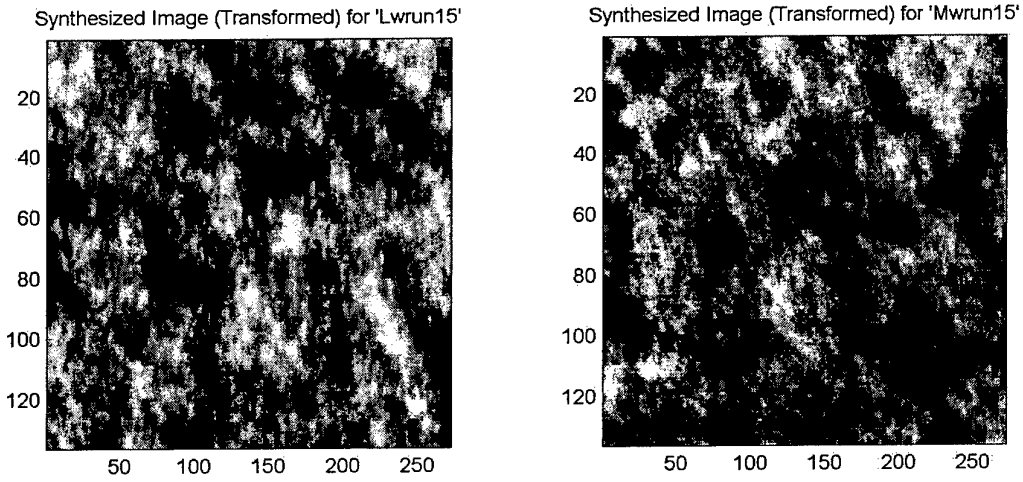

Figure 71 – Synthetic Images for Run 15

3.15 Run 16

3.15.1 General Information

Flight Date: 3-7-97 DAY
Altitude: 5K ft
Depression Angle: 60 deg.
Vegetation Classes in Run: 13, 51, 15, 4, 21
Predominate Vegetation Class: 15

Ensemble Size is: 548
Number of Valid Images is: 60
Vertical Resolution is: 0.65m
Horizontal Resolution is: 0.56m

3.15.2 Histogram

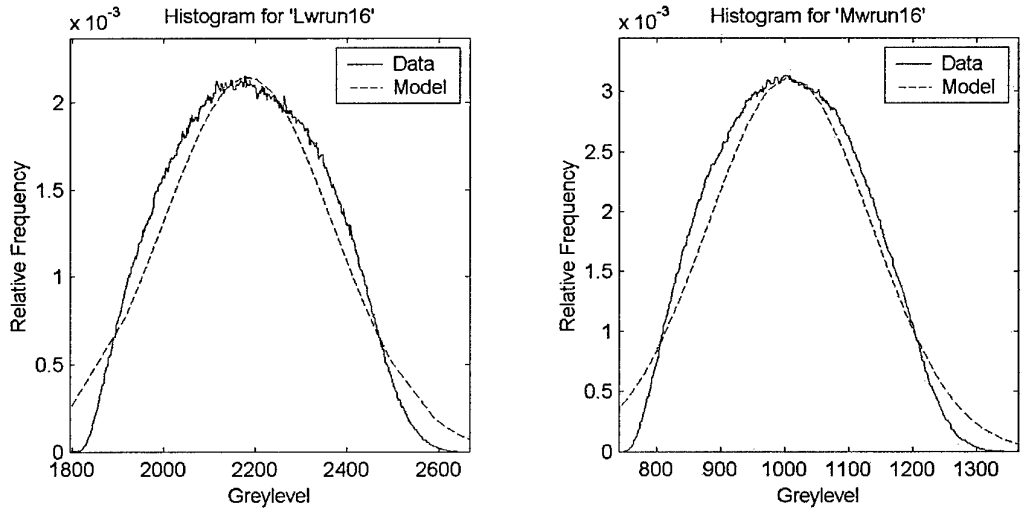

Figure 72 – Gaussian Fit – Histogram of Run 16

Histogram Information for 'Lwrun16'

Normal Model Parameters:
    Mean is: 2182.96
    Variance is: 34618.21
RMS error is: 1.63%
Chi2 P-value is: 100.00%
Model Accepted by Threshold: Yes
Model Accepted Visually: No

Histogram Information for 'Mwrun16'

Normal Model Parameters:
Mean is: 1007.99
Variance is: 16445.23
RMS error is: 2.20%
Chi2 P-value is: 100.00%
Model Accepted by Threshold: Yes
Model Accepted Visually: No

3.15.3 Auto-covariance – Horizontal

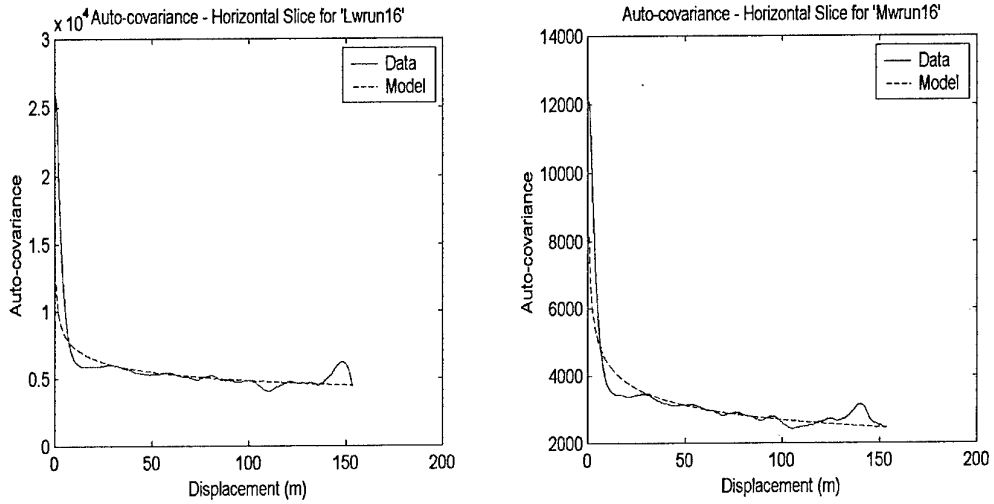

Figure 73 – Power Law Fit - Horizontal Slice of Run 16

Auto-covariance - Horizontal for 'Lwrun16'

Mean Standard deviation between images is: 1242.94
Power Law Model Parameters:
a_est is: 13110.58
b_est is: 0.00
w_est is: 0.11
RMS error is: 12.09%
Model Accepted by Threshold: No
Model Accepted Visually: No

Auto-covariance - Horizontal for 'Mwrun16'

Mean Standard deviation between images is: 654.40
Power Law Model Parameters:
a_est is: 8054.12
b_est is: 0.00
w_est is: 0.12
RMS error is: 10.14%

Model Accepted by Threshold: No
Model Accepted Visually: No

3.15.4 Auto-covariance – Vertical

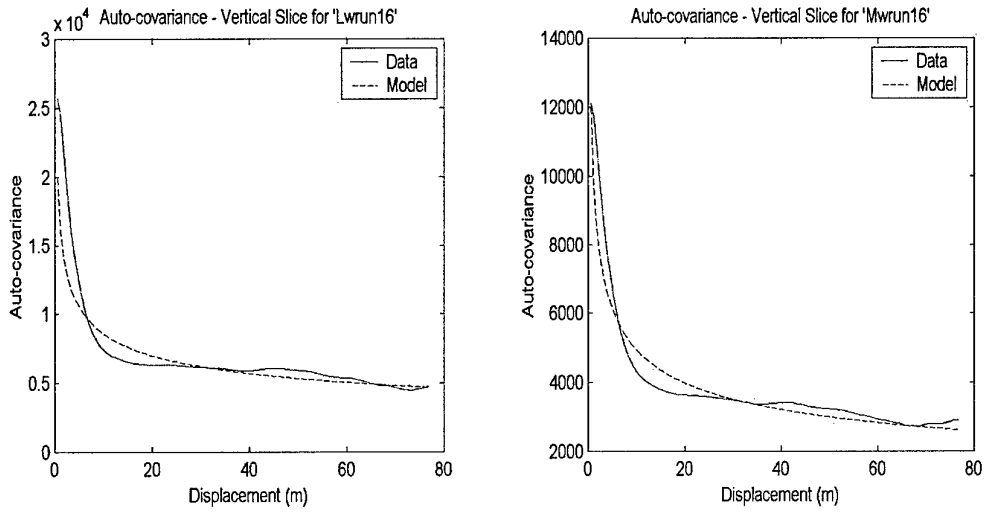

Figure 74 – Power Law Fit - Vertical Slice of Run 16

Auto-covariance - Vertical for 'Lwrun16'

Mean Standard deviation between images is: 1197.24
Power Law Model Parameters:
a_est is: 16968.82
b_est is: 0.00
w_est is: 0.15
RMS error is: 10.49%
Model Accepted by Threshold: No
Model Accepted Visually: No

Auto-covariance - Vertical for 'Mwrun16'

Mean Standard deviation between images is: 630.76
Power Law Model Parameters:
a_est is: 10116.72
b_est is: 0.00
w_est is: 0.16
RMS error is: 8.24%
Model Accepted by Threshold: No
Model Accepted Visually: No

3.15.5 Image Synthesis:

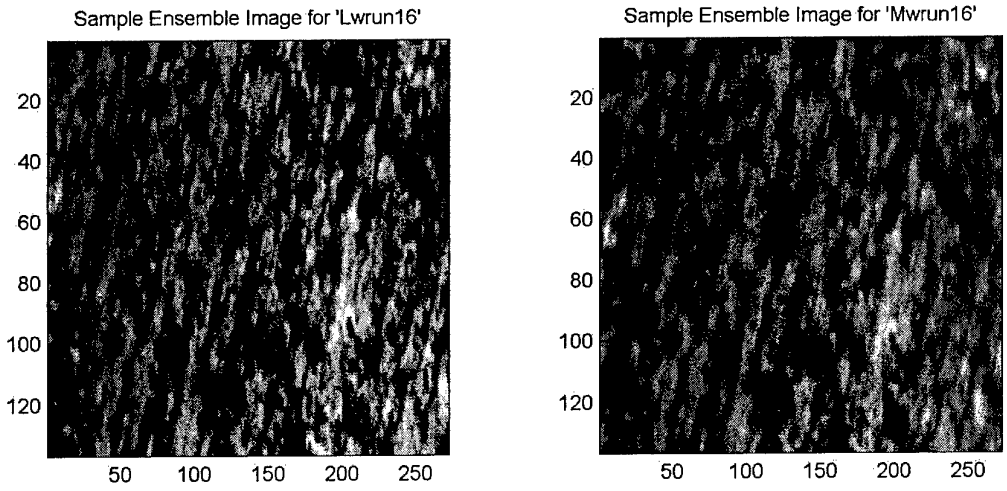

Figure 75 – Original Images from Run 16

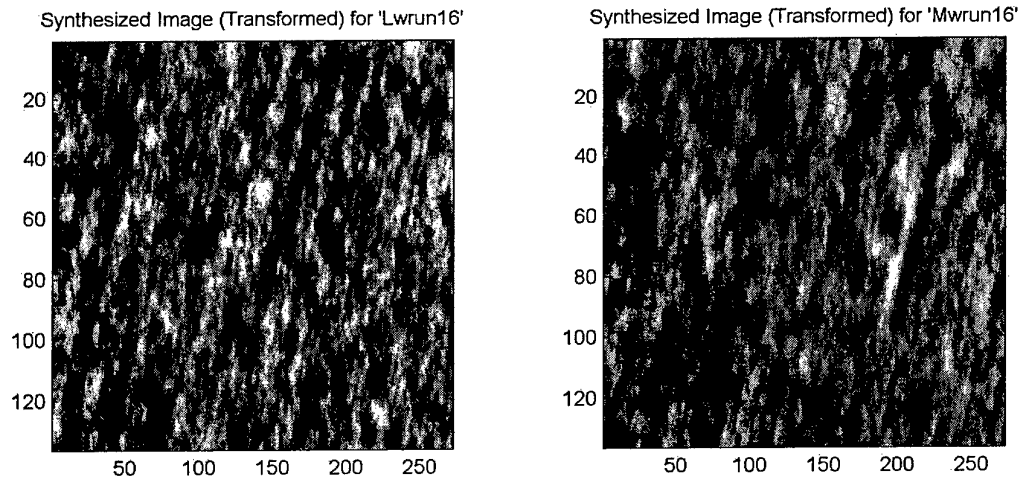

Figure 76 – Synthetic Images for Run 16

3.16 Run 17

3.16.1 General Information

Flight Date: 3-7-97 DAY
Altitude: 10K ft
Depression Angle: 60 deg.
Vegetation Classes in Run: 4, 106
Predominate Vegetation Class: 106

Ensemble Size is: 200
Number of Valid Images is: 50
Vertical Resolution is: 1.30m
Horizontal Resolution is: 1.13m

3.16.2 Histogram

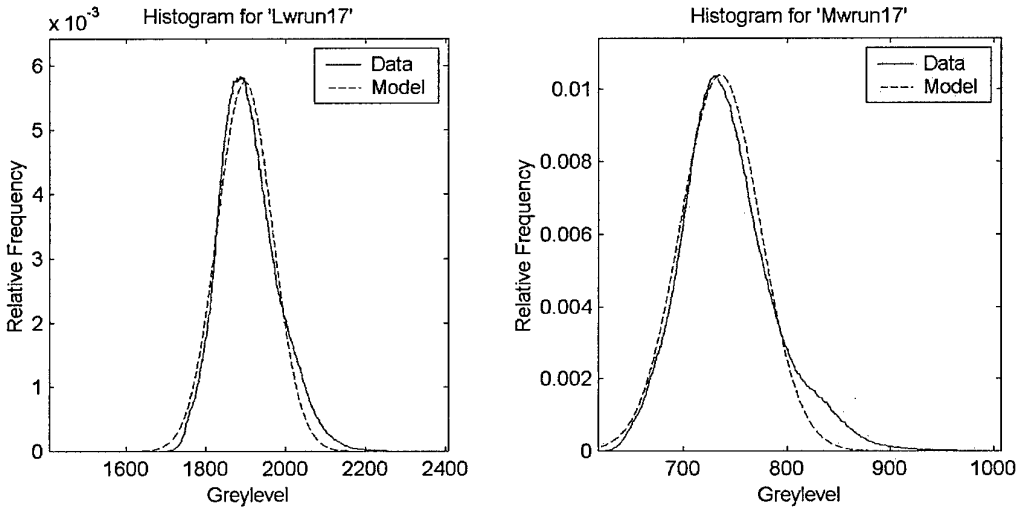

Figure 77 – Gaussian Fit – Histogram of Run 17

Histogram Information for 'Lwrun17'

Normal Model Parameters:
    Mean is: 1898.02
    Variance is: 4800.00
RMS error is: 2.24%
Chi2 P-value is: 100.00%
Model Accepted by Threshold: Yes
Model Accepted Visually: Yes

Histogram Information for 'Mwrun17'

Normal Model Parameters:
Mean is: 735.49
Variance is: 1473.30
RMS error is: 4.73%
Chi2 P-value is: 0.00%
Model Accepted by Threshold: No
Model Accepted Visually: Partially

3.16.3 Auto-covariance – Horizontal

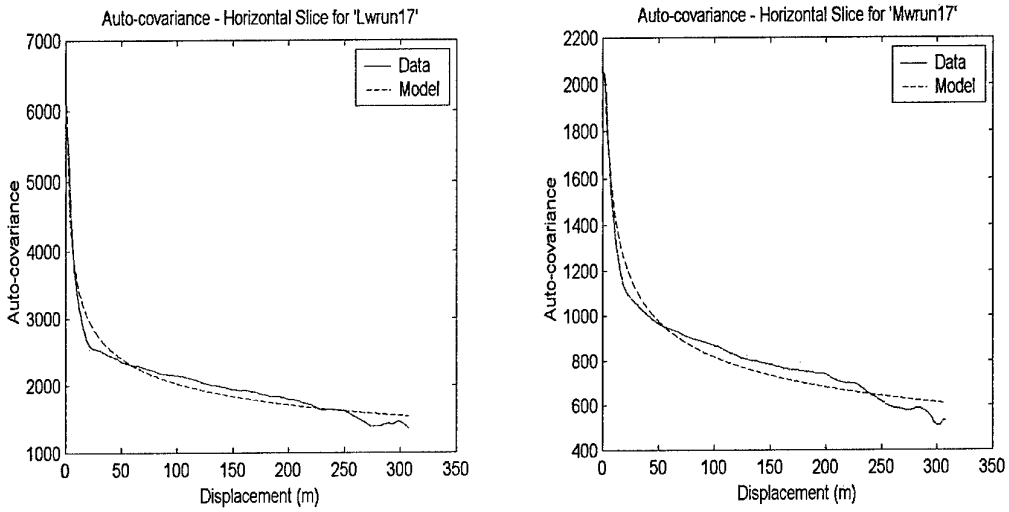

Figure 78 – Power Law Fit - Horizontal Slice of Run 17

Auto-covariance - Horizontal for 'Lwrun17'

Mean Standard deviation between images is: 546.37
Power Law Model Parameters:
a_est is: 5724.68
b_est is: 0.00
w_est is: 0.11
RMS error is: 6.50%
Model Accepted by Threshold: No
Model Accepted Visually: Partially

Auto-covariance - Horizontal for 'Mwrun17'

Mean Standard deviation between images is: 251.93
Power Law Model Parameters:
a_est is: 2248.62
b_est is: 0.00
w_est is: 0.11
RMS error is: 7.60%

Model Accepted by Threshold: No
Model Accepted Visually: Partially

3.16.4 Auto-covariance – Vertical

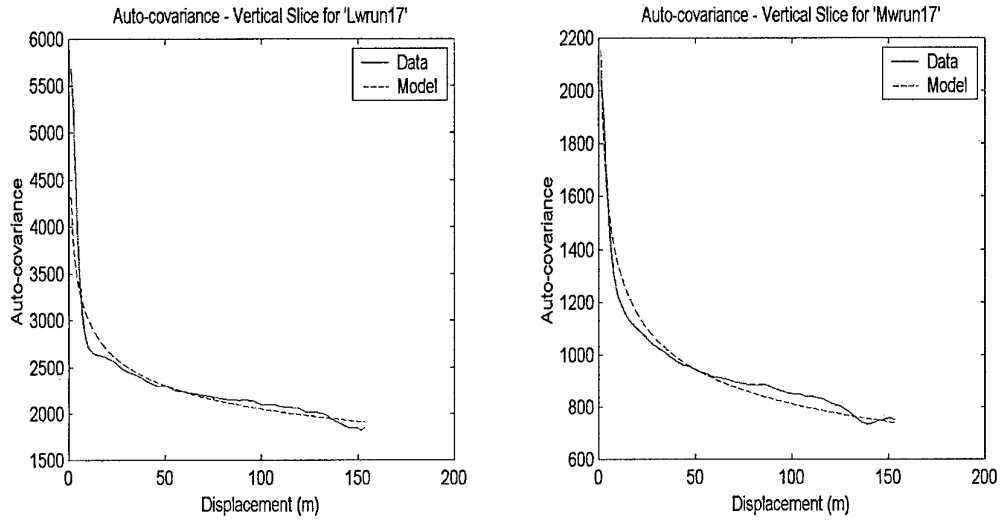

Figure 79 – Power Law Fit - Vertical Slice of Run 17

Auto-covariance - Vertical for 'Lwrun17'

Mean Standard deviation between images is: 560.96
Power Law Model Parameters:
a_est is: 4437.64
b_est is: 0.00
w_est is: 0.08
RMS error is: 4.95%
Model Accepted by Threshold: No
Model Accepted Visually: No

Auto-covariance - Vertical for 'Mwrun17'

Mean Standard deviation between images is: 255.09
Power Law Model Parameters:
a_est is: 2223.63
b_est is: 0.00
w_est is: 0.11
RMS error is: 3.99%
Model Accepted by Threshold: No
Model Accepted Visually: Partially

3.16.5 Image Synthesis:

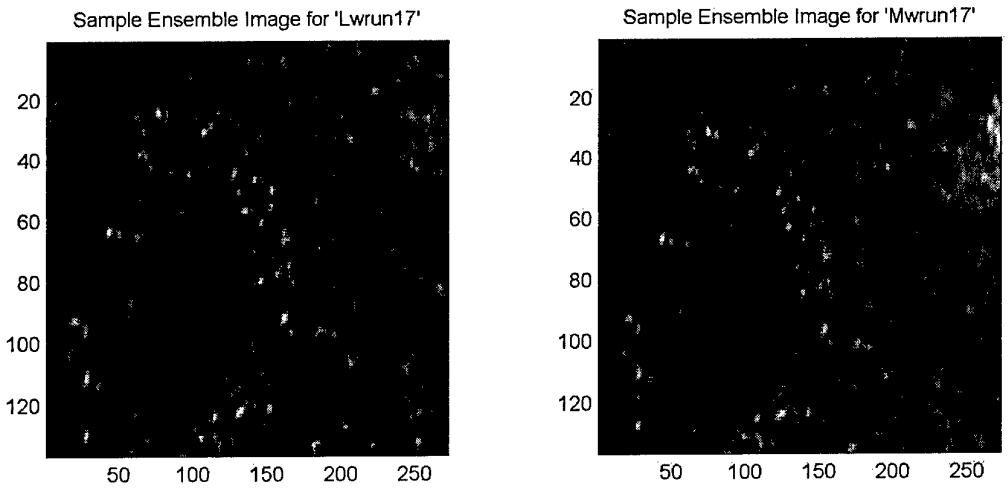

Figure 80 – Original Images from Run 17

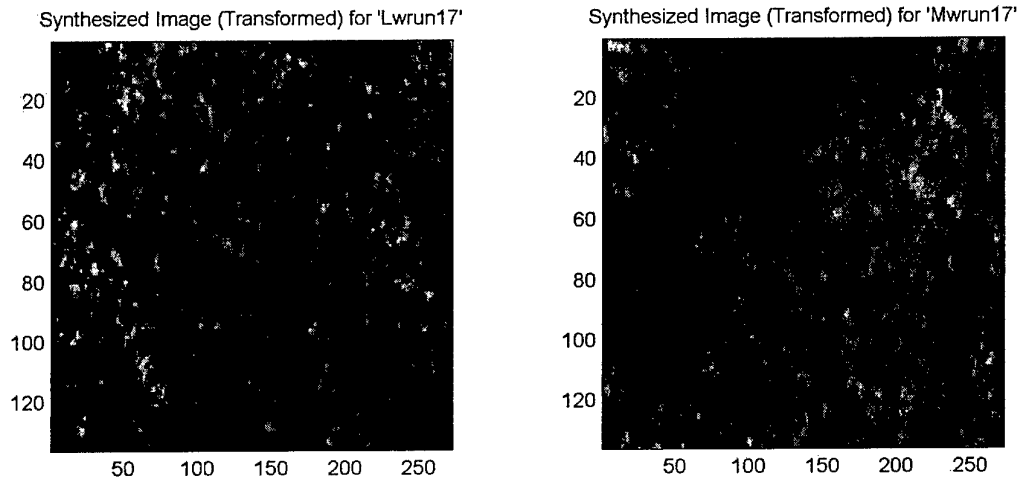

Figure 81 – Synthetic Images for Run 17

3.17 Run 18

3.17.1 General Information

Flight Date: 3-7-97 DAY
Altitude: 10K ft
Depression Angle: 60 deg.
Vegetation Classes in Run: 53, 4, 106
Predominate Vegetation Class: 53

Ensemble Size is: 251
Number of Valid Images is: 26
Vertical Resolution is: 1.30m
Horizontal Resolution is: 1.13m

3.17.2 Histogram

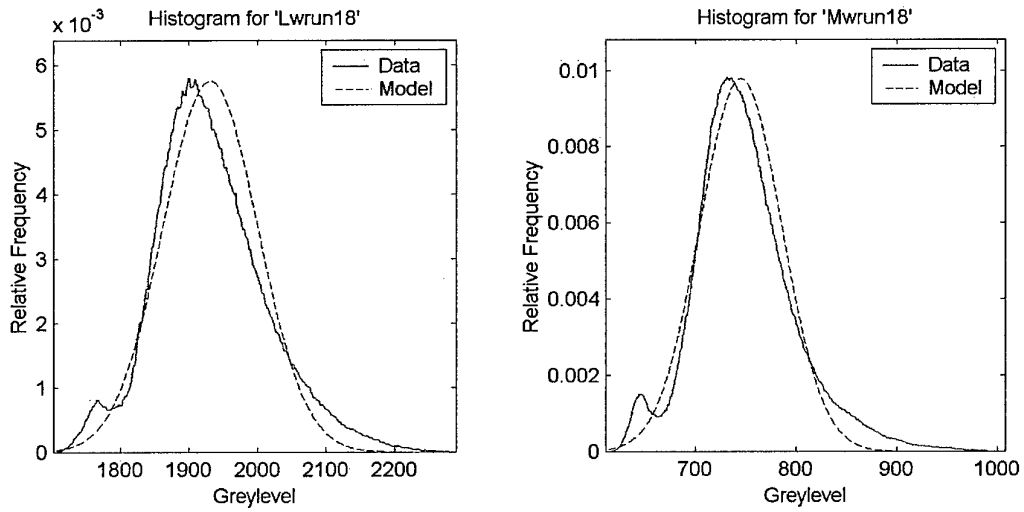

Figure 82 – Gaussian Fit – Histogram of Run 18

Histogram Information for 'Lwrun18'

Normal Model Parameters:
    Mean is: 1931.10
    Variance is: 4800.00
RMS error is: 4.56%
Chi2 P-value is: 100.00%
Model Accepted by Threshold: Yes
Model Accepted Visually: No

Histogram Information for 'Mwrun18'

Normal Model Parameters:
Mean is: 744.81
Variance is: 1663.81
RMS error is: 6.01%
Chi2 P-value is: 0.13%
Model Accepted by Threshold: No
Model Accepted Visually: No

3.17.3 Auto-covariance - Horizontal

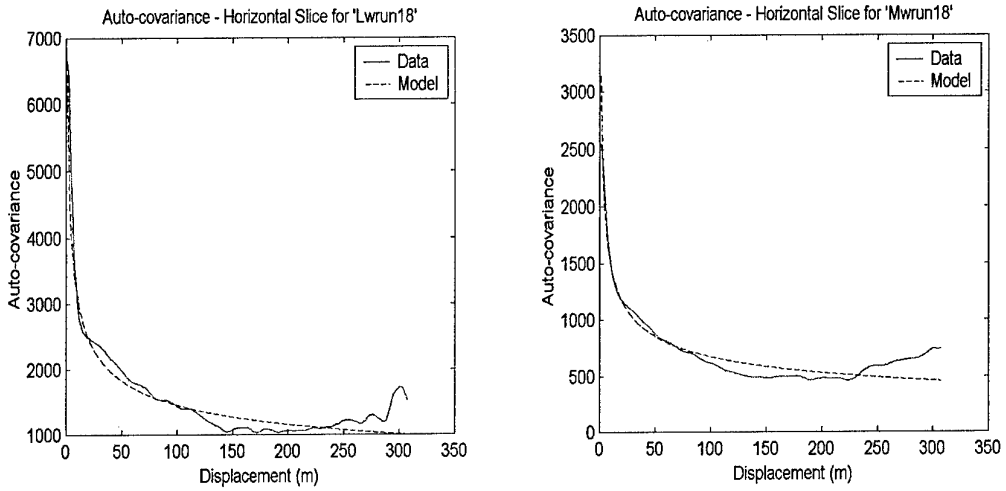

Figure 83 – Power Law Fit - Horizontal Slice of Run 18

Auto-covariance - Horizontal for 'Lwrun18'

Mean Standard deviation between images is: 1036.54
Power Law Model Parameters:
a_est is: 7730.06
b_est is: 0.00
w_est is: 0.18
RMS error is: 13.85%
Model Accepted by Threshold: No
Model Accepted Visually: Partially

Auto-covariance - Horizontal for 'Mwrun18'

Mean Standard deviation between images is: 424.45
Power Law Model Parameters:
a_est is: 3631.64
b_est is: 2.40
w_est is: 0.18
RMS error is: 16.44%
Model Accepted by Threshold: No

Model Accepted Visually: Partially

3.17.4 Auto-covariance – Vertical

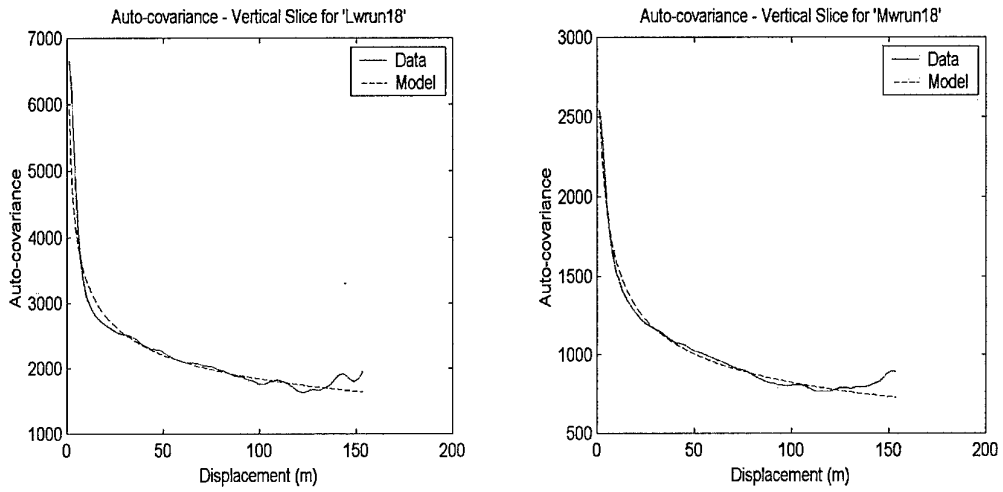

Figure 84 – Power Law Fit - Vertical Slice of Run 18

Auto-covariance - Vertical for 'Lwrun18'

Mean Standard deviation between images is: 1007.21
Power Law Model Parameters:
a_est is: 6164.67
b_est is: 0.00
w_est is: 0.13
RMS error is: 5.47%
Model Accepted by Threshold: No
Model Accepted Visually: Yes

Auto-covariance - Vertical for 'Mwrun18'

Mean Standard deviation between images is: 406.39
Power Law Model Parameters:
a_est is: 3113.55
b_est is: 1.67
w_est is: 0.14
RMS error is: 5.00%
Model Accepted by Threshold: No
Model Accepted Visually: Yes

3.17.5 Image Synthesis:

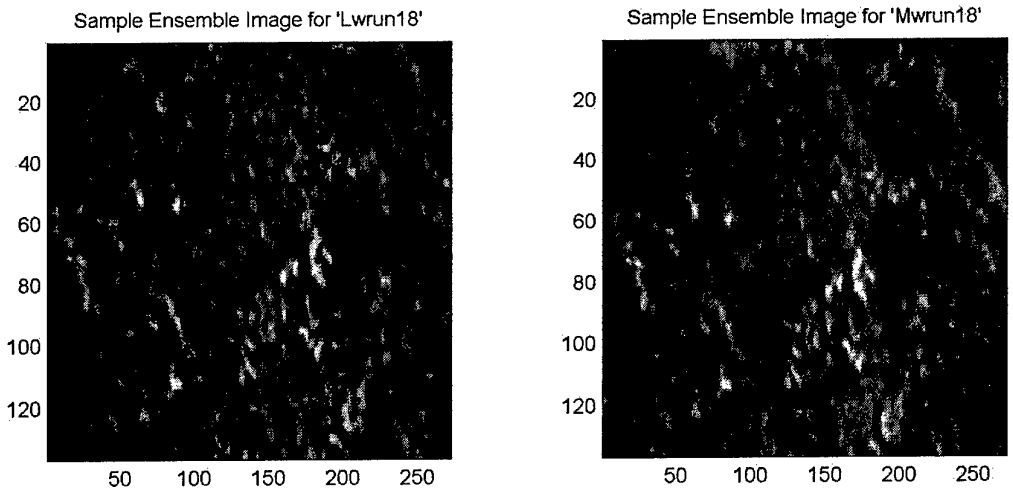

Figure 85 – Original Images from Run 18

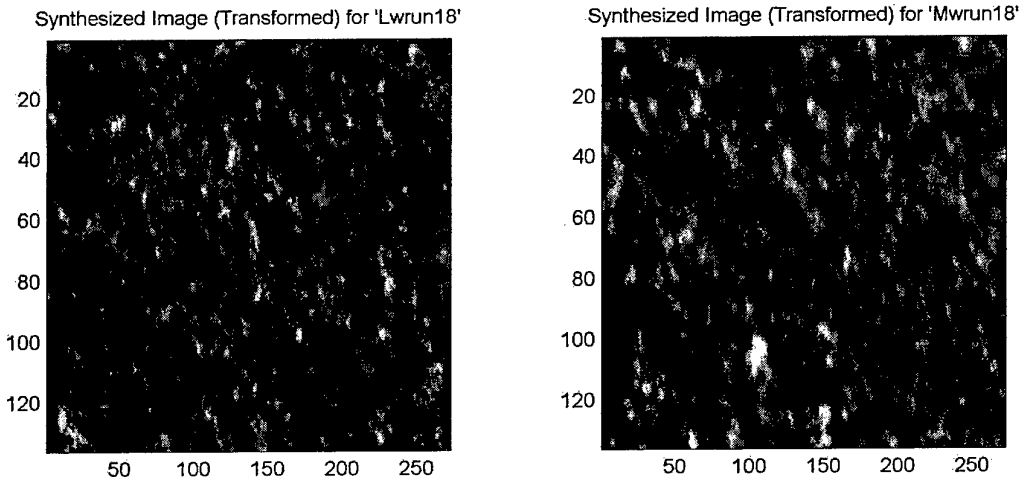

Figure 86 – Synthetic Images for Run 18

3.18 Run 19

3.18.1 General Information

Flight Date: 3-7-97 DAY
Altitude: 5K ft
Depression Angle: 60 deg.
Vegetation Classes in Run: 4, 106
Predominate Vegetation Class: 106

Ensemble Size is: 414
Number of Valid Images is: 103
Vertical Resolution is: 0.65m
Horizontal Resolution is: 0.56m

3.18.2 Histogram

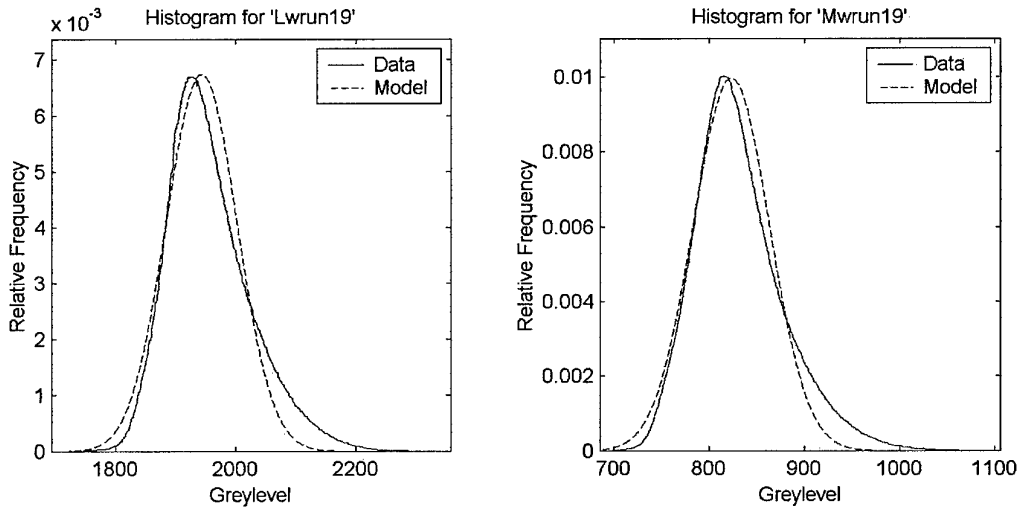

Figure 87 – Gaussian Fit – Histogram of Run 19

Histogram Information for 'Lwrun19'

Normal Model Parameters:
    Mean is: 1942.97
    Variance is: 3500.00
RMS error is: 4.03%
Chi2 P-value is: 89.65%
Model Accepted by Threshold: No
Model Accepted Visually: No

Histogram Information for 'Mwrun19'

Normal Model Parameters:
Mean is: 823.38
Variance is: 1600.00
RMS error is: 5.09%
Chi2 P-value is: 0.00%
Model Accepted by Threshold: No
Model Accepted Visually: No

3.18.3 Auto-covariance – Horizontal

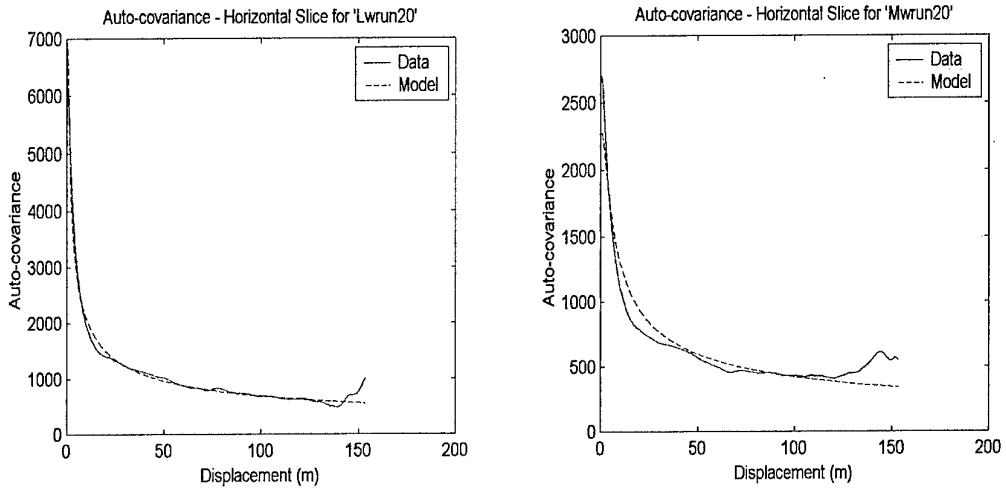

Figure 88 – Power Law Fit - Horizontal Slice of Run 19

Auto-covariance - Horizontal for 'Lwrun19'

Mean Standard deviation between images is: 186.04
Power Law Model Parameters:
a_est is: 4792.95
b_est is: 0.00
w_est is: 0.18
RMS error is: 4.10%
Model Accepted by Threshold: No
Model Accepted Visually: Yes

Auto-covariance - Horizontal for 'Mwrun19'

Mean Standard deviation between images is: 101.75
Power Law Model Parameters:
a_est is: 2483.05
b_est is: 0.00
w_est is: 0.17
RMS error is: 3.54%

Model Accepted by Threshold: No
Model Accepted Visually: Partially

3.18.4 Auto-covariance – Vertical

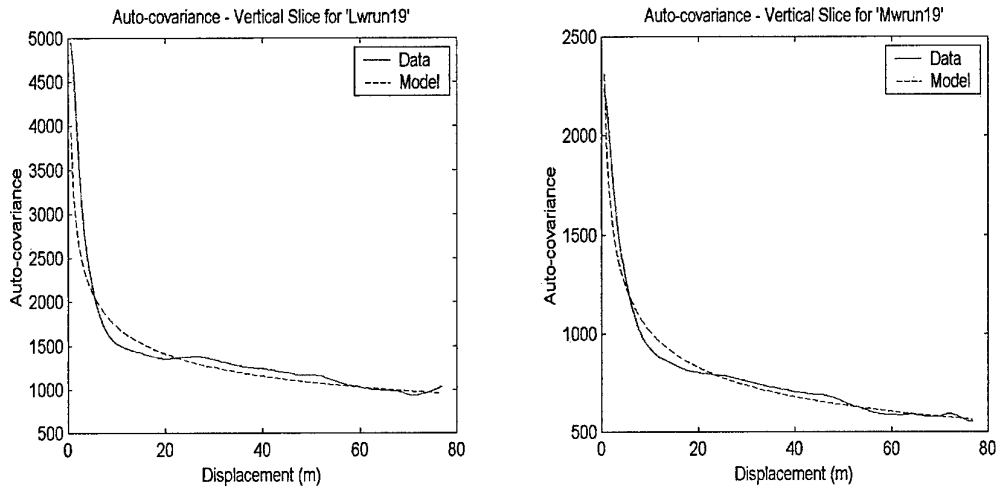

Figure 89 – Power Law Fit - Vertical Slice of Run 19

Auto-covariance - Vertical for 'Lwrun19'

Mean Standard deviation between images is: 181.17
Power Law Model Parameters:
a_est is: 3352.59
b_est is: 0.00
w_est is: 0.14
RMS error is: 7.81%
Model Accepted by Threshold: No
Model Accepted Visually: Partially

Auto-covariance - Vertical for 'Mwrun19'

Mean Standard deviation between images is: 101.26
Power Law Model Parameters:
a_est is: 1970.02
b_est is: 0.00
w_est is: 0.14
RMS error is: 4.61%
Model Accepted by Threshold: No
Model Accepted Visually: Partially

3.18.5 Image Synthesis:

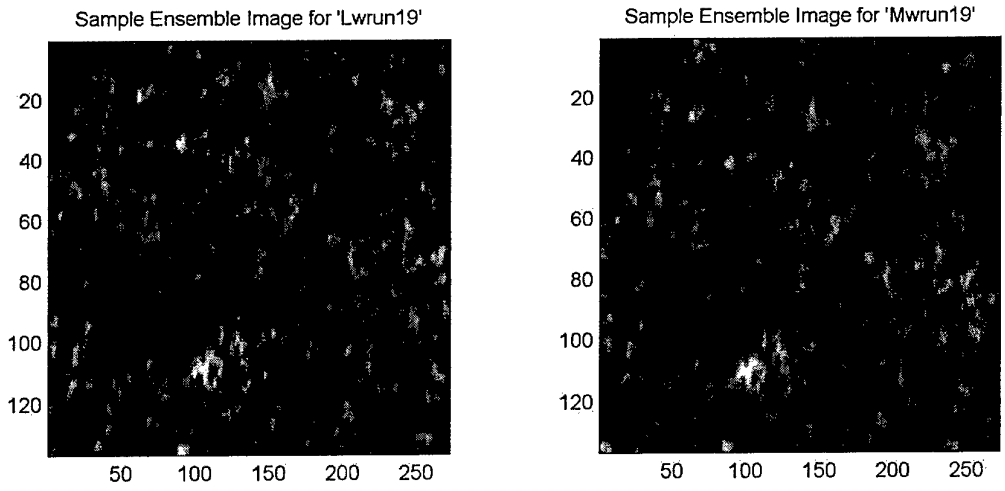

Figure 90 – Original Images from Run 19

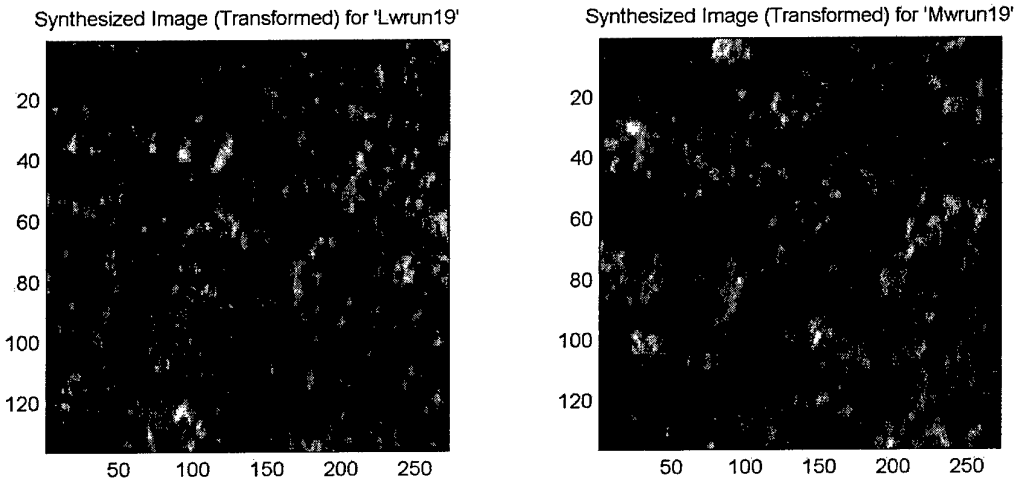

Figure 91 – Synthetic Images for Run 19

3.19 Run 20

3.19.1 General Information

Flight Date: 3-7-97 DAY
Altitude: 5K ft
Depression Angle: 60 deg.
Vegetation Classes in Run: 53, 4, 106
Predominate Vegetation Class: 53

Ensemble Size is: 495
Number of Valid Images is: 65
Vertical Resolution is: 0.65m
Horizontal Resolution is: 0.56m

3.19.2 Histogram

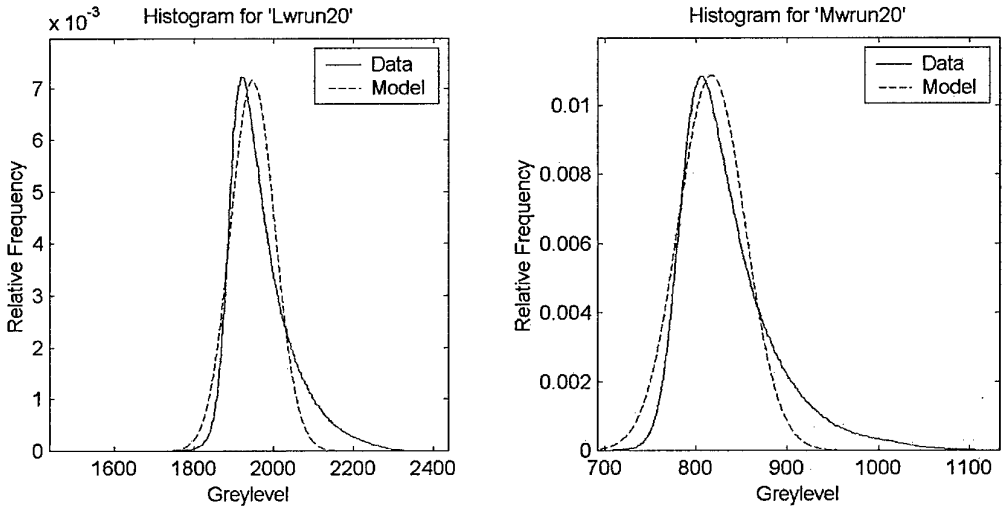

Figure 92 – Gaussian Fit – Histogram of Run 20

Histogram Information for 'Lwrun20'

Normal Model Parameters:
    Mean is: 1947.65
    Variance is: 3100.00
RMS error is: 5.28%
Chi2 P-value is: 0.00%
Model Accepted by Threshold: No
Model Accepted Visually: No

Histogram Information for 'Mwrun20'

Normal Model Parameters:
Mean is: 817.25
Variance is: 1350.00
RMS error is: 8.38%
Chi2 P-value is: 0.00%
Model Accepted by Threshold: No
Model Accepted Visually: No

3.19.3 Auto-covariance – Horizontal

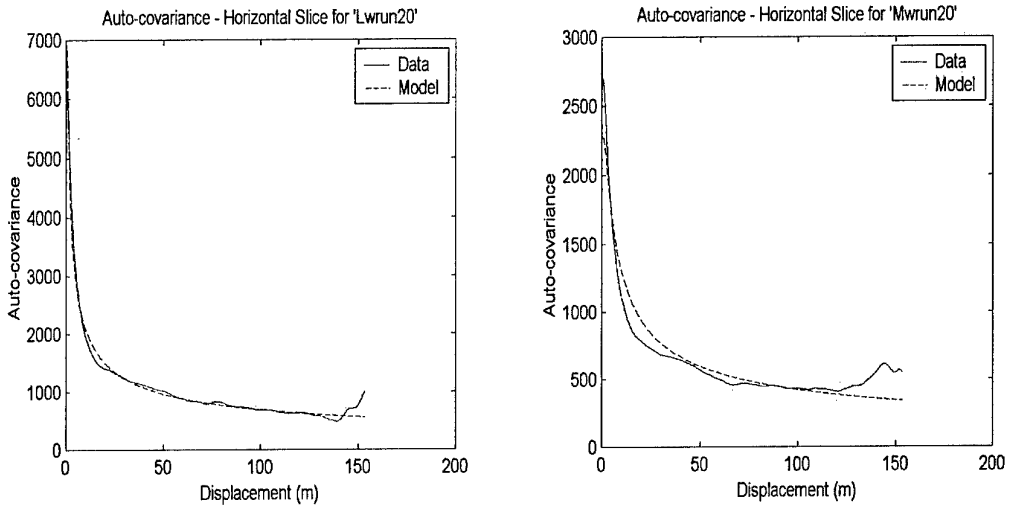

Figure 93 – Power Law Fit - Horizontal Slice of Run 20

Auto-covariance - Horizontal for 'Lwrun20'

Mean Standard deviation between images is: 211.92
Power Law Model Parameters:
a_est is: 6632.03
b_est is: 0.00
w_est is: 0.25
RMS error is: 9.38%
Model Accepted by Threshold: No
Model Accepted Visually: Yes

Auto-covariance - Horizontal for 'Mwrun20'

Mean Standard deviation between images is: 131.21
Power Law Model Parameters:
a_est is: 2656.06
b_est is: 0.00
w_est is: 0.19
RMS error is: 12.69%
Model Accepted by Threshold: No
Model Accepted Visually: Partially

3.19.4 Auto-covariance – Vertical

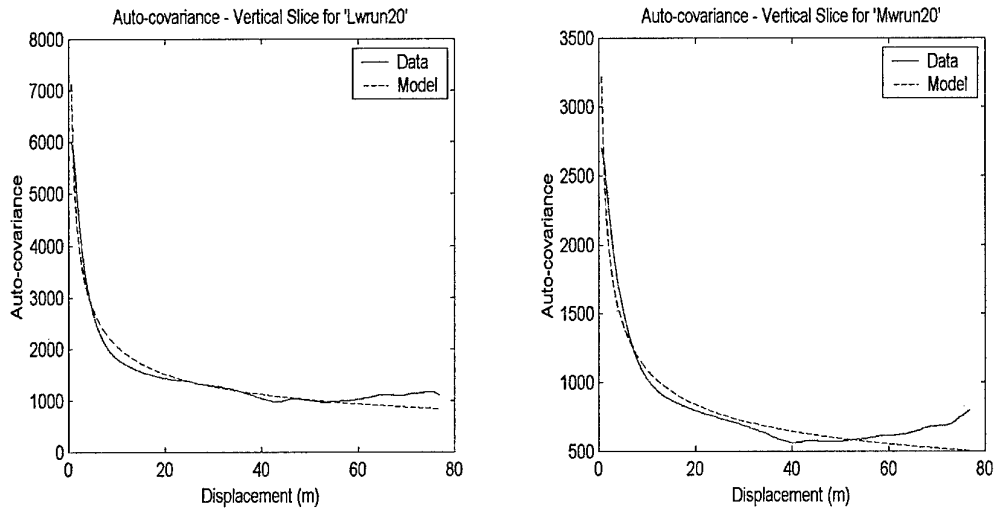

Figure 94 – Power Law Fit - Vertical Slice of Run 20

Auto-covariance - Vertical for 'Lwrun20'

Mean Standard deviation between images is: 214.62
Power Law Model Parameters:
a_est is: 5603.16
b_est is: 0.00
w_est is: 0.22
RMS error is: 11.43%
Model Accepted by Threshold: No
Model Accepted Visually: Yes

Auto-covariance - Vertical for 'Mwrun20'

Mean Standard deviation between images is: 134.95
Power Law Model Parameters:
a_est is: 2612.09
b_est is: 0.00
w_est is: 0.19
RMS error is: 12.77%
Model Accepted by Threshold: No
Model Accepted Visually: Partially

3.19.5 Image Synthesis:

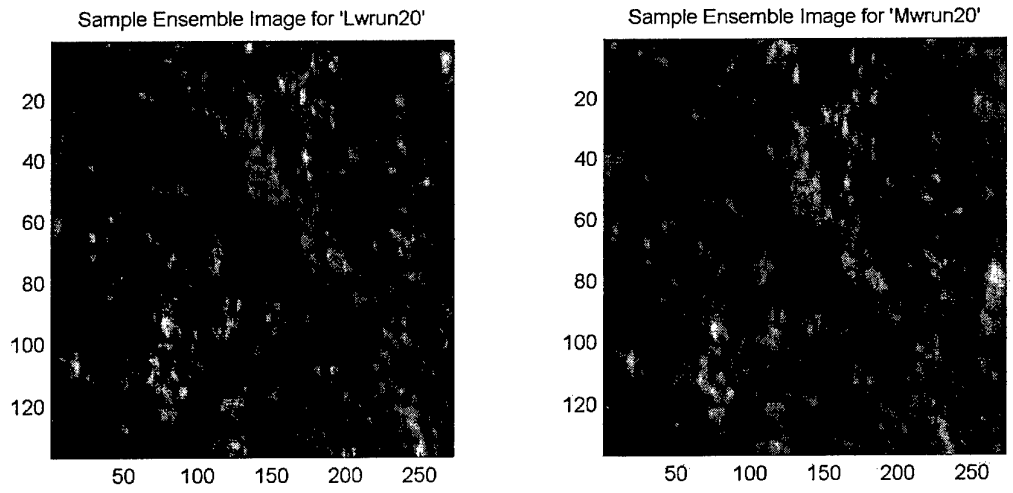

Figure 95 – Original Images from Run 20

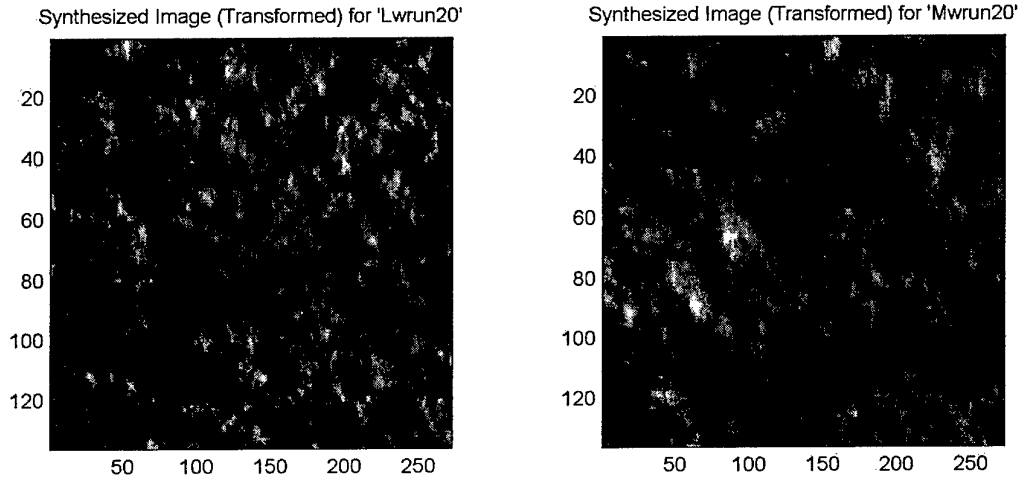

Figure 96 – Synthetic Images for Run 20

3.20 Run 21

3.20.1 General Information

Flight Date: 3-7-97 DAY
Altitude: 10K ft
Depression Angle: 60 deg.
Vegetation Classes in Run: 18, 106
Predominate Vegetation Class: 106

Ensemble Size is: 150
Number of Valid Images is: 73
Vertical Resolution is: 1.30m
Horizontal Resolution is: 1.13m

3.20.2 Histogram

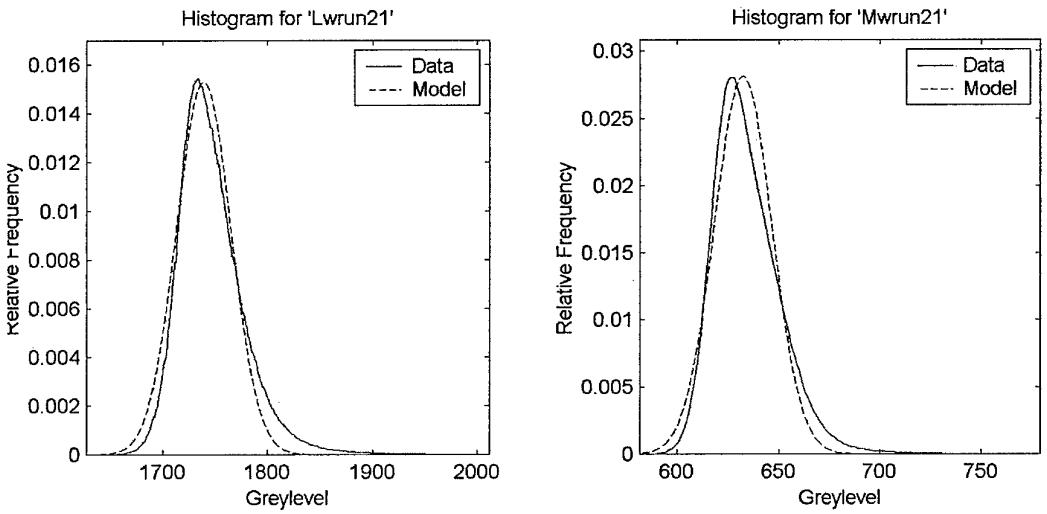

Figure 97 – Gaussian Fit – Histogram of Run 21

Histogram Information for 'Lwrun21'

Normal Model Parameters:
    Mean is: 1738.81
    Variance is: 680.00
RMS error is: 6.88%
Chi2 P-value is: 0.00%
Model Accepted by Threshold: No
Model Accepted Visually: No

Histogram Information for 'Mwrun21'

Normal Model Parameters:
Mean is: 632.47
Variance is: 201.06
RMS error is: 15.70%
Chi2 P-value is: 0.00%
Model Accepted by Threshold: No
Model Accepted Visually: No

3.20.3 Auto-covariance – Horizontal

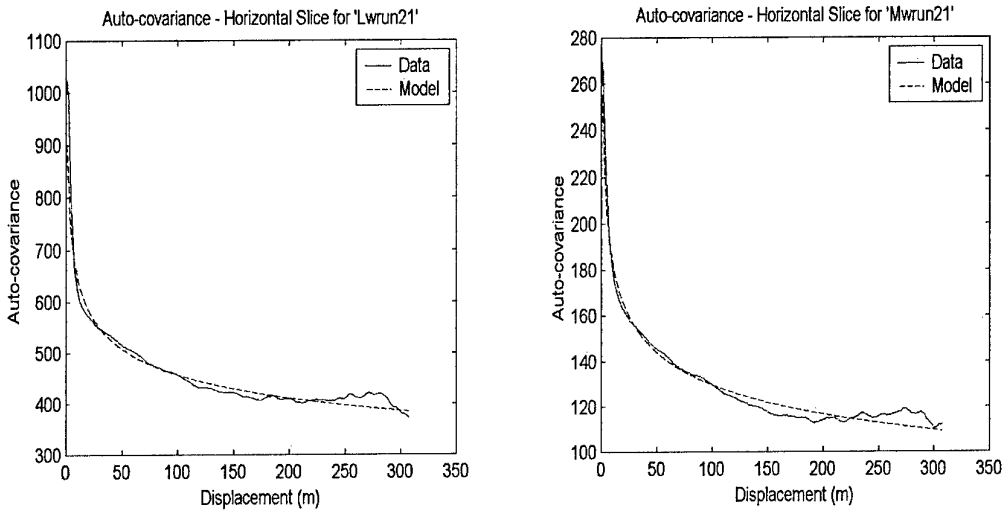

Figure 98 – Power Law Fit - Horizontal Slice of Run 21

Auto-covariance - Horizontal for 'Lwrun21'

Mean Standard deviation between images is: 94.50
Power Law Model Parameters:
a_est is: 951.44
b_est is: 0.00
w_est is: 0.08
RMS error is: 3.13%
Model Accepted by Threshold: No
Model Accepted Visually: Yes

Auto-covariance - Horizontal for 'Mwrun21'

Mean Standard deviation between images is: 21.47
Power Law Model Parameters:
a_est is: 274.83
b_est is: 0.00
w_est is: 0.08
RMS error is: 3.10%
Model Accepted by Threshold: No
Model Accepted Visually: Yes

3.20.4 Auto-covariance – Vertical

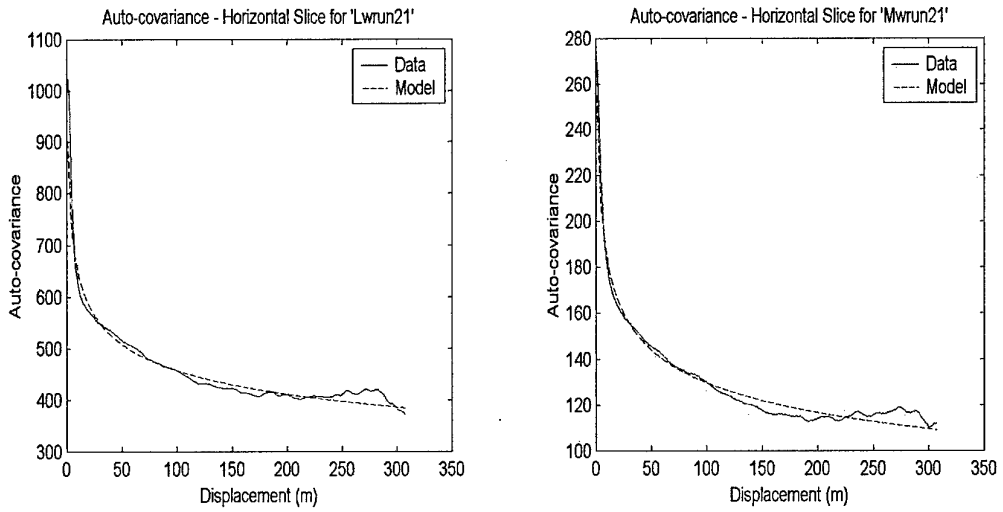

Figure 99 – Power Law Fit - Vertical Slice of Run 21

Auto-covariance - Vertical for 'Lwrun21'

Mean Standard deviation between images is: 89.90
Power Law Model Parameters:
a_est is: 971.88
b_est is: 0.00
w_est is: 0.09
RMS error is: 3.27%
Model Accepted by Threshold: No
Model Accepted Visually: Yes

Auto-covariance - Vertical for 'Mwrun21'

Mean Standard deviation between images is: 20.34
Power Law Model Parameters:
a_est is: 275.17
b_est is: 0.00
w_est is: 0.09
RMS error is: 2.33%
Model Accepted by Threshold: Yes
Model Accepted Visually: Yes

3.20.5 Image Synthesis:

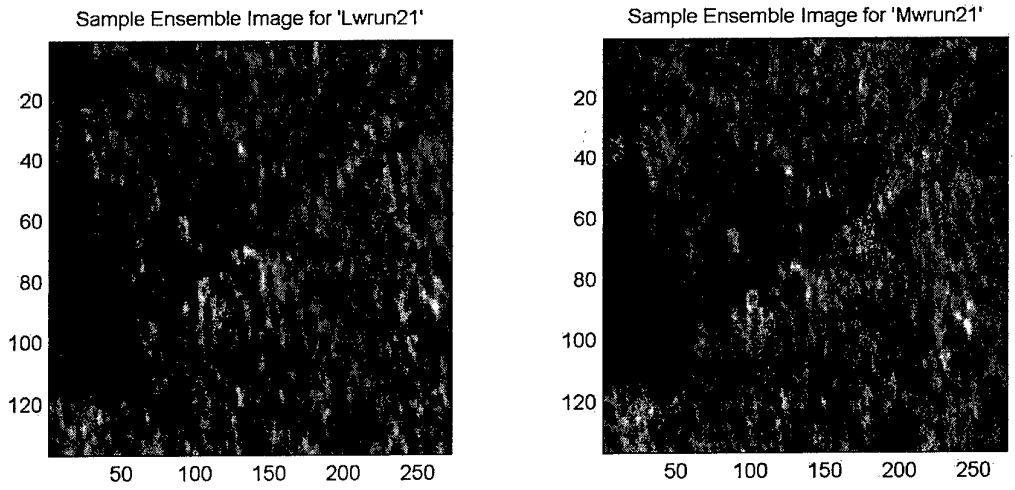

Figure 100 – Original Images from Run 21

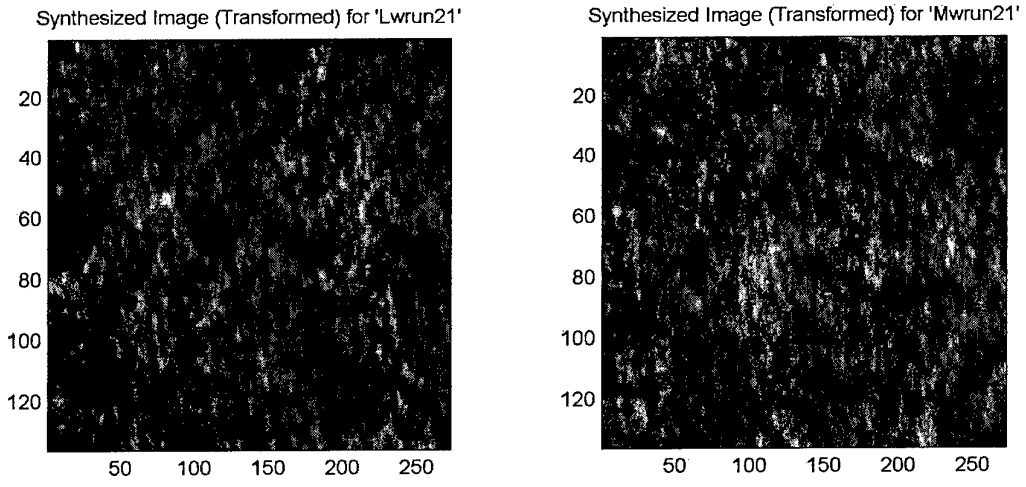

Figure 101 – Synthetic Images for Run 21

3.21 Runs 22-23

3.21.1 General Information

Flight Date: 3-7-97 DAY
Altitude: 10K ft
Depression Angle: 60 deg.
Vegetation Classes in Run: 106, 3, 47, 3, 105
Predominate Vegetation Class: 3

Ensemble Size is: 233
Number of Valid Images is: 233
Vertical Resolution is: 1.30m
Horizontal Resolution is: 1.13m

3.21.2 Histogram

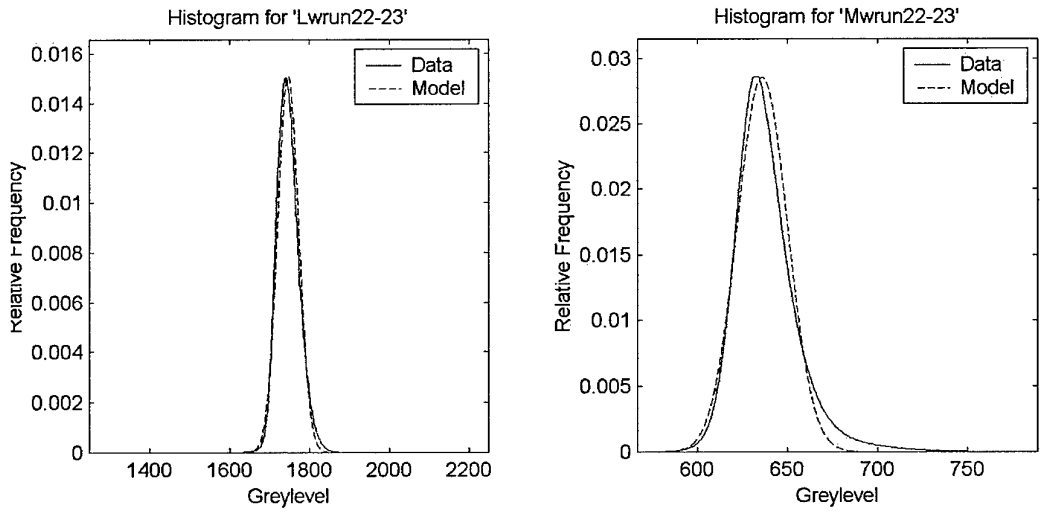

Figure 102 – Gaussian Fit – Histogram of Runs 22-23

Histogram Information for 'Lwrun22-23'

Normal Model Parameters:
    Mean is: 1745.80
    Variance is: 700.00
RMS error is: 3.68%
Chi2 P-value is: 99.99%
Model Accepted by Threshold: Yes
Model Accepted Visually: Yes

Histogram Information for 'Mwrun22-23'

Normal Model Parameters:
Mean is: 636.13
Variance is: 195.00
RMS error is: 11.87%
Chi2 P-value is: 0.00%
Model Accepted by Threshold: No
Model Accepted Visually: No

3.21.3 Auto-covariance – Horizontal

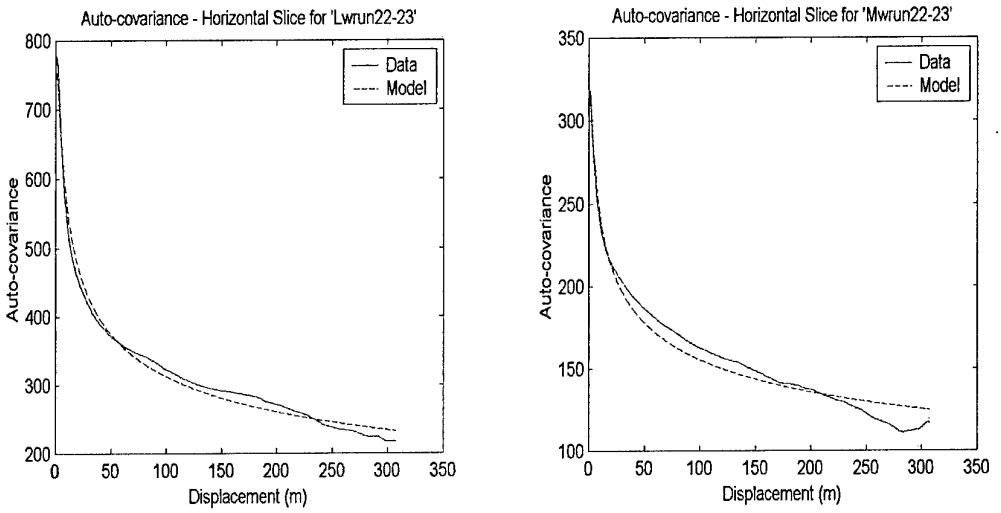

Figure 103 – Power Law Fit - Horizontal Slice of Runs 22-23

Auto-covariance - Horizontal for 'Lwrun22-23'

Mean Standard deviation between images is: 36.44
Power Law Model Parameters:
a_est is: 941.40
b_est is: 0.00
w_est is: 0.12
RMS error is: 4.31
Model Accepted by Threshold: No
Model Accepted Visually: Partially

Auto-covariance - Horizontal for 'Mwrun22-23'

Mean Standard deviation between images is: 21.43
Power Law Model Parameters:
a_est is: 360.60
b_est is: 0.00
w_est is: 0.09
RMS error is: 6.33
Model Accepted by Threshold: No
Model Accepted Visually: Partially

3.21.4 Auto-covariance – Vertical

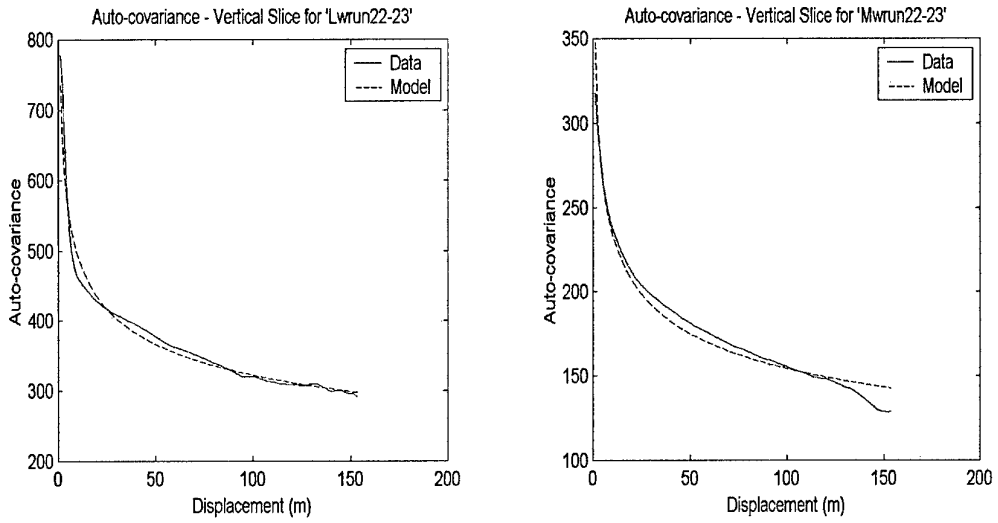

Figure 104 – Power Law Fit - Vertical Slice of Runs 22-23

Auto-covariance - Vertical for 'Lwrun22-23'

Mean Standard deviation between images is: 38.54
Power Law Model Parameters:
a_est is: 757.02
b_est is: 0.00
w_est is: 0.09
RMS error is: 2.51%
Model Accepted by Threshold: Yes
Model Accepted Visually: Partially

Auto-covariance - Vertical for 'Mwrun22-23'

Mean Standard deviation between images is: 22.22
Power Law Model Parameters:
a_est is: 357.42
b_est is: 0.00
w_est is: 0.09
RMS error is: 3.95%
Model Accepted by Threshold: No
Model Accepted Visually: Partially

3.21.5 Image Synthesis:

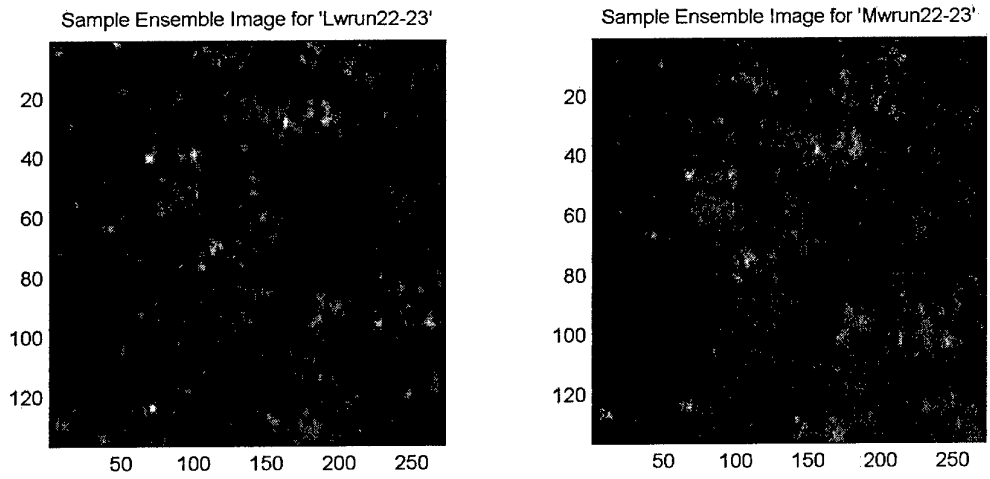

Figure 105 – Original Images from Runs 22-23

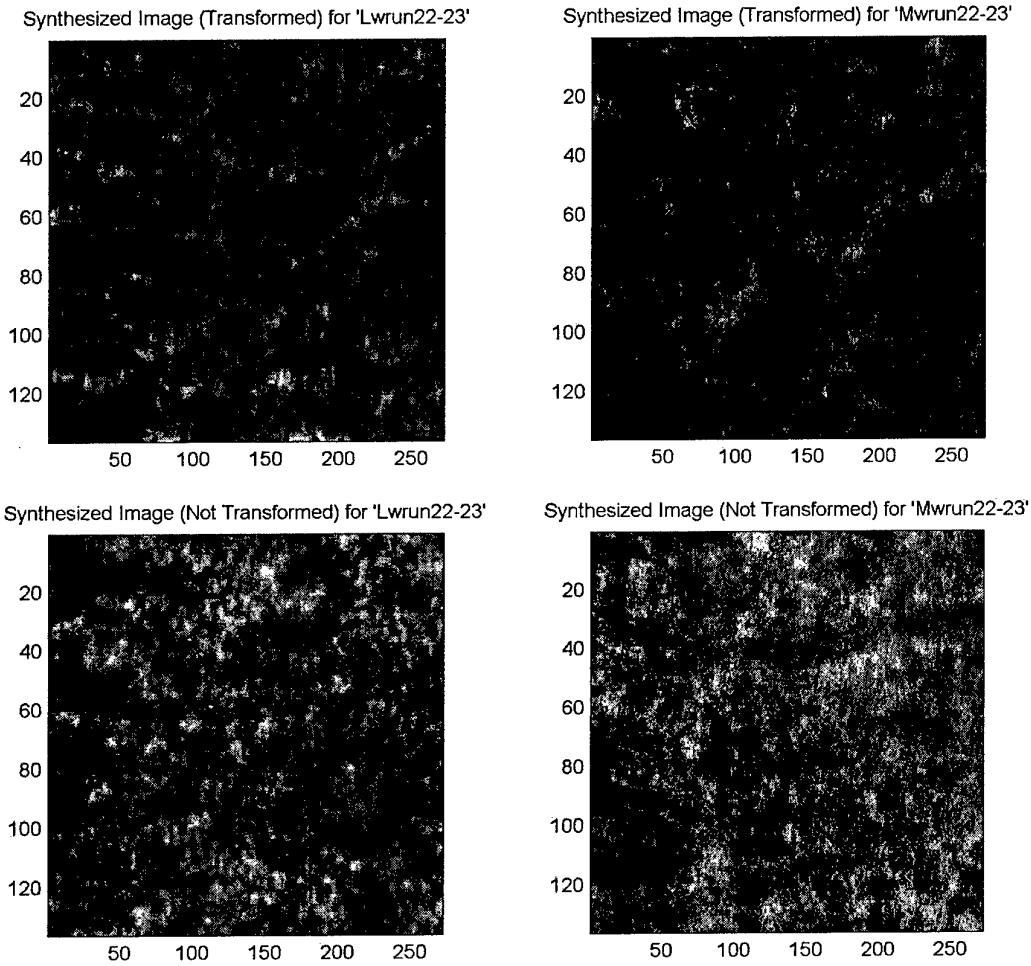

Figure 106 – Synthetic Images for Runs 22-23

3.22 Run 24

3.22.1 General Information

Flight Date: 3-7-97 DAY
Altitude: 5K ft
Depression Angle: 60 deg.
Vegetation Classes in Run: 18, 106
Predominate Vegetation Class: 106

Ensemble Size is: 350
Number of Valid Images is: 174
Vertical Resolution is: 0.65m
Horizontal Resolution is: 0.56m

3.22.2 Histogram

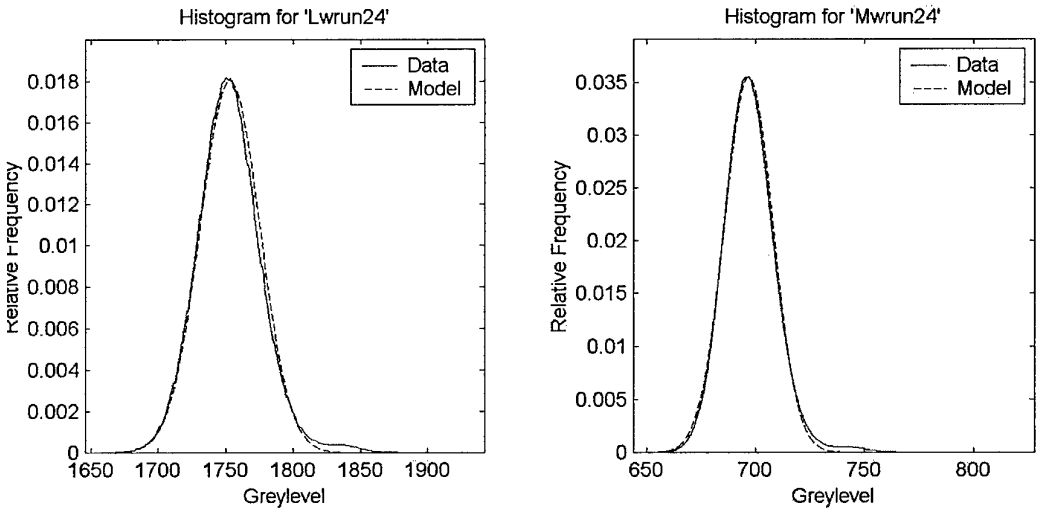

Figure 107 – Gaussian Fit – Histogram of Run 24

Histogram Information for 'Lwrun24'

Normal Model Parameters:
    Mean is: 1753.09
    Variance is: 490.00
RMS error is: 4.05%
Chi2 P-value is: 100.00%
Model Accepted by Threshold: Yes
Model Accepted Visually: Partially

Histogram Information for 'Mwrun24'

Normal Model Parameters:
Mean is: 696.84
Variance is: 126.00
RMS error is: 4.24%
Chi2 P-value is: 100.00%
Model Accepted by Threshold: Yes
Model Accepted Visually: Partially

3.22.3 Auto-covariance – Horizontal

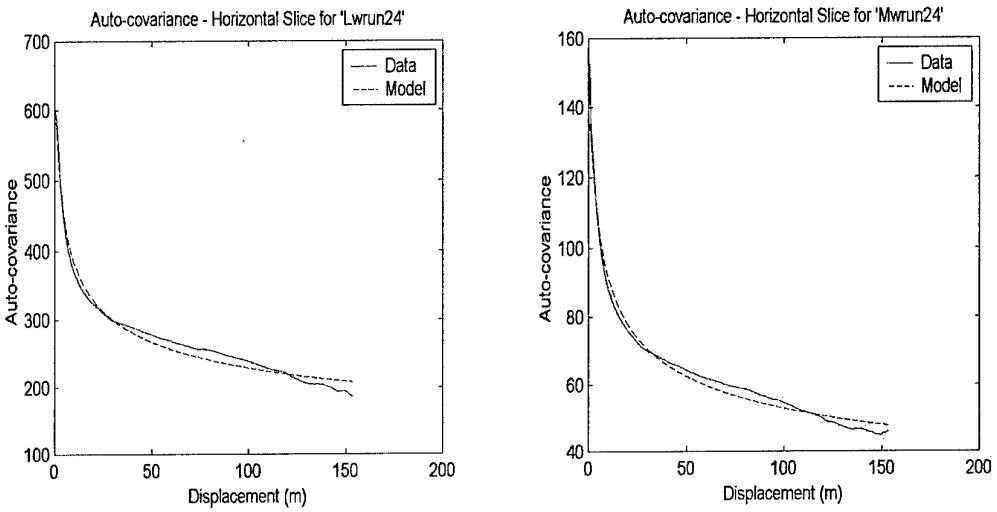

Figure 108 – Power Law Fit - Horizontal Slice of Run 24

Auto-covariance - Horizontal for 'Lwrun24'

Mean Standard deviation between images is: 56.44
Power Law Model Parameters:
a_est is: 647.27
b_est is: 1.31
w_est is: 0.11
RMS error is: 4.23%
Model Accepted by Threshold: No
Model Accepted Visually: Partially

Auto-covariance - Horizontal for 'Mwrun24'

Mean Standard deviation between images is: 15.36
Power Law Model Parameters:
a_est is: 148.29
b_est is: 0.00
w_est is: 0.11
RMS error is: 3.96%
Model Accepted by Threshold: No
Model Accepted Visually: Partially

3.22.4 Auto-covariance – Vertical

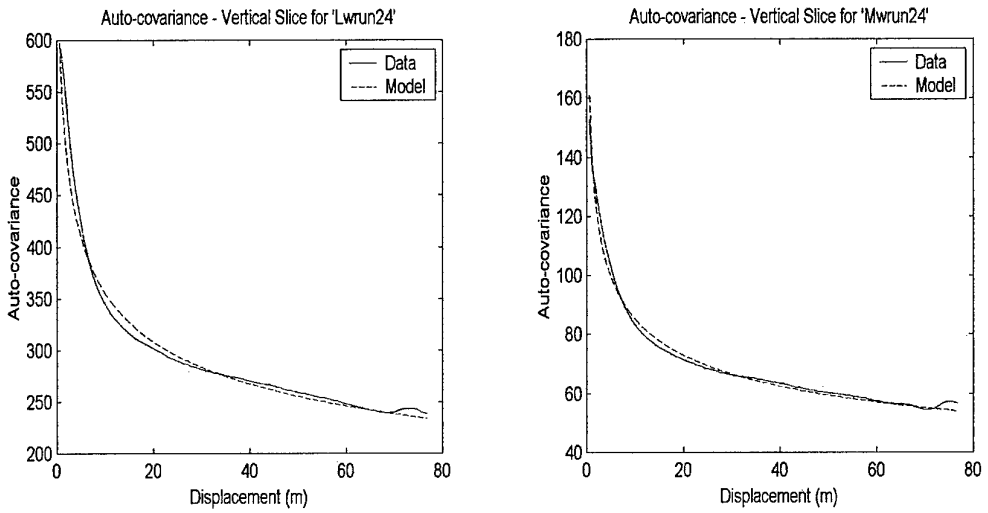

Figure 109 – Power Law Fit - Vertical Slice of Run 24

Auto-covariance - Vertical for 'Lwrun24'

Mean Standard deviation between images is: 55.40
Power Law Model Parameters:
    a_est is: 569.89
    b_est is: 0.56
    w_est is: 0.10
RMS error is: 2.36%
Model Accepted by Threshold: Yes
Model Accepted Visually: Yes

Auto-covariance - Vertical for 'Mwrun24'

Mean Standard deviation between images is: 14.76
Power Law Model Parameters:
    a_est is: 142.68
    b_est is: 0.00
    w_est is: 0.11
RMS error is: 2.09%
Model Accepted by Threshold: Yes
Model Accepted Visually: Yes

3.22.5 Image Synthesis:

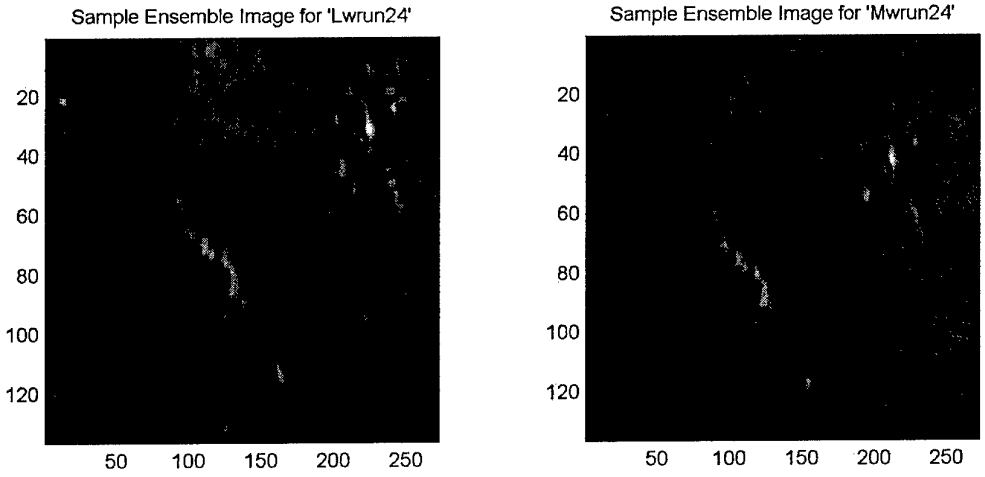

Figure 110 – Original Images from Run 24

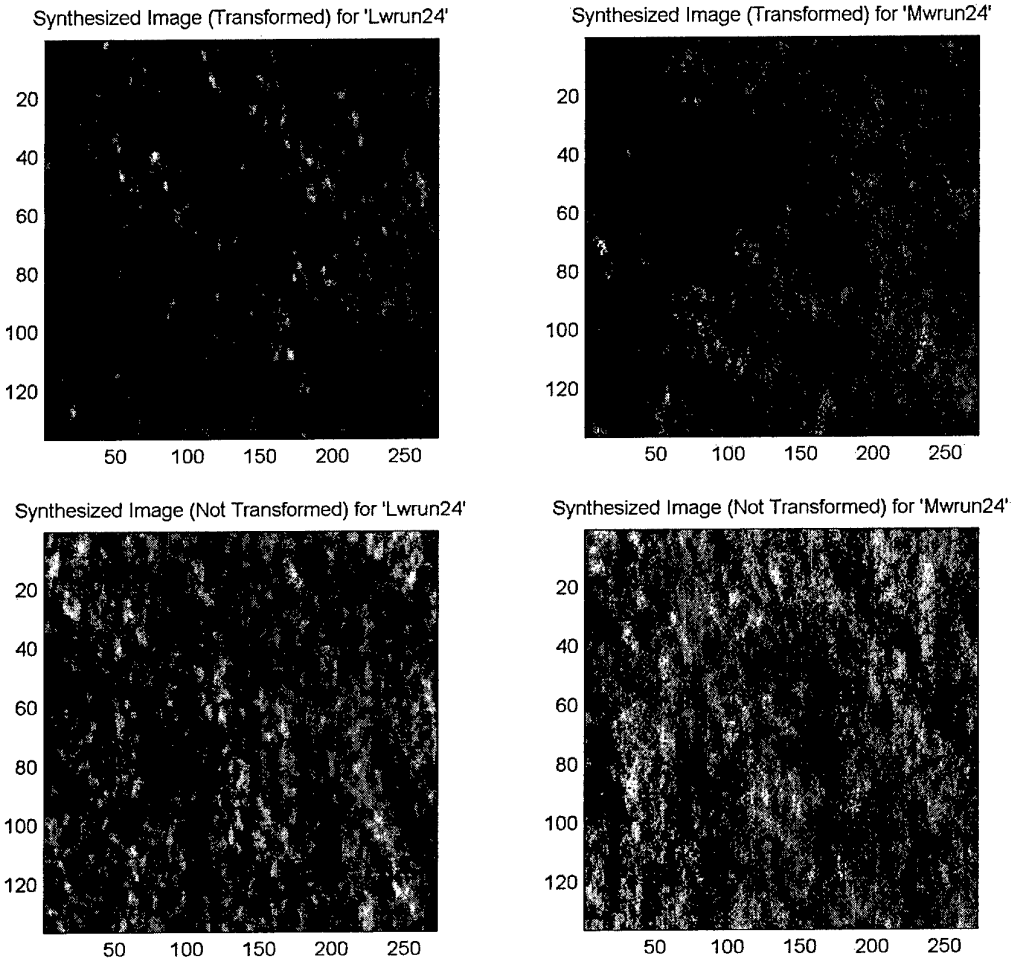

Figure 111 – Synthetic Images for Run 24

3.23 Runs 25-26

3.23.1 General Information

Flight Date: 3-7-97 DAY
Altitude: 5K ft
Depression Angle: 60 deg.
Vegetation Classes in Run: 106, 3, 47, 3, 105
Predominate Vegetation Class: 3

Ensemble Size is: 468
Number of Valid Images is: 468
Vertical Resolution is: 0.65m
Horizontal Resolution is: 0.56m

3.23.2 Histogram

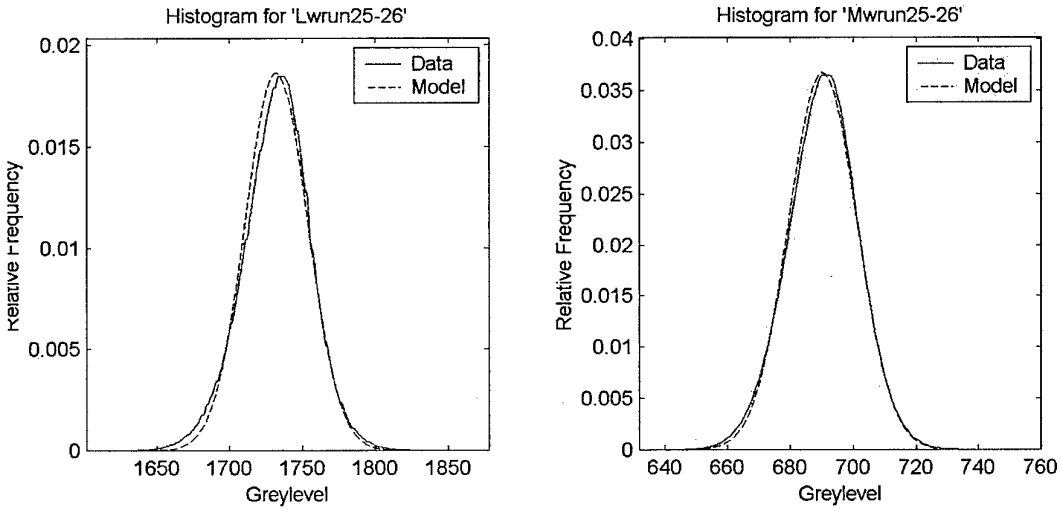

Figure 112 – Gaussian Fit – Histogram of Runs 25-26

Histogram Information for 'Lwrun25-26'

Normal Model Parameters:
    Mean is: 1732.32
    Variance is: 460.00
RMS error is: 4.98%
Chi2 P-value is: 100.00%
Model Accepted by Threshold: Yes
Model Accepted Visually: Yes

Histogram Information for 'Mwrun25-26'

Normal Model Parameters:
Mean is: 690.32
Variance is: 118.00
RMS error is: 5.28%
Chi2 P-value is: 100.00%
Model Accepted by Threshold: Yes
Model Accepted Visually: Yes

3.23.3 Auto-covariance – Horizontal

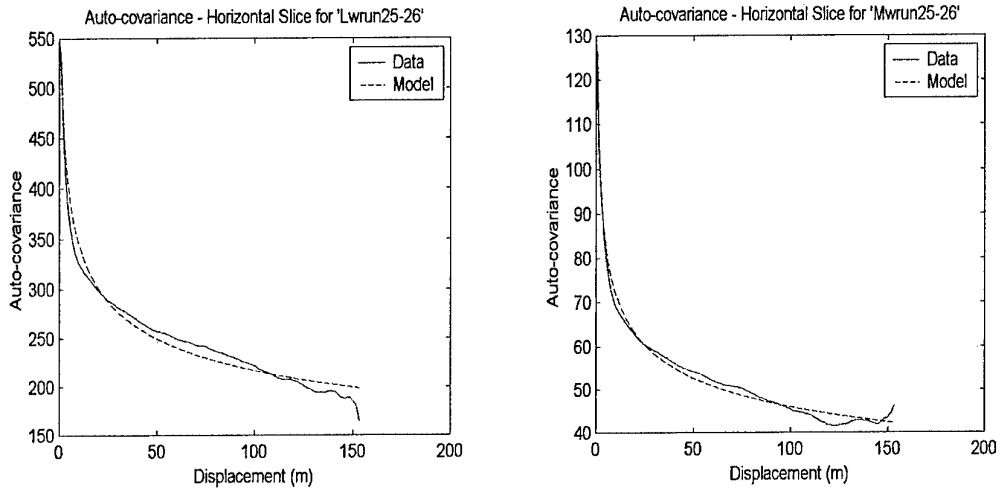

Figure 113 – Power Law Fit - Horizontal Slice of Runs 25-26

Auto-covariance - Horizontal for 'Lwrun25-26'

Mean Standard deviation between images is: 14.39
Power Law Model Parameters:
a_est is: 511.55
b_est is: 0.00
w_est is: 0.09
RMS error is: 4.53%
Model Accepted by Threshold: No
Model Accepted Visually: Partially

Auto-covariance - Horizontal for 'Mwrun25-26'

Mean Standard deviation between images is: 2.87
Power Law Model Parameters:
a_est is: 109.64
b_est is: 0.00
w_est is: 0.09
RMS error is: 2.94%
Model Accepted by Threshold: Yes
Model Accepted Visually: Yes

3.23.4 Auto-covariance - Vertical

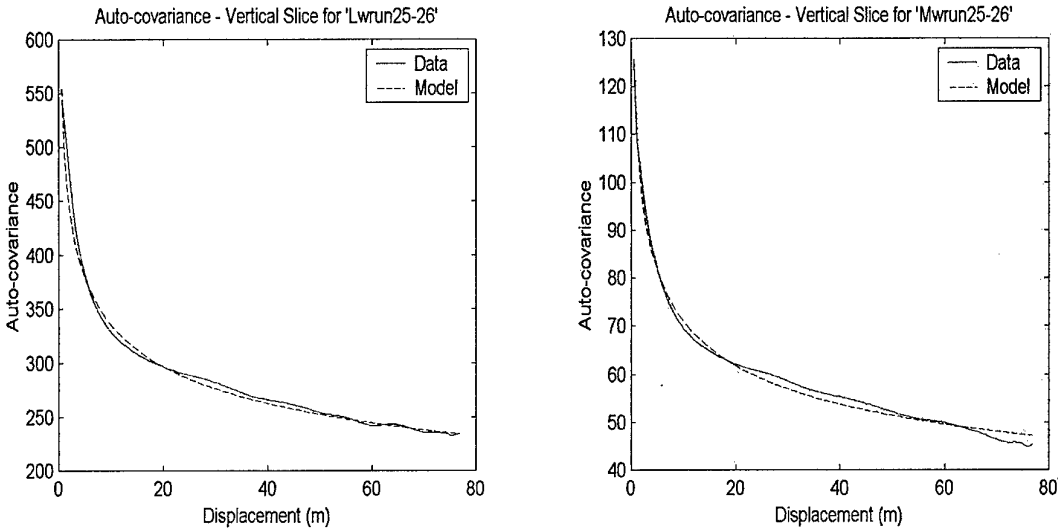

Figure 114 – Power Law Fit - Vertical Slice of Runs 25-26

Auto-covariance - Vertical for 'Lwrun25-26'

Mean Standard deviation between images is: 15.04
Power Law Model Parameters:
a_est is: 503.56
b_est is: 0.00
w_est is: 0.09
RMS error is: 1.61%
Model Accepted by Threshold: Yes
Model Accepted Visually: Yes

Auto-covariance - Vertical for 'Mwrun25-26'

Mean Standard deviation between images is: 2.99
Power Law Model Parameters:
a_est is: 112.62
b_est is: 0.00
w_est is: 0.10
RMS error is: 2.25%
Model Accepted by Threshold: Yes
Model Accepted Visually: Yes

3.23.5 Image Synthesis:

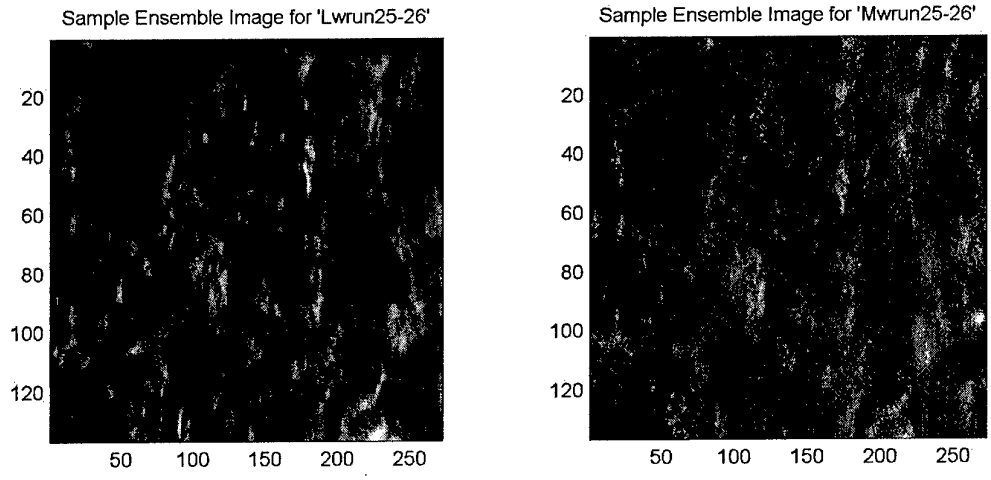

Figure 115 – Original Images from Runs 25-26

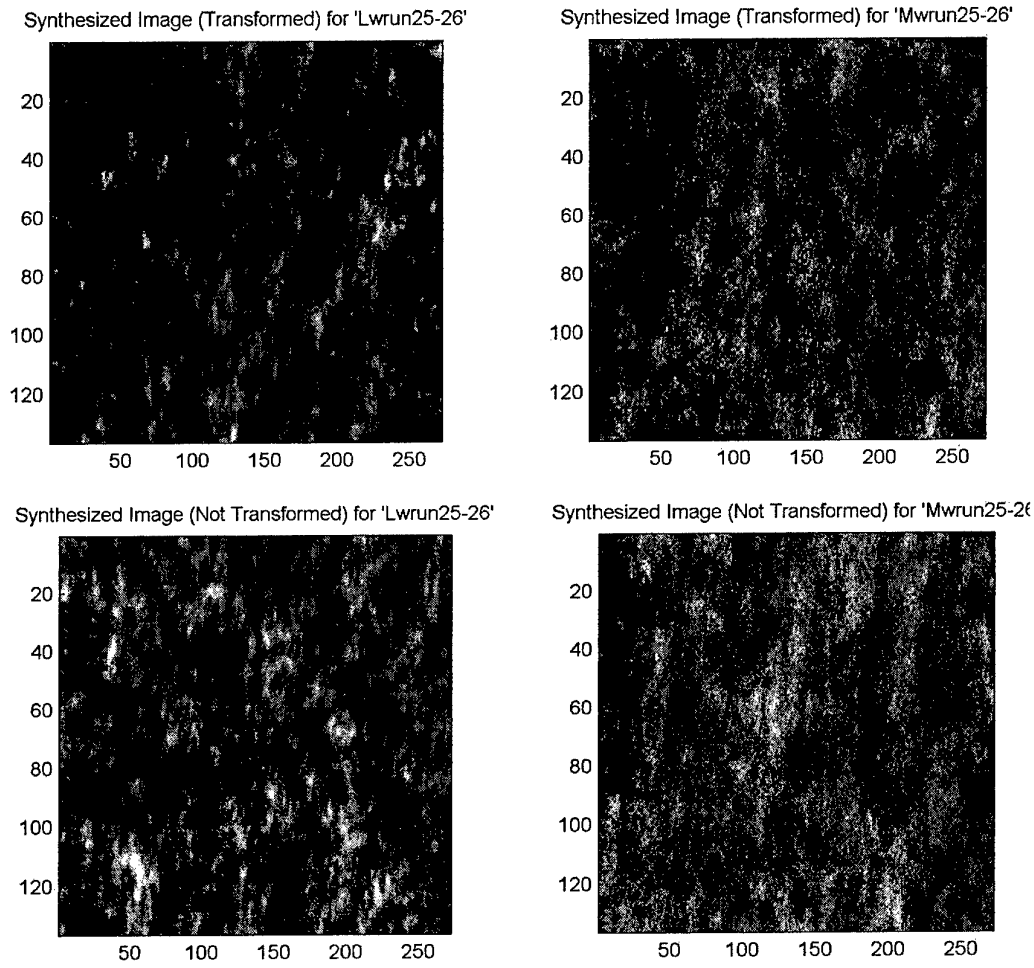

Figure 116 – Synthetic Images for Runs 25-26

4. Conclusions

4.1 Histogram Results

As the analysis of this data shows, the majority of natural terrain background is non-Gaussian. Figure 117 is a summary of the results showing the percentage of histograms which passed the Gaussian threshold, which were a partial fit and which didn't pass the hypothesis test (see section 3.2 for an explanation of the fit criteria).

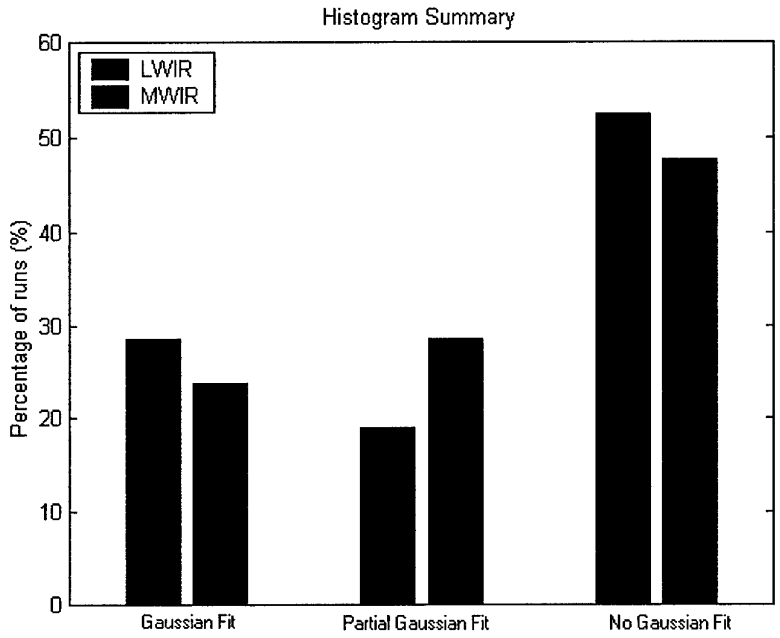

Figure 117 – Histogram Summary

4.2 Auto-covariance Results

Not all of the runs analysed fitted the power-law model. To demonstrate the relationship between ensemble size and standard deviation, Figure 118 and Figure 119 show plots of the standard deviation of the auto-covariance slices against the size of each ensemble. They indicate that as the ensemble size of a run increases, the standard deviation decreases and is more likely to fit the power-law trend.

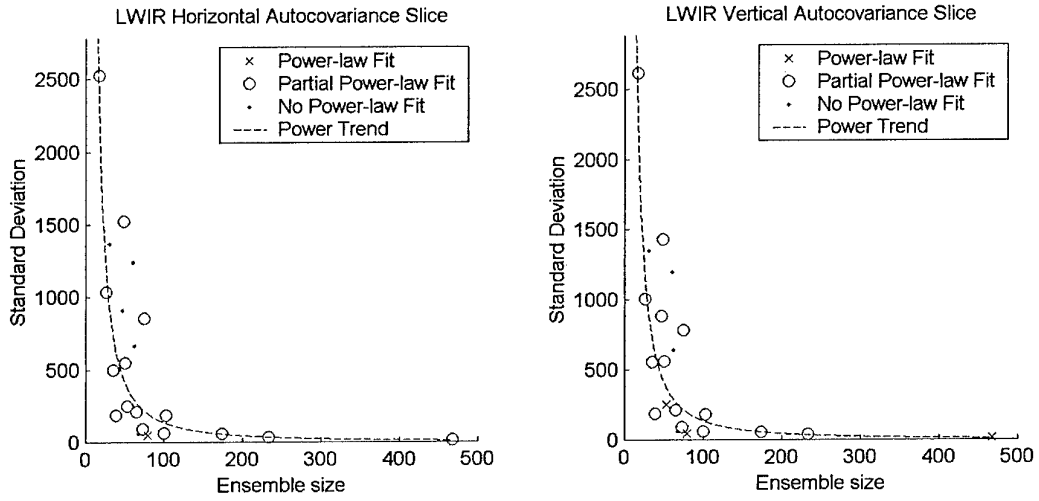

Figure 118 – LWIR Auto-covariance Summary

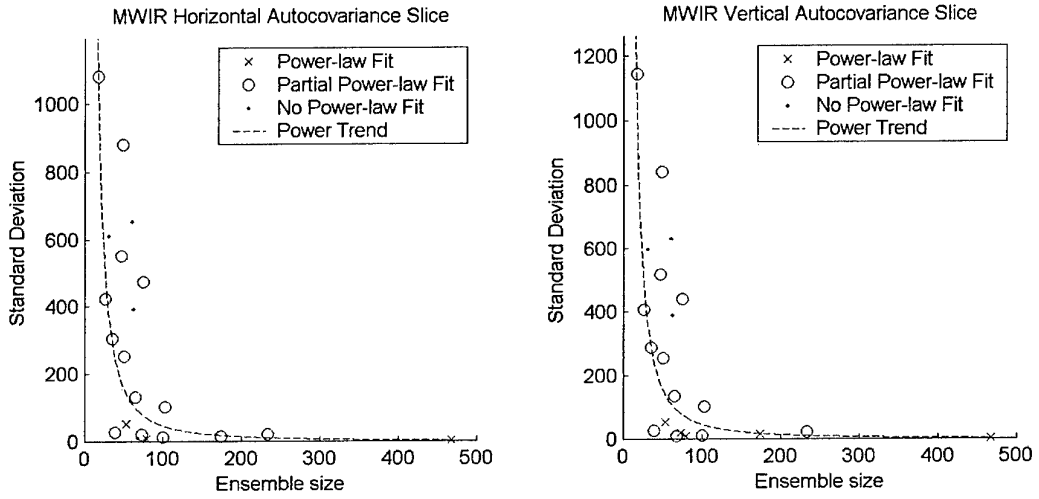

Figure 119 – MWIR Auto-covariance Summary

4.3 Stochastic Simulation Results

The majority of the transformed synthetic images appear to visually match the sample images. However, there does appear to be some differences in the constrast for images which are not transformed but pass the Gaussian hypothesis test. This difference is due to distributions having pixel values that are either really small or really large. These cause a larger dynamic range and the result is that synthetic images have an incorrect constrast. If the transformation is applied to these images before synthesis, they are forced to be truly Gaussian and reasonable simulated images result.

The more structured sparse terrain images in runs 10, 11, 13 and 15 also do not appear to match the real images closely. Here the lightness and darkness of the different regions appears correct (a property of the histogram), but the shapes of these regions are not correctly represented. The shapes are determined by higher order moments of

the random field, which are not represented by the histogram and auto-covariance estimates.

4.4 General Results and Further Work

As the 1996 trial suffered from high atmospheric absorption and low temperature contrast due to cloud cover, analysis of the 1998 trial would be the next step in a complete analysis of the data obtained. Other possible avenues of work arose from the following observations:

The auto-covariance power-law model may not be the best fit for the data analysed in this report. It could be that a different, more complex model will fit the data and help to classify the correlations in natural IR imagery.

The non-Gaussian nature of the image data and the incorrectly matched shapes for sparse terrain imagery indicates that higher order statistics are important for a complete statistical analysis. Chapple *et al.* [3] has used the same non-Gaussian simulation model and compared predicted and actual third order autocovariance functions. It was found that the simulation model gave a reasonable description of the third-order statistics, even though it was not explicitly incorporated in the model.

Alternative approaches to the stochastic simulation could include the use of a two-dimensional Markov field, [15].

5. References

[1] C.R. Dietrich and G.N. Newsam, 'A Fast and Exact method for multidimensional Gaussian stochastic simulations', Water Resource, Res. 29, pg. 2861, (1993)

[2] P.B. Chapple, D.C. Bertilone, 'Stochastic simulation of infrared non-Gaussian natural terrain imagery', Optics Communications, vol. 150, no. 1-6, pg. 71, (May 1998)

[3] P.B.Chapple, D.C.Bertilone, S. Angeli, 'Non-Gaussian stochastic model for analysis of automatic detection/recognition', Advances in Pattern Recognition Proceedings - SSPR'98 and SPR'98, pg. 897, (1998)

[4] P.B.Chapple, D.C.Berilone, R.S.Caprari, S.Angeli and G.N.Newsam, 'Target detection in infrared and SAR terrain images using a non-Gaussian stochastic model', SPIE, vol. 3699, pg. 122, (1999)

[5] D.C. Bertilone, R.S. Caprari, S. Angeli and G.N. Newsam, 'Spatial Statistics of Natural Terrain Imagery I: Non-Gaussian IR Backgrounds and Long-Range Correlations', Applied Optics 36, pg. 9167, (December 1997)

[6] D.C. Bertilone, R.S. Caprari, P.B. Chapple and S.Angeli, 'Spatial Statistics of Natural Terrain Imagery II: Visible Backgrounds and Stochastic Simulation', Applied Optics 36, pg. 9177, (December 1997)

[7] D.C. Bertilone, M. Wegener, S. Angeli, R. Joyce, 'Power-Law Correlations in Natural Infrared Imagery', Applied Optics 37, pg. 4433, (July 1998)

[8] M. Wegener, D. C. Bertilone, S. Angeli, R. Joyce, 'Preliminary Results of Statistical Analysis of Northern Australian Land Backgrounds', Not Yet Published

[9] A.M. Yaglom, 'Correlation Theory of Stationary and Related Random Functions I – Basic Results', Springer Verlag, New York, (1987)

[10] N. Ben-Yosef, K. Wilnder, S.Simhoney and G.Feigin, 'Measurement and Analysis of 2-D Infrared Natural Backgrounds', Applied Optics 24, pg. 2109, (July 1985)

[11] M.C.Phipps, M.P.Quine 'A Primer of Statistics', 2nd Edition, Prentice Hall of Australia, (1996)

[12] A.Papoulis, 'Probability, Random Variables and Stochastic Processes', 3rd Edition McGraw-Hill, New York, Sect. 8-1 and 8-4, (1991)

[13] M.J.McLachlan, T. Krishnan, 'The EM Algorithm and Extensions', Wiley & Sons, (1997)

[14] A. Jain, 'Fundamentals of Digital Image Processing', Prentice-Hall Information and System Sciences Series, New Jersey, (1989)

[15] D. Howard, 'Markov Random Fields and Image Processing', PhD Thesis for Flinders University, (March 1995).

DISTRIBUTION LIST
Statistical Analysis of Northern Australian Land Backgrounds

Luke Rosenberg and Michael Wegener

AUSTRALIA

DEFENCE ORGANISATION

Task sponsor

Director General Aerospace Development	1

S&T Program

Chief Defence Scientist	shared copy
FAS Science Policy	
AS Science Corporate Management	
Director General Science Policy Development	
Counsellor Defence Science, London	Doc Data Sheet
Counsellor Defence Science, Washington	Doc Data Sheet
Scientific Adviser to MRDC, Thailand	Doc Data Sheet
Scientific Adviser Joint	1
Navy Scientific Adviser	Doc Data Sht & Dist List
Scientific Adviser - Army	Doc Data Sht & Dist List
Air Force Scientific Adviser	Doc Data Sht & Dist List
Scientific Adviser to the DMO M&A	Doc Data Sht & Dist List
Scientific Adviser to the DMO ELL	Doc Data Sht & Dist List
Director of Trials	1

Systems Science Laboratory

Chief Weapon Systems Division	1
Research Leader MWS	1
Head Electro-optic Seekers	1
Head Missile Simulation	1
Luke Rosenberg	1
Michael Wegener	1
Derek Bertilone	1
Rob Joyce	1
Steve Angeli	1
Ninh Duong	

DSTO Library and Archives

Library Edinburgh 1 + Doc Data Sheet	
Australian Archives	1

Capability Systems Division

Director General Maritime Development	Doc Data Sheet
Director General Information Capability Development	Doc Data Sheet

Office of the Chief Information Officer

Deputy CIO	Doc Data Sheet
Director General Information Policy and Plans	Doc Data Sheet

AS Information Structures and Futures — Doc Data Sheet
AS Information Architecture and Management — Doc Data Sheet
Director General Australian Defence Simulation Office — Doc Data Sheet

Strategy Group
Director General Military Strategy — Doc Data Sheet
Director General Preparedness — Doc Data Sheet

HQAST
SO (Science) (ASJIC) — Doc Data Sheet

Navy
SO (SCIENCE), COMAUSNAVSURFGRP, NSW — Doc Data Sht & Dist List
Director General Navy Capability, Performance and Plans, Navy Headquarters — Doc Data Sheet
Director General Navy Strategic Policy and Futures, Navy Headquarters — Doc Data Sheet

Air Force
SO (Science) - Headquarters Air Combat Group, RAAF Base, Williamtown NSW 2314 — Doc Data Sht & Exec Summ

Army
ABCA National Standardisation Officer, Land Warfare Development Sector, Puckapunyal — e-mailed Doc Data Sheet
SO (Science), Deployable Joint Force Headquarters (DJFHQ) (L), Enoggera QLD — Doc Data Sheet
SO (Science) - Land Headquarters (LHQ), Victoria Barracks NSW — Doc Data & Exec Summ

Intelligence Program
DGSTA Defence Intelligence Organisation — 1
Manager, Information Centre, Defence Intelligence Organisation — 1 + (PDF version)
Assistant Secretary Corporate, Defence Imagery and Geospatial Organisation — Doc Data Sheet

Defence Materiel Organisation
Head Airborne Surveillance and Control — Doc Data Sheet
Head Aerospace Systems Division — Doc Data Sheet
Head Electronic Systems Division — Doc Data Sheet
Head Maritime Systems Division — Doc Data Sheet
Head Land Systems Division — Doc Data Sheet
Head Industry Division — Doc Data Sheet
Chief Joint Logistics Command — Doc Data Sheet
Management Information Systems Division — Doc Data Sheet
Head Materiel Finance — Doc Data Sheet

Defence Libraries
Library Manager, DLS-Canberra — Doc Data Sheet

Library Manager, DLS - Sydney West	Doc Data Sheet

OTHER ORGANISATIONS

National Library of Australia	1
NASA (Canberra)	1
Library of New South Wales	1

UNIVERSITIES AND COLLEGES

Australian Defence Force Academy	
Library	1
Head of Aerospace and Mechanical Engineering	1
Serials Section (M list), Deakin University Library, Geelong, VIC	1
Hargrave Library, Monash University	Doc Data Sheet
Librarian, Flinders University	1

OUTSIDE AUSTRALIA

INTERNATIONAL DEFENCE INFORMATION CENTRES

US Defense Technical Information Center	2
UK Defence Research Information Centre	2
Canada Defence Scientific Information Service	e-mail link to pdf
NZ Defence Information Centre	1

ABSTRACTING AND INFORMATION ORGANISATIONS

Library, Chemical Abstracts Reference Service	1
Engineering Societies Library, US	1
Materials Information, Cambridge Scientific Abstracts, US	1
Documents Librarian, The Center for Research Libraries, US	1

SPARES	5
Total number of copies:	40

This page intentionally left blank

DEFENCE SCIENCE AND TECHNOLOGY ORGANISATION DOCUMENT CONTROL DATA	1. PRIVACY MARKING/CAVEAT (OF DOCUMENT)

2. TITLE	3. SECURITY CLASSIFICATION (FOR UNCLASSIFIED REPORTS THAT ARE LIMITED RELEASE USE (L) NEXT TO DOCUMENT CLASSIFICATION)
Statistical Analysis of Northern Australian Land Backgrounds	Document (U) Title (U) Abstract (U)
4. AUTHOR(S) Luke Rosenberg and Michael Wegener	5. CORPORATE AUTHOR Systems Sciences Laboratory PO Box 1500 Edinburgh South Australia 5111 Australia

6a. DSTO NUMBER	6b. AR NUMBER	6c. TYPE OF REPORT	7. DOCUMENT DATE
DSTO-TR-1456	AR-012-812	Technical Report	July 2004

8. FILE NUMBER	9. TASK NUMBER	10. TASK SPONSOR	11. NO. OF PAGES	12. NO. OF REFERENCES
J9505/25/33	AIR 99/133	DGAD	104	14

13. DOWNGRADING/DELIMITING INSTRUCTIONS	14. RELEASE AUTHORITY
http://www.dsto.defence.gov.au/corporate/reports/DSTO-TR-1456.pdf	Chief, Weapons Systems Division

15. SECONDARY RELEASE STATEMENT OF THIS DOCUMENT

Approved for Public Release

OVERSEAS ENQUIRIES OUTSIDE STATED LIMITATIONS SHOULD BE REFERRED THROUGH DOCUMENT EXCHANGE, PO BOX 1500, SALISBURY, SA 5108

16. DELIBERATE ANNOUNCEMENT

No Limitation

17. CASUAL ANNOUNCEMENT Yes

18. DEFTEST DESCRIPTORS

Imagery, Infra-red imaging, Clutter, Image filter

19. ABSTRACT

A substantial amount of work into the statistical analysis of both visual and infra-red imagery has been undertaken in the recent years at DSTO. This report is a summary of the results from the analysis of a trial held in Northern Australia in 1997. The first and second order statistics of land background infra-red pixel intensities were estimated and Gaussian and power-law models were rigorously tested, before a stochastic simulation of the data was performed. A point-wise non-linear transform was applied for those ensemble images without a Gaussian distribution.